NTNU – Trondheim
Norwegian University of
Science and Technology

Negative Refraction in Non-Magnetic Metamaterials

Christopher Andrew Dirdal

Nanotechnology
Submission date: June 2012
Supervisor: Johannes Skaar, IET

Norwegian University of Science and Technology
Department of Electronics and Telecommunications

Abstract

The discoveries and subsequent developments within the field of metamaterials have opened up for novel light-matter interactions towards the engineering of light behavior. The astonishing phenomenon of negative refraction remains challenging to realize for visible frequencies, and non-magnetic gain metamaterials have been proposed towards this end. This thesis pursues this idea by presenting a conceptual framework for which to understand the requirements and possibilities emerging from the causal behavior of the dielectric response ϵ_r. This results in clear and concrete instructions on how ϵ_r must be designed towards negative refraction. These are offered in terms of a novel perspective employing zero- and pole placements in rational functions and analysis of ϵ_r in its complex plane.

A number of negative index systems are evaluated including two component media and low gain negative index media. Negative index concepts are introduced to the Electromagnetically Induced Transparency system. A strategy towards design and realization of arbitrary dielectric responses in terms of Krein and Nudel'man causal extrapolation is also presented.

Sammendrag

De senere års utvikling innen metamaterialer gjør det mulig å skreddersy vekselvirkninger mellom materialer og det elektromagnetiske feltet. Fenomenet kjent som negativ brytning lar seg imidlertid fremdeles vanskelig realisere ved synlige frekvenser, og aktive ikke-magnetiske metamaterialer har derfor blitt foreslått som en mulig farbar vei for å oppnå dette. Denne masteroppgaven forfølger denne ideen videre ved å kartlegge de muligheter og begrensinger slike materialer besitter for å muliggjøre negativ brytning, med hensyn på valg av dielektrisk respons ϵ_r. Denne rapporten vil presentere klare og konkrete forslag til hvordan ϵ_r må være, og dette blir gjort ved bruk av rasjonelle funksjoner samt ved analyse av ϵ_r i dets komplekse plan.

Denne rapporten behandler flere negativ brytningsmedier, deriblant to-komponent og lav-forsterkningsmedier. I tillegg er negativ brytningsteori introdusert til et atom-koherent system. Et forslag til prosedyre er lagt frem for realisering av vilkårlige dielektriske responser som baserer seg på Krein og Nudel'man ekstrapolering.

Preface

And the end of all our exploring
Will be to arrive where we started
And know the place for the first time.
– T.S. Eliot

This master thesis, initially being titled *Metamaterials and Coherent Control*, was at its inception concerned mainly with achieving negative refraction in coherent control systems such as Electromagetically Induced Transparency (EIT). Earlier work by Professor Johannes Skaar had demonstrated that negative refraction can be achieved through means of steep variation in the imaginary part of the refractive index n. As the EIT system is particularly known for its steep response features arising out of atomic coherence phenomena, it therefore seemed like a promising route towards achieving a non-magnetic, negative index medium. However, following several failed attempts at demonstrating this in terms of semi-classical field theory, it not only became clear that the EIT system was less promising than anticipated, but also that steep variations alone are not *enough*: There was more to be said concerning the conditions under which negative refraction is achieved, especially with regards to the dielectric constant ϵ_r. The attention of this thesis was therefore directed towards investigating the circumstances under which a particular ϵ_r may cause negative refraction. Though the subsequent investigation has taken different directions over the course of this thesis, the common thread is emphasized as the results are presented here, by first considering the *general* and then moving on to the *specifics*. Discussions and analysis are presented along the way, before everything is then summed up in the final concluding remarks, as well as there being presented an outlook for further inquiry.

This master thesis concludes a five year journey, under which I have ventured joyfully challenged at the Norwegian University of Science and Technology. For the opportunities and knowledge that has been given me I am immensely grateful. I must thank Professor Johannes Skaar for generously providing guidance on this thesis, my family and girlfriend Eva for their encouragement, and God for the privilege it is to wonder at the laws of nature.

Kjeller, *Christopher A. Dirdal*
15th of June 2012

Contents

1 Introduction

1.1 Background

Over the centuries our understanding of materials and their potential use have gained ever newer dimensions. We no longer understand materials solely in terms of their bulk properties such as their tensile strength and density, but increasingly in terms of *functionality*. While until recently one has perhaps most often spoken of a material's *electronic properties*, the *optical properties* of a material have grown in importance. This due to new developments within the field of *photonics*, of which an example would be *photonic crystals*. These are structured materials in which a periodically varying dielectric constant may be used as an analog to the periodic potentials considered in solid state physics. Hence a photonic crystal results in *bloch-wave solutions* and displays a number of interesting phenomena such as *photonic band gaps* and *light trapping*.

During recent years a novel method of controlling electromagnetic wave behavior has emerged through the fabrication of *metamaterials*. Such materials rely on structuring composite materials so as to give desired *effective optical parameters* that are not observed in their constituent, bulk materials. Through such materials a number of astonishing and often counterintuitive phenomena can be realized. In 2006 Pendry et. al [1] suggested that one may use metamaterials to redirect electromagnetic fields at will, even to bend light around objects like a rock diverts water in a stream. This concept is known as *optical cloaking*, as it would lead to the object becoming invisible! Short time afterwards, Schurig et al. [2] presented a physical realization of such a system that successfully bends radiation in the microwave region around a copper cylinder. Another interesting phenomena demonstrable in metamaterials is *negative refraction*, with which this thesis is concerned. In such media the index of refraction becomes negative, which therefore represents an entirely new platform of manipulating light which is of significant impact to both existing and future photonic technologies. One exciting application was suggested by Pendry in 2000 regarding a *perfect lens* [3]: A negative index material may be used as a non-diffraction limited lens, capable of imaging structures that are much smaller than the wavelength of light. Attempts at realizing such a lens have been performed with varying success, e.g. in [4].

If one compares the early development of photonics to that of solid state physics, one may observe several similarities: While the question asked in solid state physics was *how may we control the electrical properties of a material?*, the field of photonics asks similarly *how may we control their optical properties?* It is hard to overstate the impact that the field of solid state physics has played upon modern society: From the development of the first transistor in 1947 to everyday electronic devices today, this field continues to shape the modern world. This therefore raises expectations on what unrealized potential there lies within the field of photonics and metamaterials for the future.

1.2 Overview and scope of report

This thesis seeks to evaluate the general conditions under which a given dielectric response ϵ_r will lead to negative refraction in non-magnetic gain media. Passive media with magnetic responses generally display considerable loss along with having a weak magnetic response, and therefore pose a significant challenge towards achieving negative refraction at optically visible frequencies. As has been suggested in e.g. [5, 6] this thesis therefore considers the possibility of using non-magnetic *gain* media instead, and seeks to identify the conditions under which a given ϵ_r enables negative refraction. However, it is simultaneously desired that the amount of gain in such systems be small: Considerable gain can lead to the medium becoming electromagnetically unstable, and it is often difficult to achieve large gain at optically visible frequencies. Sections 3 and 4 will therefore identify the conditions under which a suitable ϵ_r may meet these requirements by identifying the relevant parameters and constraints towards achieving negative refraction.

In order to identify the conditions upon the dielectric response ϵ_r one must consider both the relationship between ϵ_r and the refractive index n, and the consequences stemming from their *causal nature*. For example, both ϵ_r and n obey the Kramers-Kronig relations, meaning that $\mathrm{Im}(\epsilon_r)$ is uniquely determined by $\mathrm{Re}(\epsilon_r)$, $\mathrm{Im}(n)$ is uniquely determined by $\mathrm{Re}(n)$ and vice versa. Now choosing $\mathrm{Re}(n) < 0$ therefore has *causal* consequences for how $\mathrm{Im}(n)$ is identified, as well as for $\mathrm{Re}(\epsilon_r)$ and $\mathrm{Im}(\epsilon_r)$. As considerations upon causality therefore play great importance towards achieving negative refraction, the relevant concepts and equations to causality are introduced in section 2.

Section 5 will propose the Electromagnetically Induced Transparency (EIT) system as a possible negative index system, which will then be evaluated in terms of the findings in sections 3 and 4. In section 6 a strategy towards the realization of arbitrary dielectric responses will be presented, which bases itself upon several of the concepts that will have emerged from sections 2, 3, and 4. Due to the general nature of the considerations presented in this thesis, the results are not limited to non-magnetic materials alone. In fact, the same conditions under which ϵ_r leads to negative refraction apply also to the product $\epsilon_r\mu_r$ of the dielectric constant and the magnetic permeability μ_r. Such considerations, as well as a summary of all the discussions of this thesis, will then finally be presented in the conclusion in section 7. The remainder of this section will outline the relevant concepts to metamaterials and negative index media.

This thesis contains many graphical plots of the optical responses of ϵ_r and n. Considering that the goal of this thesis is to achieve negative refraction within the visible spectrum, responses should be placed within the frequency bandwidth $\nu \in [400\mathrm{THz}, 788\mathrm{THz}]$. However, for simplicity the frequency axes are generally scaled to small number values. Generally, therefore, a normalization factor of about 10^{12} should be multiplied with the axes in order that the graphical plots correspond with the desired visible frequency range.

Several frequently used terms are shortened into acronyms in this

thesis. A table of their explanations is placed here for reference:

acronym	meaning	section
NIES	Negative Index by Exponential Steepness	3.2.2
ZPP	Zero-Pole Pair	4.1
EIT	Electromagnetically Induced Transparency	5
RWA	Rotating Wave Approximation	5.4

1.3 Metamaterials and negative refraction

The Greek word *meta* may be translated as *beyond*, suggesting that metamaterials have properties beyond those of conventional materials. Metamaterials can be understood as composite materials engineered for specific electromagnetic properties, many of which are not found in nature. The goal of this section is to present some of the fundamental concepts underlying metamaterials.

In order to understand the electromagnetic properties of a metamaterial, one may consider the source-free Maxwell's equations, for linear, isotropic, homogeneous media without spatial dispersion:

$$\begin{aligned} \nabla \times \mathbf{H} &= -i\nu\epsilon\mathbf{E} \\ \nabla \times \mathbf{E} &= i\nu\mu\mathbf{H} \\ \nabla \cdot \mathbf{E} &= 0 \\ \nabla \cdot \mathbf{H} &= 0 \end{aligned} \tag{1}$$

These reveal that one must look to the material parameters ϵ, the dielectric constant, and μ the magnetic permeability if one wishes to understand the electromagnetic properties of a material. In general ϵ, μ and n are complex quantities. Considering $\epsilon_r = \epsilon/\epsilon_0$:

$$\epsilon_r = \epsilon_1 + i\epsilon_2 \tag{2}$$

If the medium is passive then there is loss in the electric field amplitude described by $\mathrm{Im}(\epsilon_r) = \epsilon_2 \geq 0$. If the medium is active then there is a gain in the medium described by $\mathrm{Im}(\epsilon_r) = \epsilon_2 < 0$. In metamaterials the medium is *structured* in order to give certain desired ϵ and μ responses. One also uses electromagnetic waves with wavelengths that are much longer than any feature size of the structured metamaterial in order that ϵ_r and μ_r turn into *effective parameters*. In order to explain this, the perhaps simplest metamaterial shall be considered: The Bragg stack of Fig. 1.

If one assumes this stack to continue to infinity in both left and right directions, then the solutions to Maxwell's equations for this system become Bloch functions with a dispersion relation as the one displayed in Fig. 2. One notices in this dispersion relation that for certain frequencies there occur band gaps. These frequencies represent modes with wavelengths on the order of the periodicity a of the Bragg stack. The red line in Fig. 2 represents the dispersion *if the Bragg stack had been homogeneous*, that is if there were no alternating layers but only one and the same medium. One observes at the band gaps that the actual wave propagation is very unlike that found in a homogeneous

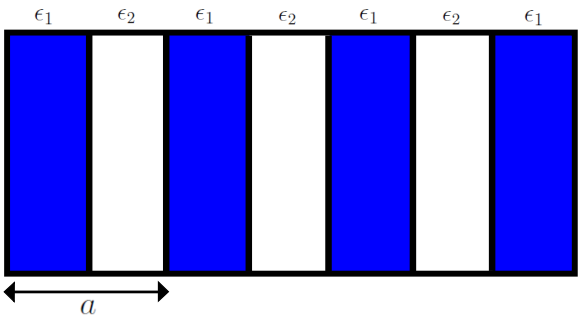

Figure 1: Stack of two alternating materials with each its own dielectric constant. The length of periodicity is given by a. The stack is assumed to continue infinitely in both directions

dispersion relationship. However, for wavelengths much longer than the periodicity, i.e. where $k = 2\pi/\lambda \to 0$ one observes that the wave dispersion relationship approaches that of a homogeneous dispersion relationship.

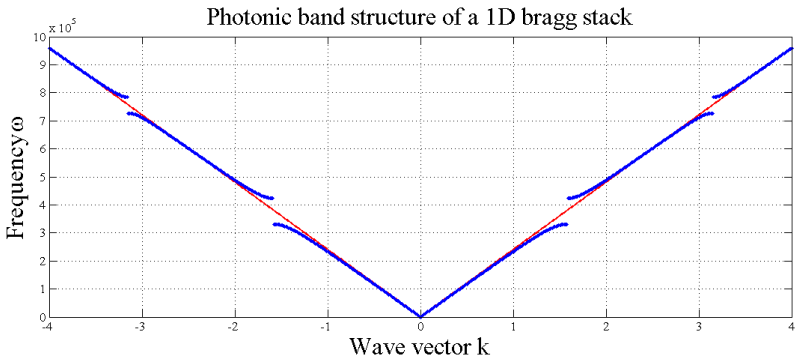

Figure 2: The blue lines correspond to the dispersion relation for the modes in the Bragg stack with alternating ϵ_1 and ϵ_2 of Fig. 1, while the red line corresponds to a homogeneous medium consisting of the effective parameter ϵ_{eff}.

This is the important point: When the wavelength is long compared to the feature size of the Bragg stack metamaterial, $\lambda \gg a$, the electromagnetic waves see an *effectively homogeneous* medium rather than a periodically alternating medium since both red and blue curves are aligned here in Fig. 2. That is, rather than behaving as though they are moving through a medium with a periodic $\epsilon(z + a) = \epsilon(z)$, the electromagnetic waves act as though they are moving through an effectively homogeneous medium $\epsilon(z) = \epsilon_{\text{eff}}$. In a general metamaterial one may have that the same occurs for μ_r. Therefore, the the two fundamental concepts relating to metamaterials have been presented: (i) Structuring of the material to influence ϵ_r, μ_r or both, and (ii) use

the media in the long wave-length limit.

It has been stated that it is possible to achieve negative refraction in a metamaterial. That is n, the index of refraction, achieves that $\mathrm{Re}(n) < 0$ at some frequency. One such metamaterial was demonstrated in the year 2000 consisting of many continuous wires and split-rings placed in a periodic array [7]. In such an arrangement, the continuous wires influence the response properties of ϵ, while the split-rings influence the magnetic properties. In this metamaterial one is able to achieve $\mathrm{Re}(\epsilon_r) < 0$ and $\mathrm{Re}(\mu_r)$ simultaneously, which as it turns out is a sufficient condition for $\mathrm{Re}(n) < 0$, the onset of negative refraction.

This metamaterial, however, only functions for microwave frequencies. Passive media with magnetic responses generally display considerable loss along with having a weak magnetic response, and are therefore often not capable of achieving negative refraction at optically visible frequencies. In the following, these properties will be shown while considering the split-ring resonator and continuous wire metamaterial closer.

1.3.1 Negative dielectric constant $\mathbf{Re}(\epsilon_r) < 0$

This section considers how one may manipulate ϵ_r by the use of an array of continuous wires in order to get $\mathrm{Re}(\epsilon_r) < 0$ for specific frequencies.

Thin continuous metallic wires may be approximated to resemble the response of plasma. Consider therefore a free point charge q under monochromatic electromagnetic radiation. Newton's 2nd law gives:

$$m\ddot{x}(t) = qE\exp(-i\nu t) \tag{3}$$

Here m is the mass of the charge q, E is the electric field amplitude, t represents time and ν represents frequency. Integrating both sides gives the displacement of the charge

$$x(t) = X\exp(-i\nu t), \quad X = -\frac{qE}{m\nu^2} \tag{4}$$

Hence one may thereby express the polarization density of the plasma as

$$P = NqX = -\frac{Nq^2E}{m\nu^2} \tag{5}$$

N is the number of free charges per volume. Note that as $\nu \to 0$, the polarization diverges as one expects for a medium consisting entirely of free charges. In a linear medium the polarization density may be related to the electric field through the electric susceptibility χ as

$$P = \epsilon_0\chi E \tag{6}$$

Hence, comparing (5) and (6), one may express the relative dielectric constant $\epsilon_r = \epsilon/\epsilon_0$ as

$$\epsilon_r = 1 + \chi = 1 - \frac{Nq^2}{\epsilon_0 m \nu^2} \tag{7}$$

One may define a plasma frequency ω_p so that

$$\epsilon_r = 1 - \frac{\omega_p^2}{\nu^2}, \quad \omega_p^2 = \frac{Nq^2}{\epsilon_0 m} \tag{8}$$

As predicted, negative $\mathrm{Re}(\epsilon)$ is attainable for $\nu < \omega_p$.

1.3.2 Negative magnetic permeability $\mathbf{Re}(\mu_r) < 0$

This section considers how one may manipulate μ_r by the use of an array of metallic split ring resonators in order to achieve $\mathrm{Re}(\mu_r) < 0$ for specific frequencies.

Figure 3, displays a single split-ring and its equivalent circuit. The voltage source for this RLC circuit equals the emf induced in the split-ring resonator due to the varying magnetic field flux through it, the inductance arises due to the self-inductance of the ring, the capacitance arises over the air gap, and there is an electrical resistance within the ring. In the following, circuit analysis will be employed to demonstrate that the split-ring resonator displays a Lorentzian response.

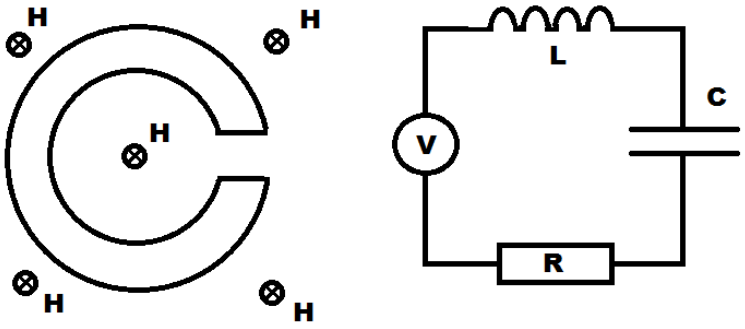

Figure 3: Split ring resonator and its corresponding RLC circuit

According to Faraday's law of induction one has:

$$V = -\frac{d\Phi}{dt} = \pi a^2 \mu_0 \frac{dH(\nu, t)}{dt} = -i\nu\pi a^2 \mu_0 H(\nu, t) \tag{9}$$

Using Kirchoff's voltage law on the equivalent RLC circuit one finds

$$V = (-i\nu L - \frac{1}{i\nu C} + R)I \tag{10}$$

The magnetization density of the split-ring is $M = NI\pi a^2$, where N is the number of split-ring resonators per unit volume. Inserting (9) into (10), one may solve for the current, and hence express the magnetization density as

$$M = -\frac{i\nu(\pi a^2)^2 N\mu_0 H(\nu,t)}{-i\nu L - \frac{1}{i\nu C} + R} \tag{11}$$

Inserting this expression of M into the known relation $B = \mu_0(H + M) = \mu_0\mu_r H$, one may find the relative magnetic permeability $\mu_r = \mu/\mu_0$:

$$\mu_r = 1 + \frac{(\pi a^2)^2 N\nu^2 \frac{\mu_0}{L}}{\nu^2 - \frac{1}{LC} + i\nu\frac{R}{L}} \tag{12}$$

As may be seen from Equation (12), the permeability is approximately Lorentzian if $\frac{R}{L} \ll \frac{1}{LC}$. Under this assumption one may therefore safely assume that the magnetic permeability may be described by the Lorentzian resonator:

$$\mu_r = 1 + \chi_0 \frac{\omega_0^2}{\omega_0^2 - \nu^2 - i\nu\Delta\nu} \tag{13}$$

Here $\omega_0 = 1/\sqrt{LC}$ and $\Delta\nu = R/L$ are the central frequency and bandwidth, respectively, and the resonator strength is described by the constant χ_0. Furthermore, one may separate (13) into real and imaginary parts

$$\mathrm{Re}(\mu_r) = 1 + \chi_0 \frac{\omega_0^2(\omega_0^2 - \nu^2)}{(\omega_0^2 - \nu^2)^2 + (\nu\Delta\nu)^2} \tag{14}$$

$$\mathrm{Im}(\mu_r) = \chi_0 \frac{\omega_0^2\nu\Delta\nu}{(\omega_0^2 - \nu^2)^2 + (\nu\Delta\nu)^2} \tag{15}$$

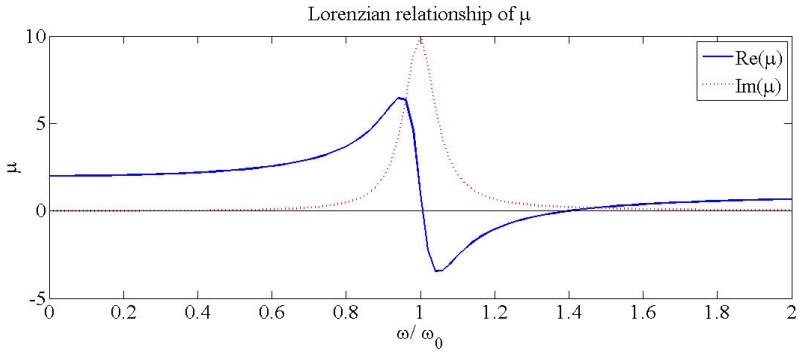

Figure 4: Plot of the permeability in a Lorentzian model

Viewing Fig. 4 one observes that there is a bandwidth in which $\mathrm{Re}(\mu)$ is negative. However it is also clear that $\mathrm{Im}(\mu_r)$, which represents absorption, is large in the same region. Is there any way this absorption can be made smaller? One may observe from the Equations (14) and (15) that $\mathrm{Im}(\mu_r)$ approaches zero faster than does $\mathrm{Re}(\mu_r) - 1$, meaning that as $\chi_0 \to \infty$, $\mathrm{Im}(\mu_r)$ will drop to zero for a frequency at

which $\mathrm{Re}(\mu_r)$ is finite and negative. Hence if χ_0 can be made sufficiently large then it is possible to achieve $\mathrm{Re}(\mu_r) < 0$ and $\mathrm{Im}(\mu_r) \approx 0$ for a limited bandwidth.

This analysis reveals the problem with magnetic resonances in passive media for visible frequencies: There will be significant loss present in magnetic responses at negative refraction because the magnetic response is χ_0 is generally small for visible frequencies. It is for this reason that this thesis therefore considers non-magnetic media.

1.4 Wave solutions in negative index materials

Now that the principles behind metamaterials have been considered, as well as one particular metamaterial realization of negative refraction, it is interesting to ask what the electromagnetic wave solutions look like within such media. To gain a little insight into such wave behavior one must once again turn to Maxwell's equations (1). Assuming plane wave solutions of the form $\mathbf{E} = \mathbf{E}_0 \exp(i\mathbf{k}\cdot\mathbf{r} - i\nu t)$ and $\mathbf{H} = \mathbf{H}_0 \exp(i\mathbf{k}\cdot\mathbf{r} - i\nu t)$, and inserting these into Maxwell's equations gives:

$$\begin{aligned} \mathbf{k}\times\mathbf{E} &= \nu\mu\mathbf{H} \\ \mathbf{k}\times\mathbf{H} &= -\nu\epsilon\mathbf{E} \end{aligned} \tag{16}$$

Then defining the fields to be $\mathbf{E}_0 = E\hat{\mathbf{x}}$, $\mathbf{H}_0 = H\hat{\mathbf{y}}$ and $\mathbf{k} = -\mathrm{k}\hat{\mathbf{z}}$, one may find:

$$\begin{aligned} kE &= -\nu\mu H \\ kH &= -\nu\epsilon E \end{aligned} \tag{17}$$

Multiplying these two equations together gives $k^2 = \mu\epsilon\nu^2$, which one may then compare with the phase velocity of the modes $v_p = \nu/k$ and the definition of the refractive index $n = c/v_p$ to find:

$$n^2 = \epsilon_r\mu_r \tag{18}$$

This therefore displays the relationship between the refractive index n, ϵ_r and μ_r which will be of use later.

So how does an electromagnetic plane wave behave in a negative refractive index material? For a normal media where $\mathrm{Re}(\epsilon_r) > 0$ and $\mathrm{Re}(\mu) > 0$ at a given frequency, (16) shows that $\mathbf{E}\times\mathbf{H}$ points in the direction of $\mathbf{k}$. When this is the case, one says one is dealing with a *right-handed medium*. However, consider (16) for the condition $\mathrm{Re}(\epsilon_r) < 0$ and $\mathrm{Re}(\mu_r) < 0$ as in the negative index metamaterial considered in the previous section. One now observes the surprising fact that $\mathbf{k}$, $\mathbf{E}$ and $\mathbf{H}$ form a *left-handed system* as seen in Fig. 5. What is even more strange, is that the wave vector points in the opposite direction of the Poynting vector $\mathbf{S}$, which points in the direction of energy transfer! For right-handed media $\mathbf{k}$ and $\mathbf{S}$ are parallel.

The phenomenon of negative refraction can be demonstrated for a plane wave traveling across an interface between a left- and right-handed media displayed in Fig. 6. By noting that (i) the normal component of the Poynting vector must be continuous due to the fact that there is no accumulation of energy at the boundary, (ii) the tangential

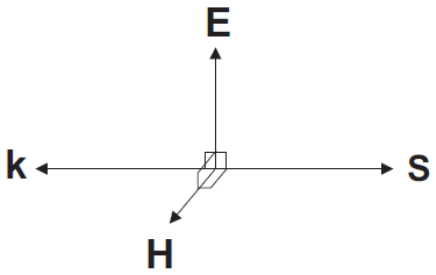

Figure 5: Left handed system in which the wave vector and Poynting vector point in opposite directions. Hence phase velocity and energy propagation point in opposite directions! This figure is taken from [8].

components of the electric and magnetic fields must be continuous due to boundary conditions, one arrives at the displayed refraction [8]. The angle of refraction in the medium on the right has the negative angle of that one would expect in a normal medium. Hence it is called negative refraction. This phenomena was proposed by Veselago in 1968 [9].

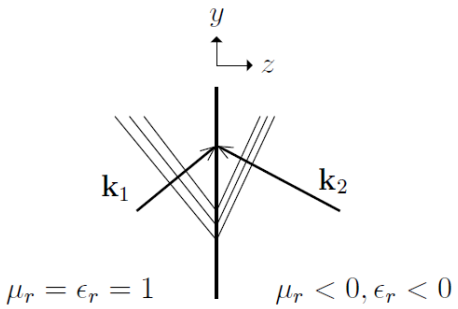

Figure 6: Negative refraction across an interface between a right handed system and a left handed system. This figure is taken from [8].

As discussed earlier, due to the problems with magnetic resonances it is desired to achieve negative refraction in non-magnetic media. Firstly, can this be done? And secondly what will the wave solutions look like in such media? It turns out that by using an active non-magnetic medium, negative refraction can be achieved even though the medium is right-handed! This may be shown through a simple argument: Imagine a passive medium where $\mathrm{Re}\{\epsilon_p(\nu_n)\} < 0$ and $\mathrm{Re}\{\mu_p(\nu_n)\} < 0$ at a frequency ν_n, so that at this frequency one has negative refraction $n_p = -\sqrt{|\epsilon_p(\nu_n)||\mu_p(\nu_n)|}$. Next, imagine an active medium which is such that $\epsilon_a(\nu) = \epsilon_p(\nu)\mu_p(\nu)$ and $\mu_a(\nu) = 1$ for all frequencies ν. Since $n_a(\nu) = n_p(\nu)$, the active medium therefore produces negative refraction at ν_n even though both $\mathrm{Re}\{\epsilon_a(\nu_n)\}$ and

Re$\{\mu_a(\nu_n)\}$ are positive. This argument holds as long as ϵ_p, ϵ_a, μ_p and μ_a can in fact be chosen the way suggested. Though it may not seem apparent that this should be the case, right-handed media that display negative refraction have been proposed in literature [5, 6]. Now, assuming that a medium can be constructed in the way described, will the plane wave in an active medium behave in the same way as in a passive medium? Not exactly. The behavior of a wave incident on an active negative index medium is discussed in [10] and a figure from this article is presented in Fig. 7. The shape of the transmitted wave will have the same appearance in both active and passive media as they both display the same refractive index. However, the passive medium is a left handed medium, so that the Poynting vector will point towards the right while the wave vector will point towards the left. For the active medium however, being a right handed medium, both the Poynting vector and the wave vector points to the left. That is, back towards the source! The amplitude of the active wave will also be larger as it draws energy from the active medium.

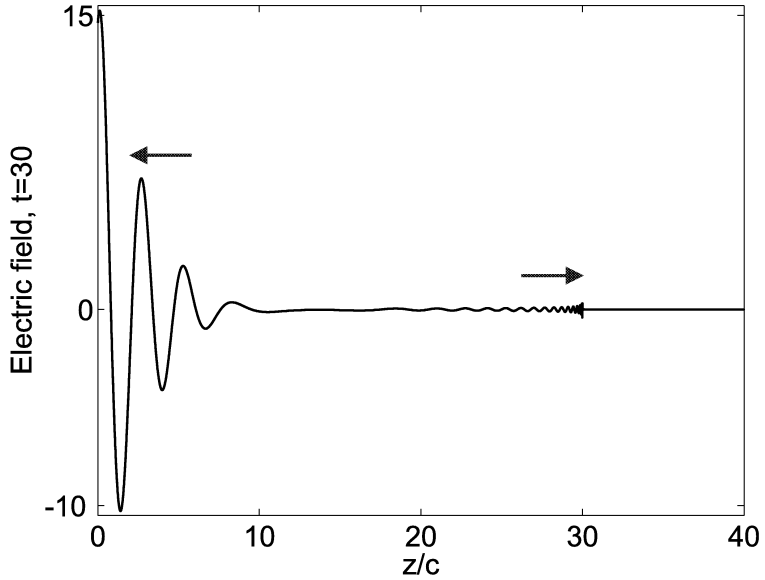

Figure 7: The wave propagation of a plane wave incident to an active negative index medium at $z = 0$ [10]. The arrow towards the right displays the forerunner of the wave, while both the wave vector and the Poynting vector point towards the left for the region $z/c \leq 10$.

2 Causality, Kramers-Kronig relations and analyticity

Any electromagnetic medium must be *causal* in the microscopic sense. That is, no polarization or magnetization can exist in the medium be-

fore there has been applied an electric or magnetic field, respectively. This fact, trivial though it may seem, turns out to have thorough-going consequences. In the end it is the requirements of the Kramers-Kronig relations, which assume causality, that dictate under what circumstances negative refraction is permissible as shall be shown in sections 3, 4, and 6.

One consequence of causality is that the optical parameters representing the electric susceptibility χ, the dielectric response ϵ_r, magnetic permeability μ_r and the refractive index n must all be described by *analytic functions*[1] for some region in the upper complex half-plane [10]. For passive media it can be taken for granted that this requirement is fulfilled in the whole upper half-plane, however as is pointed out in [10], for active media there exist conditions under which the refractive index n becomes non-analytic there. Such media turn out to be *electromagnetically unstable* and are not suitable for the purposes of this thesis. This poses a threat toward possible negative index realizations in non-magnetic media, because such media must necessarily be active as is explained in section 3.1.1. One must therefore verify that the refractive indexes of such media in fact are analytic in the whole upper complex frequency plane for the purposes of this thesis. This section seeks to explain how ϵ_r must be in order to ensure the analyticity of n, as well as define causality and derive the Kramers-Kronig relations.

It will be assumed that $\mu_r = 1$ here and for the rest of this report, in line with the fact that this project considers non-magnetic media. Therefore this section will proceed with examining the conditions under which χ, ϵ_r and n are analytic. The same arguments apply to the analyticity of μ_r, however, but will not be discussed explicitly.

2.1 Causality and Kramers-Kronig relations

At the application of a field pulse at time t, a polarization density of magnitude $\epsilon_0 x(t)$ is induced, where $x(t)$ is a scalar function of time. For a linear medium, the time domain polarization is then a superposition of earlier effects of the field $\mathcal{E}(\tau)$ for $\tau \leq t$, defining a convolution:

$$\mathbf{p}(t) = \epsilon_0 x(t) * \mathcal{E}(t) = \epsilon_0 \int_{-\infty}^{\infty} x(\tau)\mathcal{E}(t-\tau)d\tau \tag{19}$$

Assuming causality means that

$$x(t) = 0, \quad \text{for} \quad t < 0 \tag{20}$$

i.e. there exists no polarization before the field has been turned on. Calculating the polarization in the frequency domain involves calculating the Fourier transform of the convolution defined in (19) by the use of (20) giving:

[1] Definition from Wolfram Mathworld: A complex function is said to be analytic on a region **R** if it is complex differentiable at every point in **R**. If a complex function is analytic on a region **R**, it is infinitely differentiable in **R**. A complex function may fail to be analytic at one or more points through the presence of singularities, or along lines or line segments through the presence of branch cuts.

$$\mathbf{P}(\nu) = \epsilon_0 \chi(\nu) \mathbf{E}(\nu) \tag{21}$$

Here $\chi(\nu)$, the Fourier transform of $x(t)$, is the susceptibility, by which the dielectric function is defined $\epsilon_r(\nu) = 1 + \chi(\nu)$. $\mathbf{P}(\nu)$ and $\mathbf{E}(\nu)$ are the frequency domain polarization and electric field, respectively.

From here on, media that are microscopically unstable are excluded, that is, $x(t)$ and $\chi(\nu)$ are assumed to be square integrable. Causality then results in the fulfillment of the Kramers-Kronig relations, which relate the real and complex parts of the susceptibility by:

$$\begin{aligned} \mathrm{Im}(\chi) &= \mathscr{H}\mathrm{Re}(\chi) \\ \mathrm{Re}(\chi) &= -\mathscr{H}\mathrm{Im}(\chi) \end{aligned} \tag{22}$$

Here $\mathscr{H}$ represents the Hilbert transform. As a consequence of $x(t)$ being real in (20) one has that $\chi(-\nu) = \chi^*(\nu^*)$, and therefore also $\epsilon_r(-\nu) = \epsilon_r^*(\nu^*)$. Using this symmetry relation in (22), along with the expression for the Hilbert transform $\mathscr{H}$, one may derive:

$$\mathrm{Im}\ \chi(\nu) = \frac{2}{\pi}\mathcal{P}\int_0^\infty \frac{\nu \mathrm{Re}\chi(\omega)}{\nu^2 - \omega^2} d\omega \tag{23}$$

$$\mathrm{Re}\ \chi(\nu) = -\frac{2}{\pi}\mathcal{P}\int_0^\infty \frac{\omega \mathrm{Im}\chi(\omega)}{\nu^2 - \omega^2} d\omega \tag{24}$$

The $\mathcal{P}$ here represents the Cauchy principal value. These are the equations which are most commonly referred to as the Kramers-Kronig relations. They show that $\mathrm{Re}(\chi)$ is uniquely determined by $\mathrm{Im}(\chi)$, and vice versa. Since $\chi = \epsilon_r - 1$, it follows that (23) and (24) apply for $[\epsilon_r - 1]$ as well.

2.2 Analyticity of χ, ϵ_r and n

In order to show that causality leads to analyticity, this discussion will base itself on what is known as the Titchmarch theorem[2]. This states that if the susceptibility χ fulfills causality, it follows that χ must also be an analytic function in the upper complex frequency plane. Therefore, since $\chi = \epsilon_r - 1$ is analytic, it follows that ϵ_r is analytic as well.

[2]Titchmarsh Theorem: if $\chi(\nu)$ is square integrable over the real ν-axis, then any one of the following implies the other two:

1. Causality: The fourier transform $x(t) = F_\nu[\chi(\nu)]$ is zero for $t < 0$
2. Analyticity: The function $\chi(\nu)$ is analytic for $\mathrm{Im}(\nu) > 0$. Furthermore, $\chi(\nu)$ is uniformly square integrable along a line parallel to the real axis in the upper half-plane: $\int_{-\infty+i\gamma}^{\infty+i\gamma} |\chi(\nu)|^2 d\nu < k$ for some number k and all γ.
3. Kramers-Kronig: The real and imaginary parts of $\chi(\nu)$ (where $\nu \in \mathbb{R}$) are Hilbert transforms of each other.

What about n? From (18) one has $n = \sqrt{\epsilon_r}$. If $\epsilon_r = 0$ at ν_0 then $|dn/d\nu|_{\nu=\nu_0} \to \infty$, making n non-analytic at this frequency. It is therefore not given that n should be analytic just because ϵ_r is: All zeros in ϵ_r represent points of non-analyticity in n. It is shown in [10] that if n is not analytic, then the medium is electromagnetically unstable. For the purposes of this report, therefore, one must demand that ϵ_r not have any zeros in the upper complex plane. As long as this is the case, then n is analytic and the stability of the medium is ensured.

Actually, it is clear from (18) that n can have both a positive or negative global sign. How does one know which one to use? As n can be negative for certain frequencies, one cannot determine the global sign of n from an individual frequency. Instead the sign of n is found by evaluating the behavior of n for all frequencies. The procedure is as follows: The fact that χ is square integrable again means that $|\chi(\nu)| \to 0$ as $\nu \to \infty$. Therefore

$$n = \pm\sqrt{1+\chi(\nu)} \approx \pm(1+\frac{\chi}{2}) \to \pm 1 \quad (\nu \to \infty) \tag{25}$$

Since $\chi = 0$ at $\nu \to \infty$, one cannot have negative refraction here. Therefore the correct global sign is positive, by convention. Considering the above, one also has that $\epsilon_r \to 1$ for $\nu \to \pm\infty$.

2.3 How to evaluate n for active media

Based on [10] and the discussions above, here follows a basic "cookbook recipe" on how to find and evaluate n for an active medium where $\mu = 1$.

1. Examine whether ϵ_r contains zeros in the upper half of the complex frequency plane.
2. If there are no zeros, then n takes the analytic form:

   $$n = \pm\sqrt{|\epsilon|}\exp(i\theta_\epsilon/2) \tag{26}$$

   where the argument $\theta_\epsilon = \arg(\epsilon)$ is *unwrapped* so as to ensure continuity in n.
3. Determine the global sign of the above expression by evaluating it for $\nu \to \infty$, and choose the sign that gives $n \to +1$

3 How does one obtain negative refraction in non-magnetic media for a given ϵ_r?

The fundamental question lying behind this section, and indeed most of this thesis, relates to how ϵ_r must be chosen in order to achieve negative refraction in non-magnetic media. One may rightfully ask why such special attention should be given to this parameter when in fact the phenomena of negative refraction is only encountered when observing *another* optical parameter, namely the index of refraction.

There is, however, good reason for this: It is the dielectric function ϵ_r that describes the material-specific properties of any given non-magnetic medium, and hence it is *the* optical parameter which is most directly related to the given medium. As has been shown in section 1.3 it is the parameter one seeks to solve for when considering the fields of the medium. For this reason, when faced with the task of constructing a medium that should display negative refraction, one has no other choice than to start with the dielectric constant ϵ_r.

Another interesting question is whether one can achieve negative refraction with little, or perhaps even *arbitrarily little*, gain in ϵ_r. This is because any requirement of significant gain represents a challenge towards the realization of negative refraction: Firstly because large gain can cause the medium to become unstable, and secondly because achieving siginificant gain at optical frequencies is challenging. Therefore, if one should be able to find systems for which negative refraction is achieved without gain in non-magnetic media, then the possibility of realizing negative index media for optical frequencies will achieve a new height of realism.

So then, how does one choose ϵ_r towards these goals? What requirements must one demand? This section will seek to outline the main general requirements and raise questions for further investigation in sections 4 and 5. This section will proceed by first considering ϵ_r in its complex plane, and then considering the requirements imposed due to causality.

3.1 Considerations from the complex plane of ϵ_r

3.1.1 Criterion 1: Gain

The first requirement upon a given dielectric function ϵ_r towards the achievement of negative refraction in n, is that there must be gain in the system. That is, $\mathrm{Im}(\epsilon_r) < 0$ for a frequency region in vicinity of the occurrence of negative refraction. Why is this the case?

Consider Fig. 8a displaying the polar path of the dielectric function ϵ_r. The plot may be understood in the following way: From section 2 one knows that as $\nu \to \infty$ then $\epsilon_r \to 1$ due to causality. Thereby, while tracing the path displayed for ϵ_r one starts with the frequency placed at infinity and then moves down to an observation frequency ν_{obs}. As observed, therefore, the pathway begins at $\epsilon_r = 1$ and moves along the arrow direction until reaching $\epsilon_r(\nu_{\mathrm{obs}})$ at a phase angle $\arg(\epsilon_r) = \theta_\epsilon$. What does the corresponding complex plane of the refractive index n look like for this given ϵ_r? According to (26), one has that $\arg(n) = \theta_\epsilon/2$ which therefore leads to the path plotted in Fig. 8b. In the same way as for ϵ_r, the path for n starts at $n = 1$ for $\nu \to \infty$ and ends at $n(\nu_{\mathrm{obs}})$ at the phase angle $\arg(n) = \theta_\epsilon/2$. Notice from the plot that $\mathrm{Re}\ n(\nu_{\mathrm{obs}}) \approx -1$, meaning that the particular ϵ_r in this example has lead to the occurrence of negative refraction at ν_{obs}.

Notice from Fig. 8b that one only achieves $\mathrm{Re}(n) < 0$ as long as $\pi/2 < \arg(n) < 3\pi/2$, which places n in the second and third quadrants. This means that $\pi < \theta_\epsilon < 3\pi$ since $\theta_\epsilon = 2\arg(n)$. Any

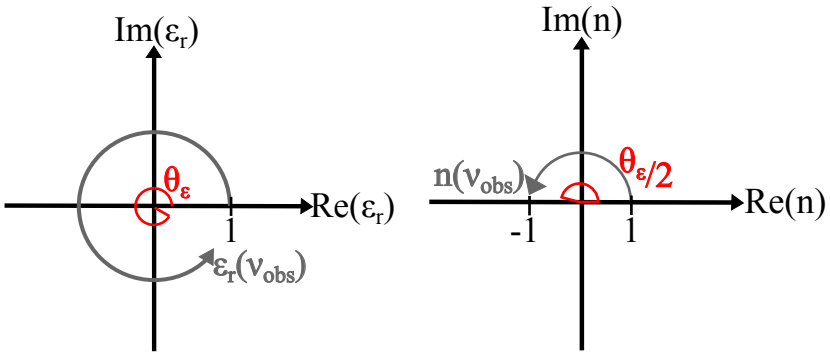

(a) Complex plane of ϵ_r (b) Complex plane of n

Figure 8: Visualizing the relationship between the polar paths in the complex planes of ϵ_r and n.

polar path of ϵ_r that is to start at $\epsilon_r = 1$ for $\nu \to \infty$ and end up at $\epsilon_r(\nu_{\text{obs}})$ where $\pi < \theta_\epsilon < 3\pi$ must therefore move within the lower complex plane where $\text{Im}(\epsilon_r) < 0$. This means that, for a frequency region between ν_{obs} and $\nu \to \infty$ there will be gain. One observes this in Fig. 8a where the polar path moves through the third and fourth quadrant. This is in fact always the case when one wishes to have negative refraction in a non-magnetic medium, and hence one must require that such media be active.

Why does one not necessarily require gain if the medium *is* magnetic? For a magnetic medium the refractive index is not only determined by the dielectric constant ϵ_r but also by the magnetic permeability μ_r. The refractive index is therefore given by:

$$n = \sqrt{(|\epsilon_r||\mu_r|)}\exp[(\theta_\epsilon + \theta_\mu)/2] \tag{27}$$

Here $\theta_\mu = \arg(\mu_r)$. One observes here that $\arg(n) = (\theta_\epsilon + \theta_\mu)/2$. In order to achieve negative refraction, one must again demand that $\pi/2 < \arg(n) < 3\pi/2$, which in this case can e.g. be achieved by having $\theta_\epsilon = \theta_\mu = \pi$. This does not require the polar path of ϵ_r or μ_r to move into the lower complex plane, and hence gain is not required.

3.1.2 Criterion 2: Polar path around the origin

One observes in Fig. 9a and Fig. 9b two polar paths of ϵ_r that are unable to achieve negative refraction. This despite that they both display gain, and despite that the latter path moves within all four quadrants of the complex plane. In the case of Fig. 9a one has $-\pi < \theta_\epsilon < 0$, which leads to $-\pi/2 < \arg(n) < 0$, and in the case of Fig. 9b one has $-\pi < \theta_\epsilon < \pi$, which leads to $-\pi/2 < \arg(n) < \pi/2$. If one again considers Fig. 8b, it is clear that neither of these paths result in $\arg(n)$ being large enough to cause negative refraction. Hence gain is only a necessary requirement, but not a sufficient one, towards achiev-

ing negative refraction in a non-magnetic medium. What *is* sufficient, however, is if the polar path of ϵ_r moves *around* the origin in the complex plane. When this is the case, one is ensured that enough phase has been achieved for $\mathrm{Re}(n) < 0$.

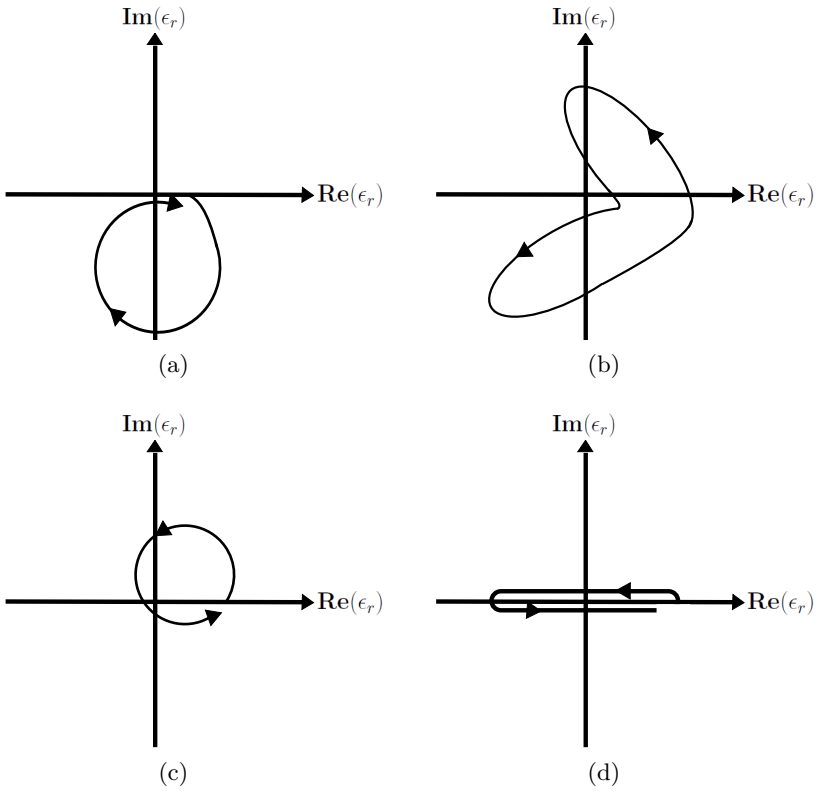

Figure 9: Various proposed polar paths of ϵ_r in the complex plane towards achieving negative refraction. Only (c) and (d) are successful.

Consider Fig. 9c and Fig. 9d. These are two polar paths of ϵ_r that move around the origin, and hence lead to negative refraction. Both paths end up almost at their start, meaning that at this point the phase is $\theta_\epsilon \approx 2\pi$. From the expression for the refractive index (26) it is clear that when $\theta_\epsilon = 2\pi$ one ends up with $\mathrm{Re}(n) = -\sqrt{|\epsilon_r|}$ and $\mathrm{Im}(n) = 0$. This is desirable because $\mathrm{Im}(n) > 0$ represents attenuation of electromagnetic fields in the medium. Therefore, though it is sufficient that the polar path of ϵ_r move around the origin in the complex plane, the closer it comes to enclosing an ellipse the better.

So far three polar paths of ϵ_r have been presented which all lead to the occurrence of negative refraction. When comparing Fig. 8a, Fig. 9c and Fig. 9d, one observes that the amount of $\max\{-\mathrm{Im}(\epsilon_r)\}$ decreases for each system. That is, Fig. 8a requires the most gain, while Fig. 9d requires the least (assuming they have been plotted on the same scale). This suggests that although gain is a necessary

requirement, it does not necessarily have to be large. In fact, in the case of Fig. 9d it seems that it can be made arbitrarily small. Is this realistic? Here one needs to be cautious: Notice that in this section ϵ_r has simply been treated as a complex function. No assumptions have been made upon it other than that $\epsilon_r \to 1$ for $\nu \to \pm\infty$. However, it is known from section 2 that the dielectric response must be *causal* and obey the Kramers-Kronig relations. Therefore, though this section has served to show how a given ϵ_r will lead to negative refraction, one must therefore bear in mind that it is not given that any particular suggested ϵ_r is causal. In other words, even though a polar path such as the one displayed in Fig. 9d will lead to negative refraction at arbitrarily low gain, it is not known that it in fact is possible to create this ϵ_r in a causal medium. For these reasons, the next section will present the requirements upon ϵ_r known from the Kramers-Kronig relations.

3.2 Criterion 3: Causality

Considerations on possible routes toward negative refraction can be derived from causality arguments as has been done in [6]. Consider the imaginary refractive index n for a hypothetical medium in Fig. 10. The refractive index n is such that $\mathrm{Im}(n) = 0$ in the frequency region $\omega_1 < \nu < \omega_2$, and that the observation frequency ν_{obs} is situated somewhere within this region. By the Kramers-Kronig relation (24) in section 2, when replacing $\chi(\nu)$ with $[n(\nu) - 1]$, one can therefore set up the following equation:

$$\mathrm{Re}\ n(\nu_{\mathrm{obs}}) = 1 - \frac{2}{\pi}\int_0^{\omega_1} \frac{\mathrm{Im}\ n(\omega)\ \omega}{\nu_{\mathrm{obs}}^2 - \omega^2} d\omega + \frac{2}{\pi}\int_{\omega_2}^{\infty} \frac{\mathrm{Im}\ n(\omega)\ \omega}{\omega^2 - \nu_{\mathrm{obs}}^2} d\omega \quad (28)$$

From this expression one may observe two possibilities by which one can make $\mathrm{Re}(n) < 0$:

i. Large positive $\mathrm{Im}(n)$ below the working frequency, or large negative $\mathrm{Im}(n)$ above the observation frequency ν_{obs}

ii. Steep drop in $\mathrm{Im}(n)$ immediately below the observation frequency ν_{obs}

Possibility (i) leads to $\mathrm{Re}(n) < 0$ by holding $\mathrm{Im}(n)$ in the second term large and positive, or holding $\mathrm{Im}(n)$ in the third term large and negative.

The fact that possibility (ii) leads to $\mathrm{Re}(n) < 0$ may be understood qualitatively as follows. If one has $\nu_{\mathrm{obs}} \approx \omega_1$, then one acquires a large value in term two of (28) which contributes to make $\mathrm{Re}(n) < 0$. However, since $\mathrm{Im}(n)$ is assumed to be zero for $\omega_1 < \nu_{\mathrm{obs}} < \omega_2$, while it is assumed to have a finite, positive magnitude for $\nu \leq \omega_1$, then it is clear that $\mathrm{Re}\ n(\nu_{\mathrm{obs}}) < 0$ is only possible if $\mathrm{Im}(n)$ drops steeply as $\nu \to \nu_{\mathrm{obs}}^-$. A quantitative description of this effect is offered in [6].

These discoveries are interesting as they indicate what may be possible:

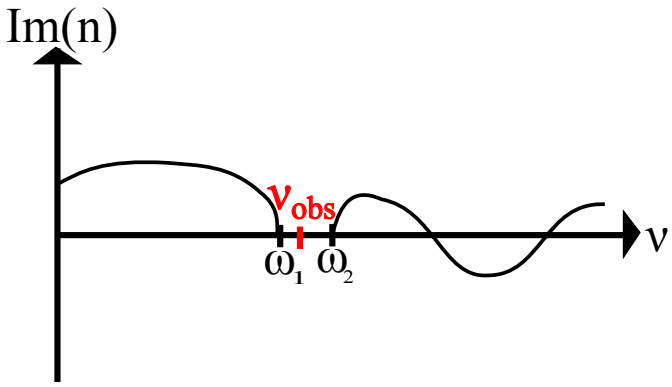

Figure 10: Displaying the complex component of the refractive index vs. frequency in a hypothetical medium to illustrate (28).

a **Low negative Im(n):** For example, what if one wishes to achieve negative refraction with low negative Im(n)? Upon viewing (28) it seems this can be done by having high positive Im(n) and/or sharp variations below the working frequency.

b **Low positive and negative Im(n):** What if one wishes neither large positive nor negative Im(n)? From (28) one observes one therefore needs to have a sharp variation in Im(n) below the working frequency.

So how are these concepts useful in practice? In order to demonstrate this, two cases of suggested negative index material realizations from literature will now be considered.

3.2.1 Two-Component System: High loss, low gain realization

It has been suggested that one can achieve negative refraction at optical frequencies using two-component media [5]. That is, by use of a dielectric response with one passive and one active component of the following form:

$$\epsilon_r = 1 + \frac{\alpha}{\omega_\alpha^2 - \nu^2 - i\nu\Gamma_\alpha} + \frac{\beta}{\omega_\beta^2 - \nu^2 - i\nu\Gamma_\beta} \tag{29}$$

In this expression one can identify two Lorentzian functions with each their own amplitude $\alpha > 0$ and $\beta < 0$, their own respective resonance frequencies ω_α and ω_β, and their own widths described by Γ_α and Γ_β. It has been suggested that such a medium may for example be realized in non-magnetic medium with two atomic or molecular constituents, where one is in the ground state and the other in the excited state [5, 11].

Fig. 11 presents an example of one such medium. Viewing the dielectric response in Fig. 11a, one observes that the amount of passive response amplitude (Im(ϵ_r) > 0) is a lot larger and broader than there

is an amount of active response amplitude ($\mathrm{Im}(\epsilon_r) < 0$). In Fig. 11b one observes that negative refraction is achieved: $\mathrm{Re}(n) < 0$ occurs around $\nu \approx 55$. Considering that $\mathrm{Im}(n)$ is large prior to the negative refraction, one can understand this behavior in terms of (28) by possibility (i) presented earlier. That is, for this system one achieves negative refraction due to the large $\mathrm{Im}(n)$ below the onset of negative refraction.

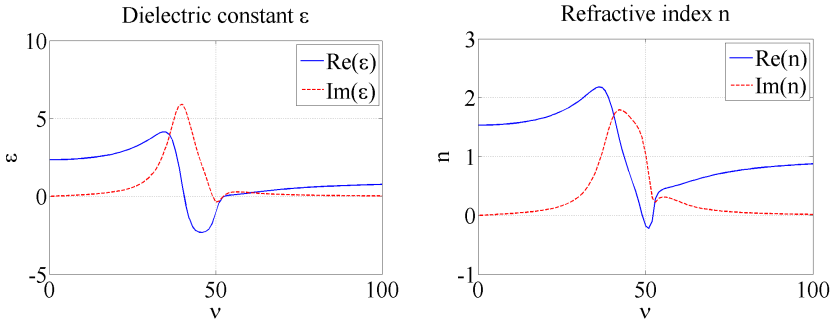

(a) (b)

Figure 11: A two-component medium described by (29) where $\alpha = 1.5$ and $\beta = -0.15$: A superposition of a passive and an active Lorentzian response. Achieves negative refraction around $\nu = 50$ due to the large amount of $\mathrm{Im}(n)$ and $\mathrm{Im}(\epsilon_r)$ below this frequency.

3.2.2 NIES: Steep variation realization

The article [6] suggests a medium that may achieve negative refraction through steep variation, that is, through possibility (ii) identified earlier regarding (28). The dielectric constant ϵ_r, its complex plane, and the refractive index of this system are plotted in Fig. 12. The refractive index, displayed in Fig. 12b, contains a sharp drop below $\nu = 1$, which accordingly causes $\mathrm{Re}(n)$ to become negative here. Hence, by making this drop even steeper, one is able to achieve a larger amount of negative refraction. The amount of negative refraction achieved turns out to be logarithmically dependent upon the gradient of the drop; i.e. negative refraction in this system requires *exponential steepness* [6]. This system is therefore given the acronym NIES: *Negative Index by Exponential Steepness*, and it will be revisited upon several occasions during this master thesis.

By looking at the dielectric response of this system in Fig. 12a, one observes that considerable gain is involved. The advantage of this system is that the needed gain can be reduced: As the drop in $\mathrm{Im}(n)$ is made steeper, less gain is required to achieve the same amount of negative refraction. That is, the steeper the drop is made, the less gain will be necessary. Therefore, if one makes the drop sufficiently steep, one can in fact achieve a large amount of negative refraction

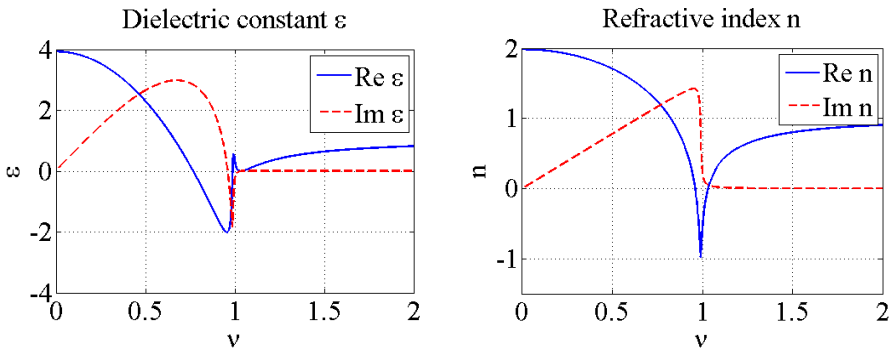

(a) Dielectric response ϵ_r

(b) Refractive index n

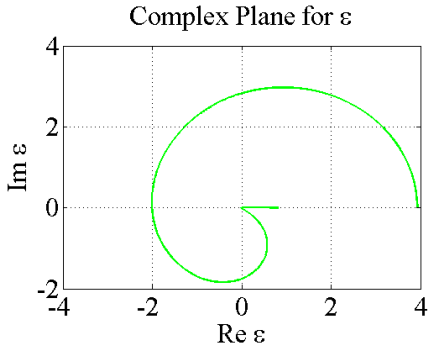

(c) Complex plane of ϵ_r

Figure 12: The NIES system: A steep drop in $\mathrm{Im}(n)$ at $\nu = 1$ is shown to lead to negative refraction in (b). The corresponding ϵ_r is displayed in (a), and the complex plane of ϵ_r is displayed in (c).

with *arbitrarily low gain*. For this reason, this system is very interesting indeed. Should one manage to realize it, a great milestone would have been overcome towards the achievement of negative refraction at optical frequencies. A system thought to be able to imitate this response will be considered and evaluated in section 5.

In order to verify that one in fact can achieve negative refraction with arbitrarily low gain, an expression for n will now be presented. The article [6] shows that the response may be written as an integral of Lorentzian functions:

$$n = 1 + \alpha \int_0^{\omega_1} \frac{\omega_0^2}{\omega_0^2 - \nu^2 - i\nu\Gamma} d\omega_0 \tag{30}$$

$$= 1 + \alpha \left[\omega_1 - \left[i\sqrt{\omega^2 + i\omega\Gamma} \right] \arctan\left(\frac{\omega_1}{i\sqrt{\omega^2 + i\omega\Gamma}} \right) \right] \tag{31}$$

The parameter ω_0 represents the resonance frequency, and Γ describes the width, of each Lorentzian. The parameter α represents a normal-

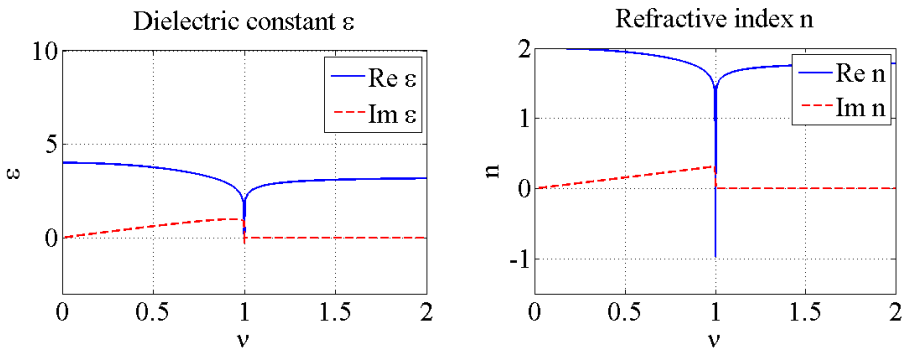

(a) Dielectric response ϵ_r (b) Refractive index n

Figure 13: The NIES system where $\Gamma = 5{\cdot}10^{-13}$ leading to extreme steepness in $\mathrm{Im}(n)$ at $\nu = 1$. The response has been normalized by the adjustment of α in (31) so that $\mathrm{Re}(n) = -1$. Hence the same amount of negative refraction is achieved here as in Fig. 12 with almost no gain displayed in (a).

ization coefficient with units Hz^{-1}, and the upper frequency before the sharp drop is determined by ω_1. One may understand the steepness of the drop in Fig. 12b as being determined by the steepness of the last Lorentzian summed in the integral in (30), thereby making it determined by Γ.

The drop is made steeper by making Γ smaller. Therefore, by making Γ smaller in (31) one should achieve negative refraction requiring less gain. Consider Fig. 13: Here $\Gamma = 5{\cdot}10^{-13}$, making the Lorentzians in (30) extremely narrow and steep. In return, hardly any gain at all is required for ϵ_r in Fig. 13a to achieve negative refraction at $\nu = 1$ for n in Fig. 13b. By making Γ smaller one should also expect the responses ϵ_r and n to attain greater amplitudes: This is indeed the case, however α is changed so as to normalize the response displayed in Fig. 13 in order to end up with $\mathrm{Re}(n) = -1$. This means that the amplitudes of each Lorentz function in (30) has been adjusted down. Therefore, this shows that by continually increasing the steepness of the drop in n, one can in this way achieve negative refraction at arbitrarily low gain. However, the small value of Γ used here, demonstrates the extreme steepness needed to achieve this. What is more, the frequency bandwidth at which negative refraction occurs likewise becomes extremely narrow.

The NIES system has therefore verified that negative refraction can be achieved through steep variation in $\mathrm{Im}(n)$, as expressed in possibility (ii) earlier. However, does this then mean that all that is needed is steep variation? Why then use the complicated response expressed in (30)? Could one not simply have achieved the same negative refraction at *arbitrarily low gain* with a single Lorentzian using the same Γ instead? The Lorentzian response shape is plotted in Fig. 27b of section 5.1. The answer is yes and no: Yes, the steep variation of a single Lorentzian

will lead to negative refraction, but no, it will not achieve this at arbitrarily low gain. An example showing this will be presented later in section 4.5.2.

It is clear, therefore, that although steep variation can lead to negative refraction, an additional requirement is relevant if one wishes to achieve this with arbitrarily low gain: Rather than simply have a steep drop, one must have a *special type* of steep drop. Notice in Fig. 12b and Fig. 13b that prior to the sharp drop there is a *slow rising*. That is, in contrast to a steep Lorentzian response, the response here is *asymmetric*. Had there been an equally sharp rising in $\mathrm{Im}(n)$ before the sharp drop, as is the case for a Lorentzian response, then negative refraction would not be possible at arbitrarily small gain. One must have an *asymmetric drop*: A slow rising and fast drop.

How does this *asymmetric drop* reduce the amount of gain required in achieving negative refraction? One may again understand this from (28): As one observes in the equation's second term, it is not only the steep drop that matters, but also the amount of $\mathrm{Im}(n)$ present below ν_{obs}, below the onset of negative refraction, that encourages $\mathrm{Re}(n)$ to become negative. Considering Fig. 12b it is known that as the drop is made steeper by making Γ smaller, the amount of $\mathrm{Im}(n)$ below $\nu = 1$ remains unchanged before normalization through changing α. However, had the response n rather consisted of a single Lorentzian, then the amount of $\mathrm{Im}(n)$ below the onset of negative refraction would decrease as Γ is made smaller.

3.2.3 Requirements upon ϵ_r

The requirements upon n from the Kramers-Kronig relations for the achievement of negative refraction have now been demonstrated at length. However, the primary interest of this report is to arrive at criteria for ϵ_r, not n. How may the results of these discussions therefore be related to ϵ? Consider n defined in terms of functions $u(\nu)$ and $v(\nu)$:

$$n = 1 + u(\nu) + iv(\nu) \tag{32}$$

The real term of n is therefore $1 + u(\nu)$ and imaginary term of n is $v(\nu)$. One may then express $\epsilon_r = n^2$:

$$\epsilon_r = \underbrace{\big(1 + u(\nu)\big)^2 - v(\nu)^2}_{\epsilon_1} + i\,\underbrace{2v(\nu)\big[1 + u(\nu)\big]}_{\epsilon_2} \tag{33}$$

The real term of the dielectric constant is here called ϵ_1 whereas the imaginary term is called ϵ_2.

Considering the two expressions, it is not apparent that there exists any unambiguous link between the criteria placed upon n and those placed upon ϵ_r in achieving negative refraction. For example, if one wishes a high value of $\mathrm{Im}(n) = v(\nu)$ below ν_{obs} in order to pursue possibility (i) regarding (28), it is not clear where one needs to place loss and gain in ϵ_r, because the sign of $\epsilon_2 = \mathrm{Im}(\epsilon_r)$ will depend on whether $\mathrm{Re}(n) = 1 + u(\nu)$ is positive or negative at any given frequency.

Also, one observes when comparing ϵ_r with n in Fig. 12 that their response behaviors are quite different, and it therefore does not seem intuitive that one should be able to simply transfer the conditions under which n gives negative refraction to ϵ_r.

Therefore, rather than attempt to relate the requirements upon n directly to ϵ_r through (32) and (33), some indirect considerations will be made from the following observation: It is known that one must require $\mathrm{Re}(\epsilon)$ to be negative prior to the occurrence of negative refraction in n, as is shown in Fig. 14. One observes here that one must have path (2) rather than path (1) in order for ϵ_r to acquire gain and achieve negative refraction (as was pointed out in Fig. 8 in section 3.1.1). Path (2) requires that $\mathrm{Re}(\epsilon_r) < 0$ along the way through the second and third quadrants.

This therefore shows that the question of how to make $\mathrm{Re}(\epsilon_r) < 0$ is related to the question of making $\mathrm{Re}(n) < 0$. One can set up an equivalent equation for ϵ_r as that of (28) by once again using the Kramers-Kronig relation (24) in section 2, and replacing $\chi(\nu)$ with $[\epsilon_r(\nu) - 1]$. This gives:

$$\mathrm{Re}\ \epsilon_r(\nu_{\mathrm{obs}}) = 1 - \frac{2}{\pi}\int_0^{\omega_1} \frac{\mathrm{Im}\ \epsilon_r(\omega)\ \omega}{\nu_{\mathrm{obs}}^2 - \omega^2} d\omega + \frac{2}{\pi}\int_{\omega_2}^{\infty} \frac{\mathrm{Im}\ \epsilon_r(\omega)\ \omega}{\omega^2 - \nu_{\mathrm{obs}}^2} d\omega \quad (34)$$

Hence, in order to achieve $\mathrm{Re}(\epsilon_r) < 0$ the same possibilities (i) and (ii) given earlier for n, apply for making $\mathrm{Re}(\epsilon_r) < 0$ as well. These therefore become necessary, though not sufficient, requirements for achieving $\mathrm{Re}(n) < 0$.

One is therefore left with the following result: In order to achieve negative refraction one must require that $\mathrm{Re}(\epsilon_r) < 0$ prior to the onset of negative refraction through the possible routes (i) and (ii) (regarding ϵ_r rather than n) identified earlier. It is also known that ϵ_r must be chosen so that n achieves the same possible routes (i) and (ii) (regarding n). However, from these Kramers-Kronig considerations it still remains unclear *exactly* how to make $\mathrm{Re}(n) < 0$ on the basis of how one chooses ϵ_r. The next section will pursue this further.

4 Considerations by rational functions

Seeking to concretize the concepts presented in section 3.1, and gain a better understanding of their consequences towards ϵ_r, this section will construct response functions in terms of rational functions towards the end of achieving negative refraction. The concepts stemming from the complex plane of ϵ_r and causality arguments will hence be given a more concrete appearance in terms of zeros and poles in the complex frequency plane. Rational functions, consisting of polynomials, are capable of describing a wide range of possible responses, since most functions can be approximated by a Taylor polynomial within a bandwidth. By using rational functions for the purpose of investigation, this part therefore looks very generally upon what is possible theoretically.

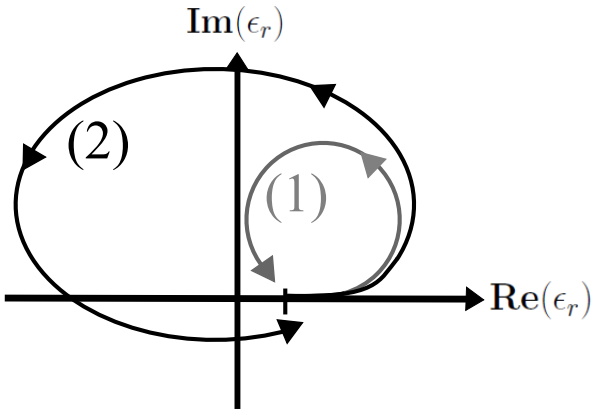

Figure 14: Two possible paths of ϵ_r. Only (2) makes $\mathrm{Re}(\epsilon_r) < 0$, which is a necessary requirement for achieving negative refraction.

4.1 Rational functions

A rational function is any function that can be written as a ratio of two polynomial functions. From the considerations on causality and the Kramers-Kronig relations in section 2, it is known that the rational function describing ϵ_r must obey:

1. $\epsilon_r \to 1$ for $\nu \to \pm\infty$
2. $\epsilon_r(-\nu) = \epsilon_r^*(\nu^*)$
3. No zeros or poles of ϵ_r in the upper complex half-plane.

Therefore, the rational functions obeying causality will have the following form:

$$\epsilon_r = \frac{(\nu-\nu_{01})(\nu-\nu_{02})...(\nu+\nu_{0k})(\nu+\nu_{01}^*)(\nu+\nu_{02}^*)...(\nu+\nu_{0k}^*)}{(\nu-\nu_{p1})(\nu-\nu_{p2})...(\nu+\nu_{pk})(\nu+\nu_{p1}^*)(\nu+\nu_{p2}^*)...(\nu+\nu_{pk}^*)} \quad (35)$$

This form will now be explained. Here both numerator and denominator are written in the factorized form. The factors of the numerator are termed *zeros* and these occur at complex frequencies $\nu_{01}, \nu_{02}, ...$ The factors of the denominator are termed *poles* and occur at complex frequencies $\nu_{p1}, \nu_{p2}, ...$ Zeros have the property that

$$\lim_{\nu\to\nu_0} \epsilon_r = 0 \quad (36)$$

Here ν_0 is the complex frequency of any zero. Poles have the property that

$$\lim_{\nu\to\nu_p} |\epsilon_r| = \infty \quad (37)$$

Here ν_p is the complex frequency of any pole. One observes that there are equally many zeros as poles in (35) in order to fulfill causality

requirement 1. It is convenient, therefore, to group them into pairs: (ν_{01}, ν_{p1}), $(\nu_{02}, \nu_{p2}), ..., (\nu_{0k}, \nu_{pk})$. Throughout this thesis such a zero-pole pair will often be referred to by the acronym ZPP. Likewise, one observes that each ZPP has a negative frequency counterpart: (ν_{01}^*, ν_{p1}^*), $(\nu_{02}^*, \nu_{p2}^*), ..., (\nu_{0k}^*, \nu_{pk}^*)$ in order to fulfill causality requirement 2. In order to fulfill causality requirement 3, one must choose zeros and poles so that $\mathrm{Im}(\nu_{01})$, $\mathrm{Im}(\nu_{02})$,..., $\mathrm{Im}(\nu_{0k}) < 0$ and $\mathrm{Im}(\nu_{p1})$, $\mathrm{Im}(\nu_{p2})$,..., $\mathrm{Im}(\nu_{pk}) < 0$. That is, placing them in the lower complex half-plane.

If one is interested in the response ϵ_r for frequencies in vicinity of the ZPPs (ν_{01}, ν_{p1}), $(\nu_{02}, \nu_{p2}), ..., (\nu_{0k}, \nu_{pk})$, and these are placed far from their complex counterparts in the complex frequency plane, one can simplify expression (35) by a *rotating wave approximation* and neglect the terms including the conjugated zero and pole frequencies. One is then left with:

$$\epsilon_r \approx \frac{(\nu - \nu_{01})(\nu - \nu_{02})...(\nu - \nu_{0k})}{(\nu - \nu_{p1})(\nu - \nu_{p2})...(\nu - \nu_{pk})} \tag{38}$$

This approximation will be used frequently in the following discussions.

4.2 Concepts

How do the placement of zeros and poles in the complex frequency plane affect the dielectric function ϵ_r in (35)? This section will present concepts necessary for answering this question. The effect upon the *phase* θ_ϵ will be considered first, before considering the effect upon the *magnitude* $|\epsilon_r|$, and then finally the effect upon the *steepness* of ϵ_r.

4.2.1 Phase θ_ϵ

How does the phase of ϵ_r as given by (35) depend on the positioning of the zeros and poles? The overall phase of ϵ_r may be expressed as

$$\theta_\epsilon \equiv \arg \epsilon_r = \arg N(\nu) - \arg D(\nu) \tag{39}$$

where $N(\nu)$ and $D(\nu)$ represent the numerator and denominator polynomials in (35), respectively. One may express $\arg\ N(\nu)$ and $\arg\ D(\nu)$ as

$$\begin{aligned} \arg N\ (\nu) &= \arg(\nu - \nu_{01}) + \arg(\nu - \nu_{02}) + ... + \arg(\nu - \nu_{0k}) \\ \arg D\ (\nu) &= \arg(\nu - \nu_{p1}) + \arg(\nu - \nu_{p2}) + ... + \arg(\nu - \nu_{p3}) \end{aligned} \tag{40}$$

The question therefore boils down to how e.g. the phases $\arg(\nu - \nu_{01})$, $\arg(\nu - \nu_{02})$ and $\arg(\nu - \nu_{p1})$, $\arg(\nu - \nu_{p2})$ depend on the positions of ν and the ZPPs. Fig. 15a displays a complex frequency plane in which two zeros, ν_{01}, ν_{02}, and two poles, ν_{p1}, ν_{p2}, are placed, as well as a observation frequency ν_{obs}. Within such a plot the phase $\arg(\nu_{\mathrm{obs}} - \nu_{01})$ may be graphically interpreted as the angle θ_{01}. Likewise the phase $\arg(\nu_{\mathrm{obs}} - \nu_{p1})$ may be graphically interpreted as the angle θ_{p1}. The

overall phase θ_ϵ can by (39) and (40) then be interpreted as the sum of all zero angles θ_{01}, θ_{02} minus all the pole angles θ_{p2}, θ_{p2}:

$$\theta_\epsilon = \theta_{01} + \theta_{02} - \theta_{p1} - \theta_{p2} \tag{41}$$

One may rearrange this and define $\theta_{\epsilon 1}$ and $\theta_{\epsilon 2}$:

$$\theta_\epsilon = \underbrace{\theta_{01} - \theta_{p1}}_{\theta_{\epsilon 1}} + \underbrace{\theta_{02} - \theta_{p2}}_{\theta_{\epsilon 2}} \tag{42}$$

Hence the overall phase θ_ϵ of ϵ_r may be expressed as the sum of the individual phase differences of the zero-pole pairs:

$$\theta_\epsilon = \theta_{\epsilon 1} + \theta_{\epsilon 2} \tag{43}$$

This has a nice graphical interpretation in Fig. 15a which displays $\theta_{\epsilon 1}$ and $\theta_{\epsilon 2}$ as blue angles in triangles set up by the ZPPs and the observation frequency.

The expressions (41) and (43) hence provide two complementary ways in analyzing the phase θ_ϵ in the complex plane. For instance, consider what happens to θ_ϵ as $\nu_{\text{obs}} \to \pm\infty$: In the first case one understands that all of the red angles in Fig. 15a become equal and therefore cancel in (41) giving $\theta_\epsilon = 0$, and in the second case one understands that all the blue angles become zero thereby making the sum (43) zero.

How do the positions of the ZPPs lead to the polar path of ϵ_r in Fig. 15b? It is clear that the phase θ_ϵ at every point along the path is given by the phase θ_ϵ from (41) and (43) in Fig. 15a. Similarly one may observe how this translates into the frequency response of ϵ_r in Fig. 15c.

4.2.2 The magnitude of $|\epsilon_r|$

Without any magnitude, there would be no polar path or any frequency response to display in Fig. 15. How is $|\epsilon_r|$ influenced by ZPP placements? For a single ZPP one may express from (38):

$$|\epsilon_r(\nu_{\text{obs}})| = \frac{|\nu_{\text{obs}} - \nu_0|}{|\nu_{\text{obs}} - \nu_p|} \tag{44}$$

The magnitude at a given observation frequency ν_{obs} is therefore given by the ratio of the distances from ν_{obs} to ν_0 and to ν_p. Fig. 16a and in Fig. 16c display two ways of increasing this ratio: Either by moving the zero and pole horizontally further apart, or by moving both zero and pole vertically closer to the real frequency axis. In order to describe these possibilities, consider first Fig. 17. Here the ZPP outlines a right angled triangle and one may express (44) as:

$$|\epsilon_r(\nu_{\text{obs}})| = \frac{d_z}{d_p} \tag{45}$$

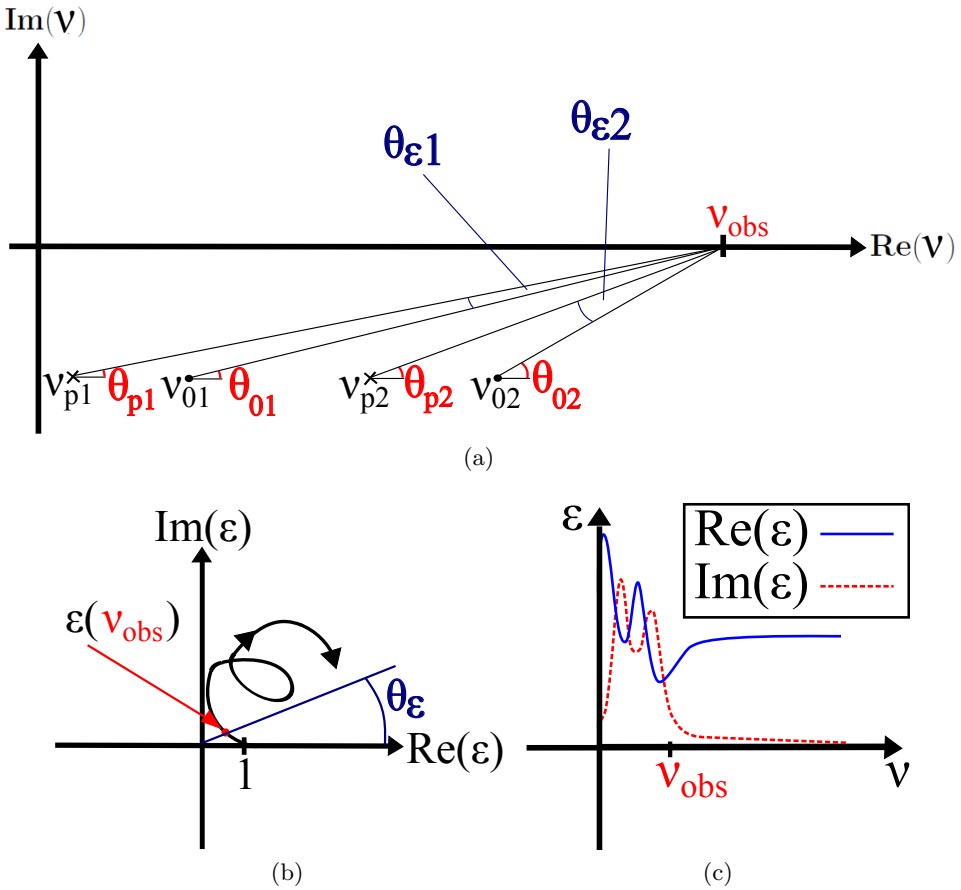

Figure 15: (a) The positions of the ZPPs, and the angles they set up with ν_{obs}. Here the crosses represent the poles and the dots represent zeros. (b) Displays the corresponding polar path of ϵ_r which starts at $\epsilon_r = 1$ for $\nu \to \infty$ and moves according to the designated direction as the frequency is moved down towards $\nu = 0$. (c) Presents the corresponding frequency response of ϵ_r.

Here d_z and d_p are the distances from ν_{obs} to ν_0, and ν_{obs} to ν_p respectively. By Pythagoras' theorem one has $d_z^2 = d_p^2 + d^2$, where d is the distance between the zero and pole. Therefore one may write:

$$|\epsilon_r(\nu_{\text{obs}})|^2 = \frac{d_p^2 + d^2}{d_p^2} = 1 + \frac{d^2}{d_p^2} \tag{46}$$

This expression is helpful in understanding the effects of moving the zeros and poles in Fig. 16. Firstly, consider making the distance between zero and poles larger as in Fig. 16a. This corresponds with making d larger in (46), which thereby makes $|\epsilon_r|$ larger at ν_{obs} as is observed in Fig. 16b. Similarly, moving the ZPP closer to the real frequency axis as is shown in Fig. 16c corresponds with making d_p smaller in (46), which also makes $|\epsilon_r|$ larger as is displayed in Fig. 16d.

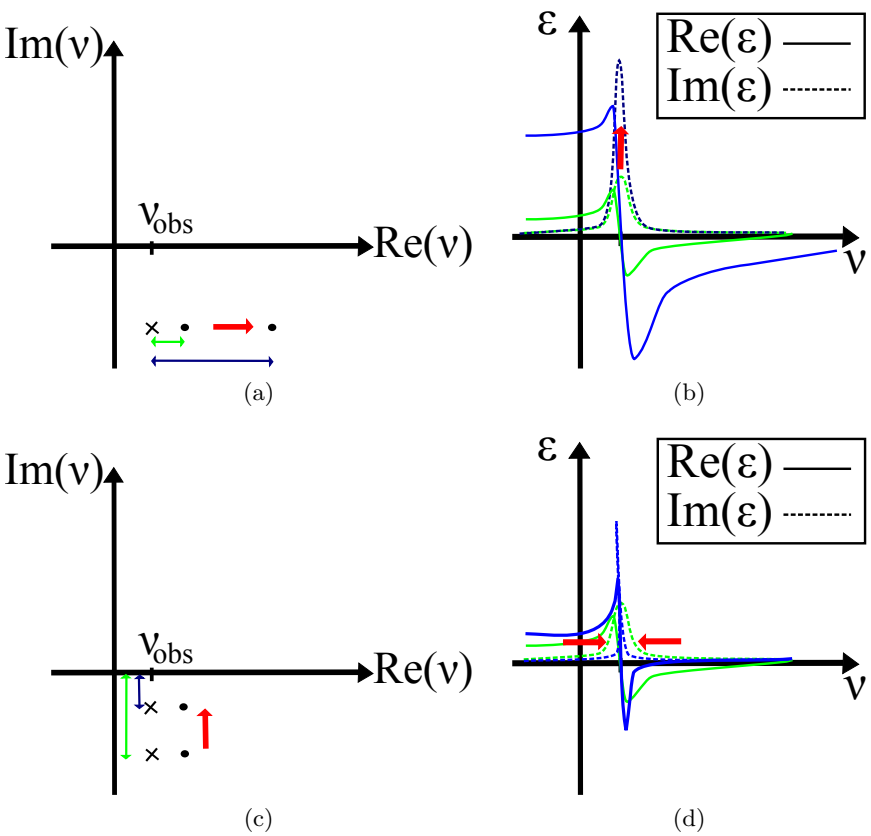

Figure 16: Displaying two different ways of altering the magnitude $|\epsilon_r|$ in terms of zero-pole movements. Zeros are represented by dots, and poles by crosses. The color green signifies the status before the change is made, whereas blue signifies the status afterwards.

Notice what happens if one should place the zero on top of the

pole in (46): This would correspond to setting $d = 0$, thereby making $|\epsilon_r| = 1$. This is consistent with the rational expression of (38) and (44), as the numerator and denominator cancel in this case.

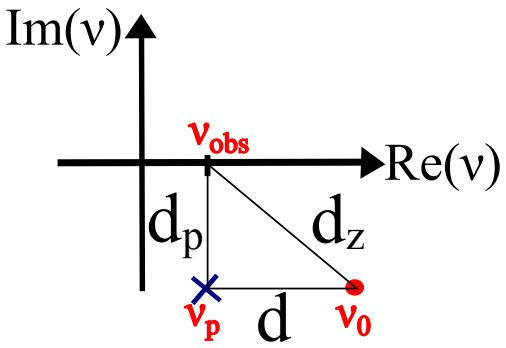

Figure 17: Schematic diagram behind (46) and (47).

4.2.3 The steepness of variation $\mathrm{d}\epsilon/\mathrm{d}\nu$

Upon comparing Fig. 16b and Fig. 16d, one observes that the movements of the ZPPs in Fig. 16a and Fig. 16c have affected the steepness of ϵ_r differently. Why is this the case? By differentiating ϵ_r of (44) and evaluating at ν_{obs} one ends up with:

$$\begin{aligned} \left|\frac{\mathrm{d}\epsilon_r}{\mathrm{d}\nu}\right|_{\nu=\nu_{\text{obs}}} &= \left\{\frac{|\nu_0 - \nu_p|}{|(\nu - \nu_p)^2|}\right\}_{\nu=\nu_{\text{obs}}} \\ &= \frac{d}{d_p^2} \end{aligned} \tag{47}$$

Here d and d_p are defined as earlier and shown in Fig. 17. Hence one sees that by making the distance from the pole to the real frequency axis smaller the steepness increases by the power of two, whereas if one increases the distance between zero and pole the steepness only increases linearly. This is the reason for the difference in shape between Fig. 16b and in Fig. 16d.

4.2.4 More zeros and poles

Most of the systems that will be discussed in this report will have more than one pair of zeros and poles in their complex frequency plane. How does one analyze such systems?

1. *Phase* θ_ϵ: Section 4.2.1 already considers the phase arising from more than one ZPP. The phases add according to (41) and (43).
2. *Magnitude* $|\epsilon_r|$: It is however clear from (38) that the magnitude

arising from each ZPP does not add, but is multiplied as shown:

$$|\epsilon_r(\nu)| = \underbrace{\frac{|\nu-\nu_{01}|}{|\nu-\nu_{p1}|}}_{\epsilon_1}\underbrace{\frac{|\nu-\nu_{02}|}{|\nu-\nu_{p2}|}}_{\epsilon_2}...\underbrace{\frac{|\nu-\nu_{0k}|}{|\nu-\nu_{pk}|}}_{\epsilon_k} \tag{48}$$

On the other hand, one can add their logarithmic magnitudes:

$$\ln|\epsilon_r(\nu)| = \ln\epsilon_1 + \ln\epsilon_2 + ... + \ln\epsilon_k \tag{49}$$

Here $\epsilon_1, \epsilon_2, ..., \epsilon_k$ are represent the identified terms in (48). Though it is not possible to sum the magnitudes, under certain circumstances it is possible to consider the magnitude arising from each ZPP independent of each other: Assume that the distance between each ZPP is much larger than the distance between each zero and pole in each ZPP. Under these circumstances in (48), if for instance ν is close to ν_{02} and ν_{p2}, then one has:

$$|\epsilon_r(\nu)| \approx \underbrace{\frac{|\nu-\nu_{02}|}{|\nu-\nu_{p2}|}}_{\epsilon_2} \tag{50}$$

This is because $\epsilon_1, \epsilon_3, \epsilon_4...\epsilon_k \to 1$ in (48) because ν is large compared to the distance between the zeros and poles in the pairs (ν_{01}, ν_{p1}), (ν_{03}, ν_{p3}), (ν_{04}, ν_{p4}), ..., (ν_{0k}, ν_{pk}).

3. *Steepness* $d\epsilon_r/d\nu$: Attempting to differentiate (38) becomes complicated when there are many zeros and poles present. However, following the argument leading to (50), it is clear that under the condition that the distance between zero and pole in each ZPP is much smaller than the distance between ZPPs, one may attribute (47) to each ZPP in order to estimate the steepness for real frequencies in their vicinity.

4.3 Desired response characteristics

The required concepts needed to analyze the complex frequency plane have now been presented and discussed. These will prove essential towards constructing responses with negative refraction and low gain. However, what exactly is desired? For example, what is meant by *low gain*? Before setting out on constructing responses, it is therefore useful to define some *figures of merit* which can help in comparing and evaluating the *quality* of the responses achieved.

a **Figure of merit 1: Low loss at negative refraction**

$$\text{large} \quad \left|\frac{-\text{Re}(n)}{\text{Im}(n)}\right| \tag{51}$$

One is interested in obtaining a large value of $|\text{Re}(n) < 0|$ simultaneously with a small value of $|\text{Im}(n)|$. Suggested realizations

in literature often have a large $\mathrm{Im}(n) > 0$ which lead to significant attenuation of electromagnetic waves within the medium at this frequency, and is therefore not wanted. An exceptional case would be if $\mathrm{Re}(n) \approx -1$ while $\mathrm{Im}(n) \approx 0$ as is the case in Fig. 12b in section 3.2.2.

b **Figure of merit 2: Low gain in ϵ_r**

$$\text{small} \quad |\max\{-\mathrm{Im}(\epsilon_r)\}| \tag{52}$$

In order to do well on this figure of merit, the amount of gain present in ϵ_r should be low. This is desired because significant amounts of gain pose stability issues, as well as it is difficult to achieve large gain at optical frequencies. An exceptional case would be if $\mathrm{Re}(n) \approx -1$ for arbitrary small gain as is the case in Fig. 13 in section 3.2.2

In order to do well on these figures of merit, the polar path of ϵ_r should move around the origin in the complex plane and almost enclose an elliptical or circular path such as in Fig. 9c and Fig. 9d in section 3.1: By achieving $\theta_\epsilon \approx 2\pi$, one is able to get negative refraction with $\mathrm{Im}(n) = 0$ as discussed in section 3.1.2. The polar path of ϵ_r should be kept near to the real frequency axis while passing through the third and fourth quadrants to minimize the amount of gain needed.

4.4 Attempting to construct negative refraction

Having now outlined the relevant concepts and the requirements in terms of the figures of merits, this section will attempt to construct desirable responses for ϵ_r by the placement of zeros and poles.

4.4.1 Fig. 18a

As a first attempt, a single ZPP in the complex plane shall be considered. This is displayed in Fig. 18a. In order to achieve a polar path of ϵ_r that moves far around the origin, the goal is therefore to make $\theta_\epsilon(\nu_{\text{obs}}) \approx 2\pi$. However, viewing the figure, it is obvious that the angle θ_ϵ will never become larger than π as long as one only has one zero-pole pair. It is therefore actually not possible to achieve negative refraction at all since this requires at least $\theta_\epsilon > \pi$. One should therefore leave this system and move on to the next.

4.4.2 Fig. 18b

Consider Fig. 18b: Ignoring the red crosses initially, one observes in this figure that there has been added N zeros and N poles in the complex plane at the position of the black dot and black cross, respectively. The multiplicity of zeros and poles at each position is indicated by the N placed aside them. Now, since each ZPP contributes to the total phase at ν_{obs} according to (43) in section 4.2, one has that the phase angle at the observation frequency becomes:

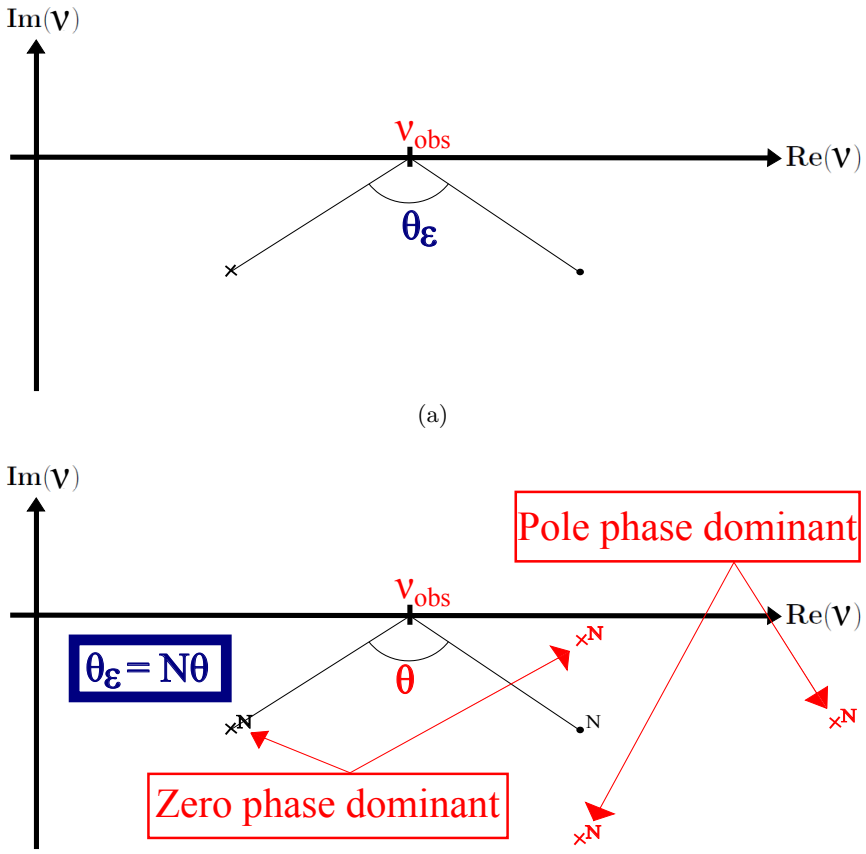

Figure 18: Suggested ZPP placements in the complex frequency plane for evaluating different configurations towards the achievement of negative refraction: (a) One ZPP. (b) Multiple ZPPs where four alternative pole positions have been suggested.

$$\theta_\epsilon = N\theta \tag{53}$$

In order to achieve enough phase angle, therefore, one can simply add a sufficient number of zero-pole-pairs in order that $\theta_\epsilon = N\theta \to 2\pi$. I.e. in the previous system of Fig. 18a, if one had placed two zero-pole pairs where the displayed ones are, one would achieve about $\theta_\epsilon \approx 4\pi/3$. Being larger than π this would enable negative refraction, however being less than 2π one would have $\mathrm{Im}(\nu) > 0$ leading to attenuation and a poor figure of merit. This could be improved by simply adding another ZPP in order to increase the phase θ_ϵ even more.

As it is thereby clear that it is possible to achieve enough phase, one should now ask where to place the zeros and poles so as to do well on the figures of merit defined in the previous section. Consider again Fig. 18b now regarding the red crosses. These represent alternative

pole positions. The goal is now to determine whether any of the four possible pole positions displayed are good with respect to achieving the desired characteristics of the responses ϵ_r and n.

Recalling (42) from section 4.2, one may also express the phase of ϵ_r as:

$$\theta_\epsilon = N(\theta_0 - \theta_p) \tag{54}$$

Here the angles θ_0 and θ_p are defined in the same way as the red angles in Fig. 15a of section 4.2.1: The vector angle from the zero or pole to the observation frequency, respectively. Firstly, consider the two bottom-right pole positions (indicated by the text *Pole phase dominant*). It is clear that for these placements one has $\theta_0 < \theta_p$. That is, one may say that the pole phases are dominant. Starting at $\nu \to \infty$ and moving down to $\nu = 0$, it is clear that the polar path of ϵ_r arising from these pole-placements will move clockwise from $\epsilon_r = 1$ at $\theta_\epsilon = 0$ through the lower complex plane, hence leading to gain. In addition, $|\epsilon_r|$ will become large when the frequency ν is in vicinity of the poles, thereby making the gain considerable. These positions are therefore not desirable.

The two remaining possibilities for placing the poles are the black and the red crosses above and to the left of the zero (indicated by the text *Zero phase dominant*). For these one has $\theta_0 > \theta_p$, and one may say that the zeros are the dominant phase. If N in (54) is chosen so that $0 \leq |\theta_\epsilon| < \pi$ for all frequencies, then the response will simply remain passive and no negative refraction will occur. However, if N is chosen so that $|\theta_\epsilon| > \pi$ when moving from $\nu \to \infty$ through $\nu = 0$ and to $\nu \to -\infty$, negative refraction will occur, and must necessarily lead to gain. The problem here becomes a trade-off between gain and phase θ_ϵ: Considering the black cross pole position, one may achieve a larger phase θ_ϵ by either (i) increasing the distance between zeros and poles, (ii) by moving the ZPPs closer to the real frequency axis, or (iii) by adding more ZPPs. However, as was outlined in section 4.2.2, (i) and (ii) are the exact same ways in which one can make the magnitude $|\epsilon_r|$ larger. Possibility (iii) will also make the magnitude larger, as this means adding more terms to the expression (38) for ϵ_r in section 4.1. Therefore, as $|\epsilon_r|$ becomes larger in general, the amount of gain will also increase. Therefore, in attempting to achieve a larger phase θ_ϵ, which is beneficial towards achieving $\mathrm{Re}(n) < 0$, one must accept more gain. In Appendix A several plots are presented to substantiate the arguments presented here.

So what does this analysis result in? Is it possible to achieve negative refraction with low gain in non-magnetic materials that meet the desired characteristics from the previous section? This section has presented some of the obstacles one faces in attempting to achieve this. One may divide them into the following:

1. **Poles:** The presence of poles are the cause of significant contributions to gain. Unfortunately, as a consequence of causality one must require an equal number of poles as zeros, and it is not clear where one should place them with respect to achieving negative refraction with a good figure of merit.

2. **Phase:** It seems that achieving a large enough phase θ_ϵ and having a low amount of gain are competing goals.

Based upon these considerations, therefore, it is not clear how negative refraction with low gain can be achieved, or if it can be achieved at all. By saying this, however, it becomes clear that this analysis has failed to account for at least one configuration: The NIES system discussed in section 3.2 (Fig. 12 and Fig. 13) from [6] does indeed display negative refraction with arbitrarily low gain simultaneously as doing well on the figures of merit defined in section 4.3. How is this then achieved? As discussed in section 3.2, this system was said to achieve negative refraction through steep variation. The question therefore becomes, what does this steepness look like in the complex frequency plane? In the following section, this steep variation medium will be investigated in the hope of understanding how its favorable characteristics emerge.

4.5 What does steepness look like in the complex plane?

It has been shown in section 3.2 that the NIES system from [6] achieves all the desired properties outlined in section 4.3 though with the necessity of steep variation: Negative refraction with arbitrarily low gain in ϵ_r and $\mathrm{Im}(n) = 0$ at the negative index frequency. The goal of this section is to analyze how this occurs in terms of the zero-pole positioning in the complex plane.

In order to do this, the expression of n will be factored. As was stated in section 3.2.2 n may be written as a sum of Lorentzians:

$$n = 1 + \alpha\left(\int_0^{\omega_1} \frac{\omega_0^2}{\omega_0^2 - \nu^2 - i\nu\Gamma} d\omega_0\right) \approx 1 + \sum_{\omega_0} \frac{\alpha\omega_0^2}{\omega_0^2 - \nu^2 - i\nu\Gamma} \quad (55)$$

The parameters ω_0 and Γ represent the resonance frequency and the width of the Lorentzian functions, respectively. α is a normalization parameter with units Hz^{-1}, and ω_1 is the frequency at which the sharp drop in $\mathrm{Im}(n)$ occurs. In Fig. 19 one has used (55) to plot n for $\Gamma = 0.01$, and ϵ_r in Fig. 19a has been found by squaring n.

The plot in Fig. 19 does not lead to a smooth curve and therefore does not sufficiently approximate the NIES response, however it is presented for further use later in the analysis of section 4.5.3. One may improve the approximation by either including more Lorentz functions in the sum (55), or alternatively by increasing the widths of each Lorentz function (at the expense of the steepness in the region of $\nu = 1$). Matlab has difficulty in factoring the polynomial expression of the sum (55) when too many Lorentzians are added, and therefore the latter option is chosen, thereby resulting in Fig. 20. Here Γ is increased from $\Gamma = 0.01$ in Fig. 19 to $\Gamma = 0.1$.

The response n may be factored after the numerator and denominator polynomials of the sum (55) have been found. A straightforward way to find these polynomials is the following: The coefficients of the

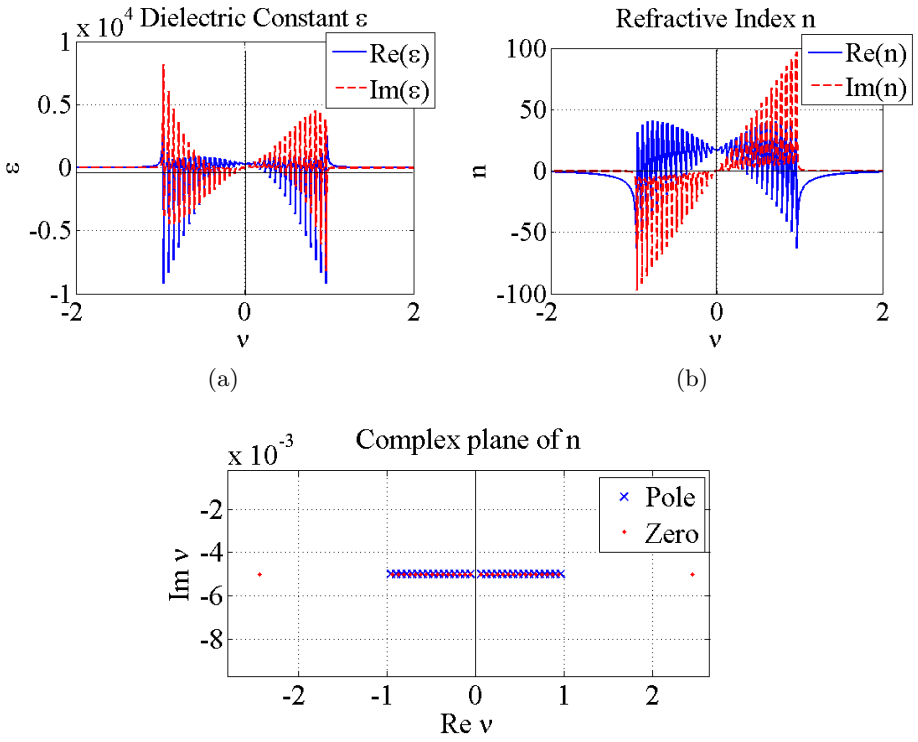

(a) (b)

(c) Complex plane: Both 19a and 19b share the same pattern, except the former has two poles/zeros on every location

Figure 19: The NIES system by (55) for $\Gamma = 0.01$.

denominator polynomial of the sum (55) are found by solving discrete convolutions of the coefficient vectors of each Lorentzian denominator polynomial, and a similar procedure is employed in finding the coefficients of the numerator polynomial of the sum. This can easily be done in e.g. Matlab, as well as factoring the resulting expression for n. The result of this is shown in Fig. 19c and Fig. 20d where the zeros and poles are displayed in the complex plane of n: They are spread out in a horizontal band along the line $\mathrm{Im}(\nu) = -\Gamma/2$. Note that contrary to earlier sections one is here dealing with the complex frequency planes of n and not of ϵ_r. However, the complex plane of ϵ_r will be identical to that of n, except that there will be two zeros and two poles at each zero-pole placement since $\epsilon_r = n^2$. The band arrangements in Fig. 19c and Fig. 20d represent a new way of placing zeros and poles that has not been considered so far in this report. It is thanks to this arrangement that this system achieves negative refraction with arbitrarily low gain. The remainder of this section will analyze n in terms of its complex plane.

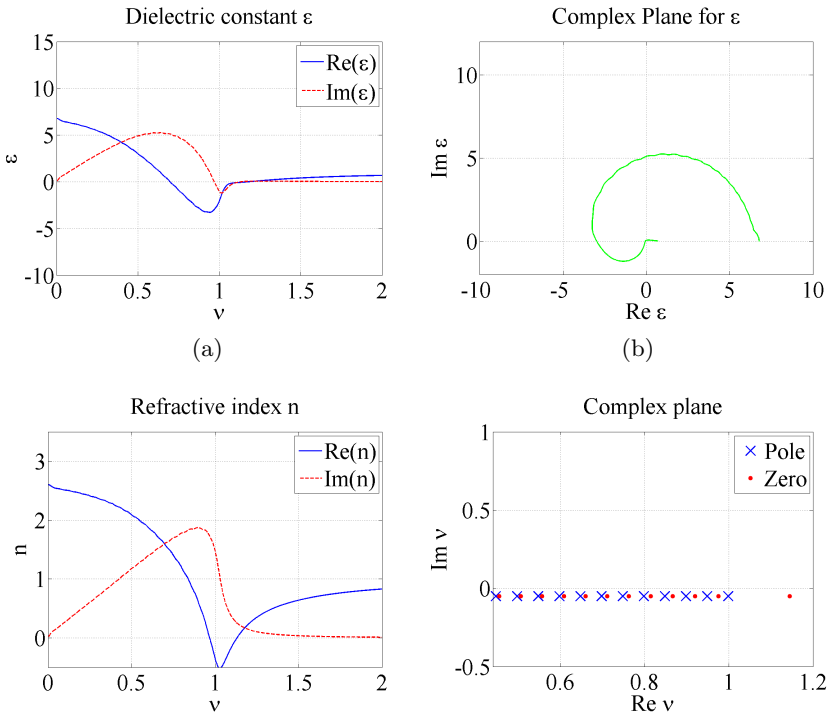

(a) (b)

(c) (d) A zoomed-in section of the complex plane of (c)

Figure 20: The NIES system by (55) for $\Gamma = 0.1$.

4.5.1 The positioning of zeros and poles

How does the positioning of the zeros and poles in this band lead to the observed response? Comparing Fig. 19b with Fig. 19c, and Fig. 20c with Fig. 20d, one observes that both $\mathrm{Im}(n)$ and the distance between ZPPs increase with frequency. Hence it seems reasonable to attribute the increase in $\mathrm{Im}(n)$ to the increased distance between zero and pole in each individual ZPP, through an increase in the resonance peak of every Lorentzian in (55). But if this is the case, why is there such an "abnormally large" distance between the zero and pole furthest to the right in Fig. 19c and Fig. 20d? Should one not then expect a much higher $\mathrm{Im}(n)$ around $\nu = 1$?

As is made clear in section 4.2.4, making the above analysis is only warranted if the distance between zero and pole in each ZPP is small compared to the distance between ZPPs. This is clearly the case for ZPPs that lie within $\nu < 0.8$ in Fig. 20d. However, for $\nu > 0.8$ one observes that the distances between zeros and poles in each pair becomes comparable to the distances between zero-pole pairs: This perhaps explains the "abnormally large" distance between zero and pole furthest to the right in Fig. 20d: That is, the positioning of this ZPP does not need to correspond with any localized feature of the

response of n in Fig. 20c. In order to test whether this analysis is valid, consider the following: What would happen if one made all the zero-pole distances in every zero-pole pair equal? One might then expect a uniform $\mathrm{Im}(n)$ with frequency. Consider Fig. 21: Fig. 21a displays a complex plane in which the distance between zero-pole pairs is small, for which $\mathrm{Im}(n)$ remains more or less uniform in Fig. 21b. On the other hand, Fig. 21c shows a complex plane where the distances between each zero and pole are large, for which the corresponding response displayed in Fig. 21d does not lead to a uniform $\mathrm{Im}(n)$ with frequency. This is therefore consistent with the analysis given: For the ZPPs in which the distance between zero and pole is small compared with the distance between ZPPs, it is clear that each ZPP may quantitatively be understood to correspond to the response $\mathrm{Im}(n)$ in vicinity of its frequency.

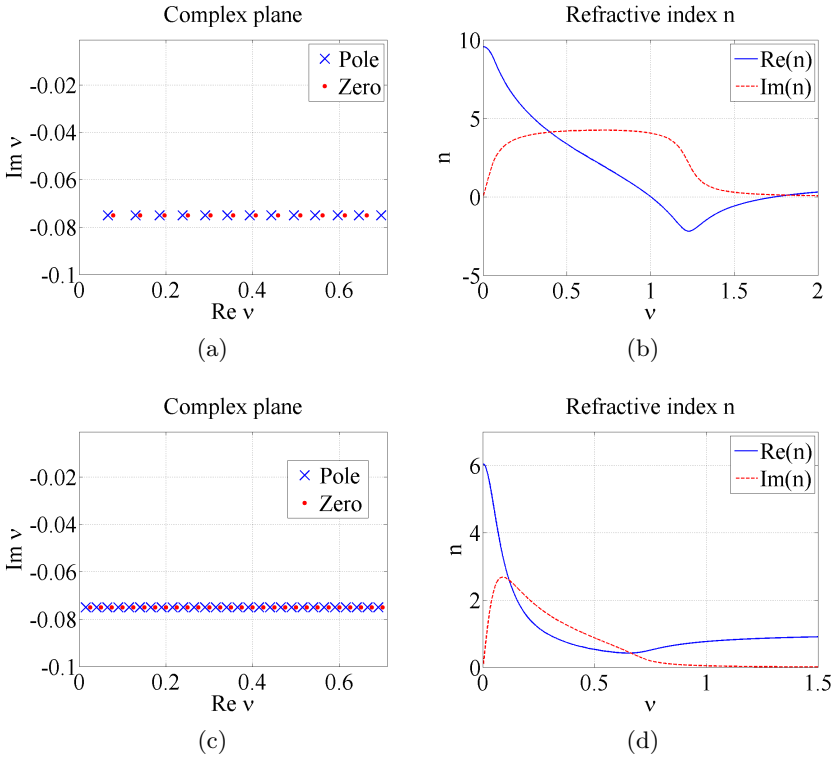

Figure 21: Testing two variants of the band arrangement displayed in Fig. 19c and Fig. 20d: (a) The distance between zero and pole in each ZPP is much smaller than the distance between ZPPs. (b) The distance between zero and pole in each ZPP is comparable to the distance between ZPPs.

4.5.2 The influence of the band

What is the influence of its arrangement of zeros and poles, and how does it contribute to allow for arbitrarily low gain in achieving negative refraction? On may divide this arrangement into two distinctive features when observing Fig. 20d:

1. *Atypical pair*: Because the ZPP furthest to the right is so atypical in comparison to the other pairs in the band, this analysis will consider this pair to be separate from the other ZPPs placed along the line $\mathrm{Im}(\nu) = -\Gamma/2$. From hereon this zero-pole pair will therefore be referred to as the *atypical pair*.
2. *Band*: The rest of the ZPPs will heron simply be referred to as the *band*. That is, from hereon the band includes all ZPPs along the line $\mathrm{Im}(\nu) = -\Gamma/2$ *except* the atypical pair.

What is the importance of this atypical pair and the band? Considering first the atypical pair, the following observation is telling: If one makes the distance between the zero and pole in the atypical pair similar to the distance between the other ZPPs near to it, it turns out that the negative refraction in Fig. 20c around $\nu = 1$ is lost. This therefore suggests that it is not the band itself that is the cause of negative refraction, but rather the atypical ZPP. Therefore, what happens if one removes the band and simply keeps the atypical pair? This is done in Fig. 22: By comparing responses in Fig. 20c and in Fig. 22c one may observe that the amount of negative refraction achieved is more or less equal. However, by comparing the polar path in the complex plane for ϵ_r in Fig. 22b with that of Fig. 20b, one observes that there is considerable more loss and gain involved without the band. This allows one to make two observations concerning the atypical pair and the band: (i) The atypical pair is the cause of negative refraction, and (ii) the band serves to lessen the amount of gain and loss present in the response.

How is it that the atypical pole and band achieve this? Firstly, again considering the atypical pair: In order that it should lead to the occurrence of negative refraction it is known that it must among other requirements acquire *enough phase*. As discussed in section 4.4 one way of achieving this is to increase the distance between zero and pole in the atypical pair. Hence, one may therefore understand the "abnormally large" distance between the zero and pole in the atypical pair as a measure to achieve enough phase to ensure negative refraction. Secondly, concerning the band, one should recall that section 4.4 identified the presence of poles as a significant obstacle towards achieving negative refraction with low gain. Hence, in Fig. 22d where there is no band present, it is the lone pole of the atypical pair that causes significant gain to occur in Fig. 22a. The band may therefore be understood as to diminish the presence of this pole. How does this occur?

Looking at the pole of the atypical pair in Fig. 20d, one notices that the zero from the neighboring ZPP in the band is close to it. It

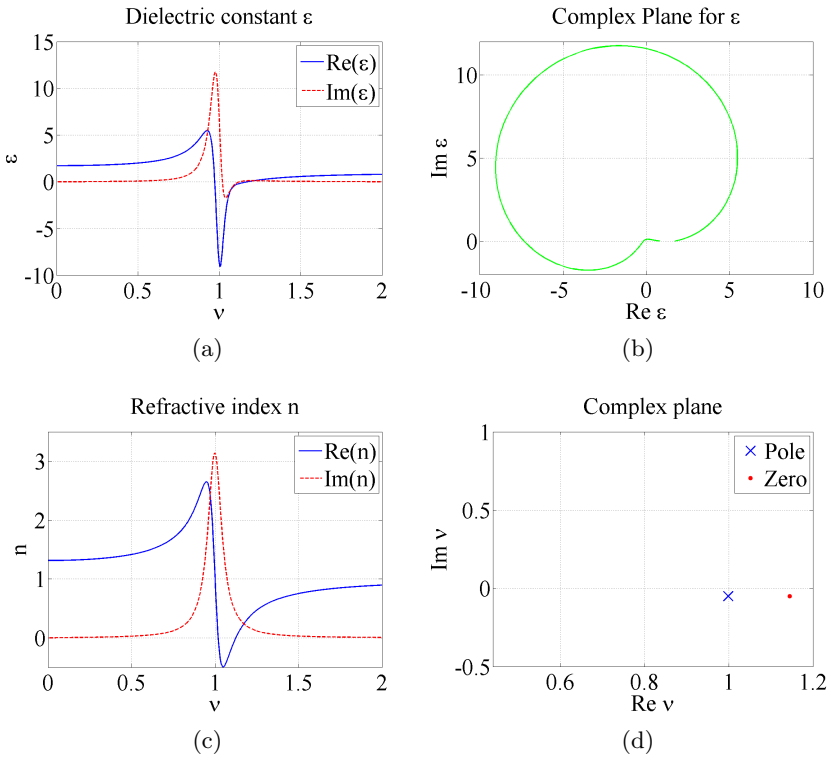

Figure 22: Removing the band of ZPPs in the NIES system. (d) Displays only the atypical pair.

is known from e.g. (46) in 4.2.2 that when a zero and pole are placed near to each other, they diminish each others presence. Hence the neighboring zero to the atypical pair serves to diminish the presence of the atypical zero. Likewise, the pole in the last ZPP of the band is close to the zero from the preceding ZPP, which serves to reduce it. And so, this diminishing effect continues along the band: The presence of the pole in the atypical pair is in a sense *smeared out* over the band. As noted concerning Fig. 20d, the distance between zeros and poles is not uniform: That is, the fact that zeros and poles are separated more at $\nu > 0.8$ this might suggest that the *smearing* is greater here.

4.5.3 Towards arbitrarily low gain

In section 3.2.2 it was shown that through making Γ, the widths of the Lorentzians in (55), small, one is able to make the drop in $\mathrm{Im}(n)$ steep enough to achieve negative refraction with arbitrarily small gain, as was exemplified in Fig. 13. How may one understand this in terms of the analysis just given? Consider Fig. 23: Here one observes two different possible arrangements of the NIES system that enable the same phase θ_ϵ, where one possibility places the band of ZPPs along

the line $\mathrm{Im}(\nu) = -\Gamma_1/2$, while the other places them along the line $\mathrm{Im}(\nu) = -\Gamma_2/2$. If one assumes that $\Gamma_1 = 0.01$ and $\Gamma_2 = 0.1$ then this corresponds to the systems of Fig. 19 and Fig. 20 respectively: It is then clear that in order to ensure that the response occurring for the arrangement at $\mathrm{Im}(n) = -\Gamma_1/2$ is smooth, one must have a higher number of ZPPs in the band, as is displayed in Fig. 23. This is because with a smaller Γ the widths of the Lorentzian functions in the sum (55) are narrower.

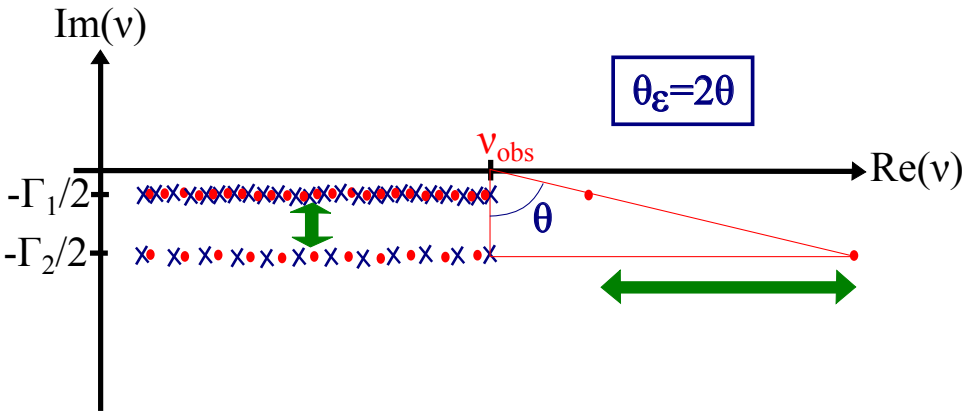

Figure 23: Two configurations of the NIES system with different Γ's displayed simultaneously. By moving the band and atypical zero up in the complex plane as shown, the distance between zero and pole is diminished leading to a reduction in the magnitude $|\epsilon_r|$ though leaving the phase θ_ϵ at ν_{obs} unchanged. This is the mechanism by which one can achieve negative refraction with arbitrarily low gain in the NIES system.

One may understand the occurrence of negative refraction at arbitrarily low gain from Fig. 23. It is observed that by making Γ smaller, the distance between zero and pole in the atypical pair can be reduced and still keep the same angle θ_ϵ. In doing this one observes that the distance between the zero and pole in the atypical pair is reduced a lot more than the distance from the ZPPs to the real frequency axis. From section 4.2.2 one thereby understands that the overall $|\epsilon_r|$ is reduced in the process. From section 4.2.3 one understands that this occurs at the cost of increased steepness. Therefore, as $\Gamma \to 0$ one has that $|\epsilon_r|$ is reduced at the cost of an increased steepness in the drop of $\mathrm{Im}(n)$.

Therefore, the secret behind arbitrarily low gain is not a consequence of the band alone, but a combination of band *and* steep variation. However, does there exist any way to achieve less gain *without* needing more steepness? Considering the arrangement located at $\mathrm{Im}(\nu) = -\Gamma_2/2$, it is clear that the larger gain of this arrangement is explained by the larger distance between zero and pole in the atypical pair. But what if one adds more ZPPs to the band: Could this increase the *smearing effect* upon the pole in the atypical pair and thereby reduce $|\epsilon_r|$? On the other hand, if it were simply the case that

the more ZPPs are placed in a band the less gain one would require, then one would expect the expression (31) of n in section 3.2.2 to not have any gain at all, because an integral of Lorentzians corresponds to an infinite number of ZPPs in the band. As this is obviously not the case, the *smearing effect* does not increase indefinitely upon addition of ZPPs. Comparing Fig. 19 and Fig. 20, it is clear that the *smearing effect* contributes as far as until the curves $\mathrm{Re}(n)$ and $\mathrm{Im}(n)$ are made smooth, but not any further than this. This is consistent with the analysis given in section 3.2.2 considering the *asymmetric drop* and the importance of the area under the $\mathrm{Im}(n)$ curve towards achieving negative refraction with arbitrarily low gain.

The consequence of this section is therefore that one observes the NIES system to achieve negative refraction at arbitrarily low gain through to both band and the steepness in the drop of $\mathrm{Im}(n)$, and that it therefore does not offer any possibility of achieving this without steepness. It therefore seems that the only possibility of achieving negative refraction with low gain in non-magnetic media occurs through demanding steepness.

4.6 What is the best achievable result without steepness?

As one observes in section 3.2.2, the steepness required for the NIES system is extreme to the extent that it is questionable whether there exists any hope of realizing such a response at all. What is then the best achievable result one may expect in a non-magnetic medium if one seeks to avoid a steep response? That is, what is the lowest amount of gain necessary to achieve negative refraction *without steepness*? Consider Fig. 24: The question one must ask is what types of polar paths in the complex plane of ϵ_r are permissible by causality. Considering that achieving sufficient phase θ_ϵ in non-magnetic media seems to be possible only either through gain or steepness, it seems one very broadly has only two possibilities: Fig. 24a and Fig. 24b both achieve $\theta_\epsilon \approx 2\pi$, the former by considerable gain and the latter through significant steepness.

Could it in fact be possible to achieve a path such as Fig. 24b without steep variation? On the basis of sections 4.4 and 4.5 it does not seem so. Therefore, assuming all routes towards achieving negative refraction without steepness must resemble Fig. 24a, this indicates the best case scenario: The circular path must have a radius $|\epsilon_r| \approx 1$ in order that $\epsilon_r \to 1$ as $\nu \to \infty$. Hence for realizations where $\mathrm{Re}(n) \approx -1$ in which steep variations are not permitted, one should expect that the the amount of gain needed to be on the order of 1. This is consistent with the known results of the Two-Component system in [5].

The Two-Component system was discussed in section 3.2.1, described by (29) and plotted in Fig. 11. Section 3.2 explains that it achieves negative refraction primarily through considerable loss below the working frequency, and does not rely upon achieving a steep response. This system may therefore be representative of the best-case

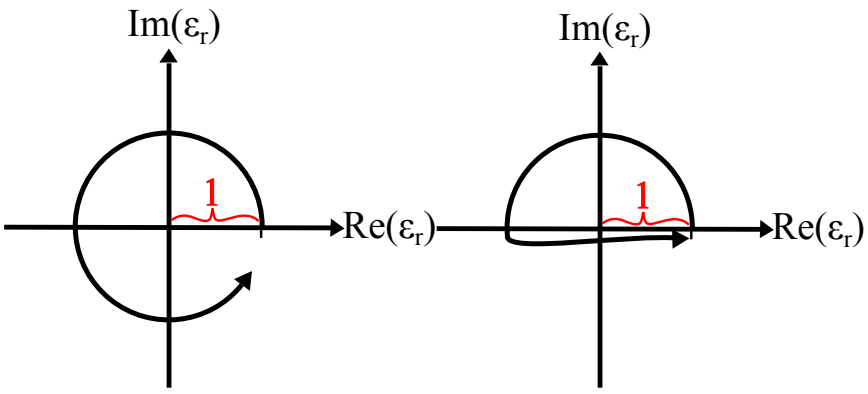

(a) Gradual variations (b) Asymmetric steep variations

Figure 24: Representing two paths to negative refraction: (a) Through significant gain and loss, (b) largely through steep variation.

one can achieve without steep variations in non-magnetic media. In order to make the analysis of this thesis complete, therefore, this system should be analyzed in the complex plane as well. The zero-pole placements in the complex frequency plane, as well as ϵ_r, n and the polar path of ϵ_r for a Two-Component medium is displayed in Fig. 25. One observes in Fig. 25d that the zeros are placed so that their phases dominate for both large and small frequencies, meaning that within these regions $|\epsilon_r|$ contributes to creating loss. It is only for frequencies around $\nu = 50$ that the pole phases dominate, for which the $|\epsilon_r|$ contributes to gain. This again occurs in the vicinity of the uppermost zero, thereby making $|\epsilon_r|$ small in this area and resulting in little gain. However, since this arrangement does not lead to a large θ_ϵ, the amount of negative refraction is also small while $\mathrm{Im}(n)$ is large. The Two-Component system therefore does badly on the figure of merits in section 4.3.

5 Electromagnetically induced transparency (EIT)

This report has so far considered the possibility of achieving negative refraction in non-magnetic media generally, and has argued that negative refraction in non-magnetic media can only be achieved with low gain if one allows for steep variations in the medium. The NIES system of section 3.2.2 has demonstrated this through an *asymmetric drop* in $\mathrm{Im}(n)$. It therefore becomes interesting to see if there exists any physical systems for which one can achieve such steep variations.

A system particularly known for its steep variation is the Electromagnetically Induced Transparency (EIT) system. Relying on atomic coherence phenomena, such systems are characteristic of having extraordinarily steep variations in their optical responses, thereby lead-

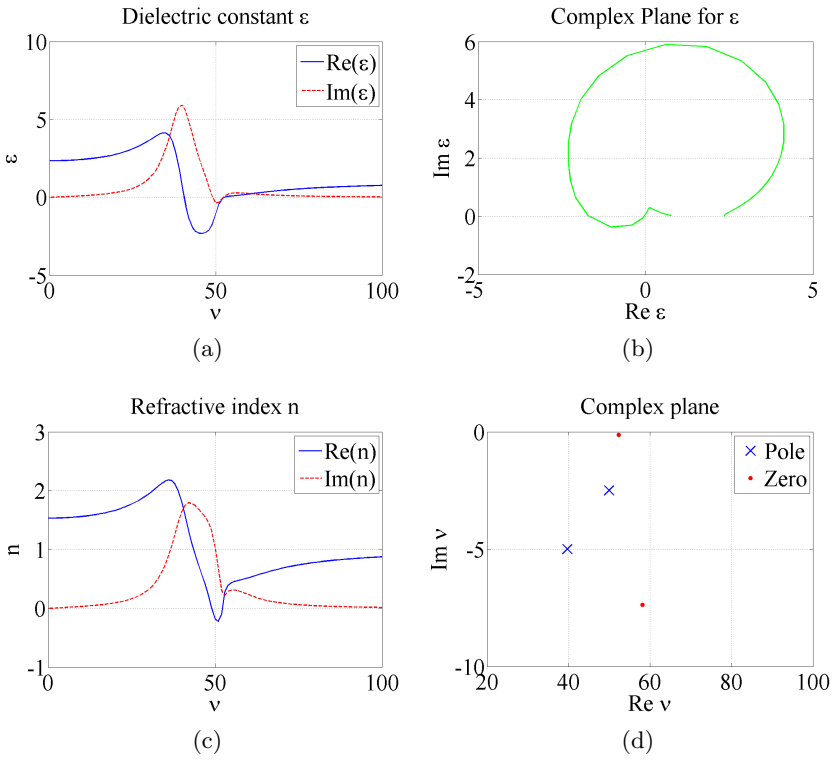

Figure 25: A two-component medium: (a) and (c) are taken from Fig. 11. (b) Displays that this system contains considerable loss, reflecting the mechanism through which negative refraction is achieved. (d) Shows the ZPP arrangement in the complex plane.

ing to effects such as ultralow group velocities ("stopping of light") and ultralarge nonlinearities [12]. For this reason, the EIT system seems a good candidate for investigation, and was also suggested for this purpose in my previous master project [11]. Indeed, as mentioned in the preface of this report, the EIT system was in fact originally the starting point of my master thesis. However, as will be argued, despite the EIT system's ability to produce steep variation, it also presents difficulties towards achieving negative refraction which in the end make the system less promising than one might have hoped for.

5.1 The model

The EIT model will be presented and derived using semiclassical theory, based upon the treatment in [13]. Consider the three level atomic system displayed in Fig. 26.

Levels $|a\rangle$ and $|c\rangle$ are coupled by a strong coherent field, whereas a weak probe field couples $|a\rangle$ to $|b\rangle$. In order to find the optical properties of the EIT system it becomes necessary to derive the dielectric

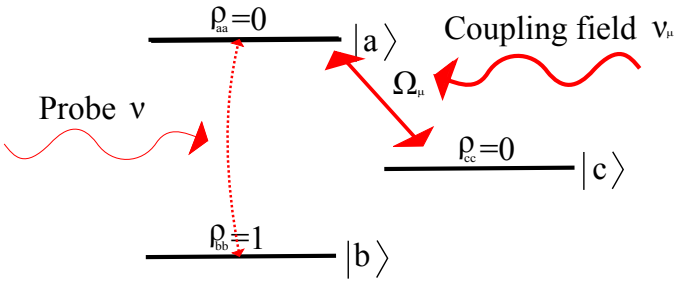

Figure 26: Three level atomic system corresponding with EIT

function $\epsilon_r(\nu)$ for the probe field. This may be expressed in terms of the electrical polarization as:

$$\epsilon_r = 1 + \chi = 1 + \frac{P_\nu(t)}{\epsilon_0 \mathcal{E} \mathrm{e}^{-i\nu t}} \tag{56}$$

Here χ is the electric susceptibility of the medium, $P_\nu(t)$ is the polarization, ϵ_0 is the permittivity of free space, $\mathcal{E}$ is the electric field amplitude, ν is frequency and t is time. The polarization may be expressed in terms of the density matrix elements of the system:

$$P(t) = e\langle\psi|\hat{x}|\psi\rangle = \wp_{ba}\rho_{ab} + \wp_{ca}\rho_{ac} + c.c. \tag{57}$$

Here e is the elementary charge, $\wp_{ba}$ and $\wp_{ca}$ are electric dipole moments corresponding to the transitions $|a\rangle \rightarrow |b\rangle$ and $|a\rangle \rightarrow |c\rangle$, and ρ_{ab} and ρ_{ac} are density matrix elements of the system. The density matrix elements may be solved by the Von Neumann equation of motion:

$$\dot{\rho} = -\frac{i}{\hbar}[\mathcal{H}, \rho] - \frac{1}{2}(\Gamma\rho + \rho\Gamma) \tag{58}$$

$\mathcal{H}$ represents the hamiltonian of the system, while Γ represents the relaxation matrix describing decay from the atomic states. One may then find for the elements ρ_{ab}, and ρ_{ab} in the density matrix:

$$\dot{\rho_{ab}} = -(\gamma_{ab} + i\omega_{ab})\rho_{ab} - \frac{i\wp_{ab}E}{\hbar}(\rho_{aa} - \rho_{bb}) + \frac{i\wp_{ac}E}{\hbar}\rho_{cb} \tag{59}$$

$$\dot{\rho_{cb}} = -(\gamma_{cb} + i\omega_{cb})\rho_{cb} - \frac{i\wp_{ab}E}{\hbar}\rho_{ca} + \frac{i\wp_{ca}E}{\hbar}\rho_{ab} \tag{60}$$

The $\gamma_{ab} = (\gamma_a + \gamma_b)/2$ and $\gamma_{cb} = (\gamma_c + \gamma_b)/2$ consist of elements from the Γ matrix and represent the decay rates from $|a\rangle$ and $|c\rangle$ to the ground state $|b\rangle$, respectively. As explained in [12, 13] one must have $\gamma_{cb} \ll \gamma_{ab}$ for EIT. The $\omega_{ab} = \omega_a - \omega_b$ and $\omega_{cb} = \omega_c - \omega_b$ are the difference in frequency between level $|a\rangle$ and $|b\rangle$, and between $|c\rangle$ and $|b\rangle$ respectively. The electric field E may be written:

$$E = \frac{\mathcal{E}}{2}(\mathrm{e}^{-i\nu t} + \mathrm{e}^{i\nu t}) + \Omega_\mu \mathrm{e}^{-i\phi_\mu}(\mathrm{e}^{-i\nu_\mu t} + \mathrm{e}^{i\nu_\mu t}) \tag{61}$$

Here $\Omega_\mu = |\wp_{ca}|\mathcal{E}_\mu/\hbar$ is the Rabi frequency of the strong coupling field with magnitude $\mathcal{E}_\mu$. Likewise, one may write $\Omega = |\wp_{ba}|\mathcal{E}/\hbar$ for the Rabi frequency of the probe field. If one assumes that the atom is initially in the ground level one may set:

$$\rho_{bb}^{(0)} = 1,\ \rho_{aa}^{(0)} = \rho_{cc}^{(0)} = \rho_{ac}^{(0)} = 0 \tag{62}$$

Furthermore, one may assume that the probe field is so weak that the population of the levels remain unaltered, therefore making ρ_{aa}, ρ_{bb} and ρ_{cc} constants with respect to time. One may likewise assume that $\rho_{ac} = \rho_{ac}^{(0)} = 0$, which allows for a simple solution to (59) and (60). Inserting (61) into (59) and (60), a *rotating wave approximation* is performed, meaning that only positive frequency terms are kept, the coupling field contributes only to the coupling transition, and the probe field contributes only to the probe transition. This gives:

$$\rho_{ab} = \frac{-i\wp_{ab}\mathcal{E}\mathrm{e}^{-i\nu t}}{2\hbar}\frac{(\gamma_{cb} + i\Delta)}{(\gamma_{ab} + i\Delta)(\gamma_{cb} + i\Delta) + \frac{\Omega_\mu^2}{4}} \tag{63}$$

The parameter Δ is the detuning, i.e. $\Delta = \omega_{ab} - \nu$. Plugging (63) into (57) and (56) gives finally:

$$\chi = \frac{i|\wp_{ab}|^2}{2\epsilon_0\hbar}\left[\frac{[\gamma_{cb} + i(\omega_{ab} - \nu)]}{[\gamma_{ab} + i(\omega_{ab} - \nu)][\gamma_{cb} + i(\omega_{ab} - \nu)] + \frac{\Omega_\mu^2}{4}}\right] \tag{64}$$

The EIT susceptibility χ is plotted in Fig. 27a, and is compared to a Lorentzian function in Fig. 27b. From this comparison, it is observed that one may interpret EIT as if it were a Lorentzian response where the absorption drops to zero at the resonance frequency. Why does this happen? As is explained in [12], there are two ways in which one can understand EIT: One in terms of a *dressed states* picture arising from a full quantization of the electric fields, and one in terms of *bare states* in the semiclassical approach. Only the latter is presented here. EIT may then be understood as an interference effect between possible transitional pathways that the system may take between states $|a\rangle$, $|b\rangle$ and $|c\rangle$. For instance, the transition $|b\rangle \to |a\rangle$ can interfere with the transition $|b\rangle \to |a\rangle \to |c\rangle \to |a\rangle$ and any higher order transitions, thereby affecting the transitional probabilities. Absorption of the probe field is canceled if these pathways interfere destructively so that there becomes no probability of transition between levels $|a\rangle$ and $|b\rangle$. In order to achieve this, the coupling field must be strong in order to make the probability amplitude of the higher order transitions large enough to cancel the probability amplitude of the $|b\rangle \to |a\rangle$ transition. The end result is that no absorption occurs at resonance as is seen in Fig. 27a.

It is due to the interference between transitional pathways that the optical response becomes so steep. This is because the absorption is only canceled at resonance, where it in fact should have been at a maximum had it not been for this interference. Therefore $\mathrm{Im}(\chi)$

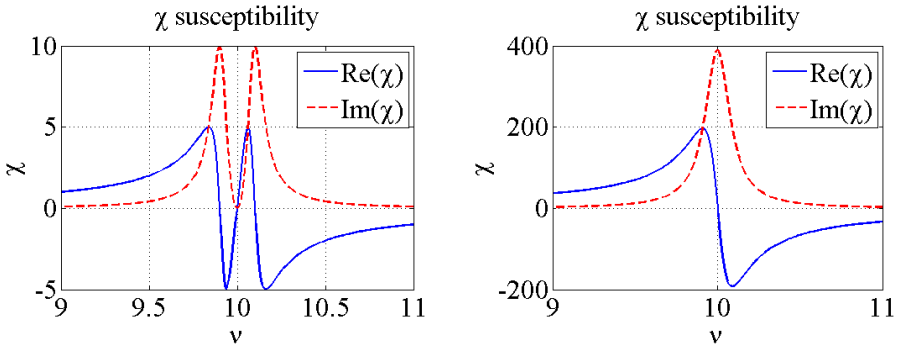

(a) Susceptibility χ (b) Lorentzian χ

Figure 27: EIT and Lorentzian responses compared.

drops very steeply around this frequency. For the purposes of achieving negative refraction, it is likely that one will need significant steepness. How does one ensure this in the EIT model? In the next section the ways in which this steepness can be controlled will be examined.

5.2 Controlling the steepness in EIT

How does one alter the steepness in the EIT response? In order to evaluate the EIT system with regards to this question it is helpful to relate the following parameters in (64) as follows: $\gamma_{cb} = \alpha\gamma_{ab}$ and $\Omega_c = \beta\gamma_{ab}$ where α and β are positive, dimensionless parameters. When this is done, one may express (64) as follows:

$$\chi = \frac{i|\wp|^2}{2\epsilon_0\hbar\gamma_{ab}} \frac{\alpha + i\frac{\Delta}{\gamma_{ab}}}{(1 + i\frac{\Delta}{\gamma_{ab}})(\alpha + i\frac{\Delta}{\gamma_{ab}}) + \frac{\beta^2}{4}} \tag{65}$$

$$= \frac{i|\wp|^2}{2\epsilon_0\hbar\gamma_{ab}} \frac{1}{(1 + i\frac{\Delta}{\gamma_{ab}}) + \frac{\beta^2}{4(\alpha + i\Delta/\gamma_{ab})}} \tag{66}$$

Once again, $\Delta = \omega_{ab} - \nu$ is the detuning of the system. It will now be considered how changing different parameters influences the response shape of χ:

1. **Lowering γ_{ab}:** This means lowering the decay rate between levels $|a\rangle$ and $|b\rangle$. The magnitude $|\chi|$ will be increased, and otherwise this has the same effect as scaling the frequency according to $\frac{\Delta}{\gamma_{ab}}$. If one normalizes χ while increasing γ_{ab}, therefore, this leads effectively to the scaling of the axes. That is, the same response shape is kept, but the response width will be decreased and sharper peaks arise. Therefore this does indeed lead to increasing the steepness of χ.
2. **Lowering γ_{cb} relative to γ_{ab}:** This means changing the relative difference between decay rates of the transitions $|c\rangle \to |b\rangle$ and

$|a\rangle \rightarrow |b\rangle$, and is described here by making α smaller. That α is small is already ensured because EIT assumes that $\gamma_{cb} \ll \gamma_{ab}$. Therefore, it is clear from (65) that making α even smaller will have little effect on the EIT response.

3. **Changing Ω_c relative to γ_{ab}:** This means changing the coupling Rabi frequency relative to the decay rate between levels $|a\rangle$ and $|b\rangle$, and is described here by altering β. What happens as one changes β? It will now be showed that this changes the distance between the two peaks in $\mathrm{Im}(\chi)$ surrounding the resonance in Fig. 27a.

   Firstly, assuming that β is large, one may calculate that the peaks occur at frequencies $\nu = \omega_{ab} \pm \gamma_{ab}\sqrt{\alpha + \frac{\beta^2}{4}} \approx \omega_{ab} \pm \gamma_{ab}\frac{\beta}{2}$ having assumed that $\beta \gg \alpha$. One may now show that as β becomes large, the two peaks become two separate Lorentz responses: If one evaluates (66) close to the right resonance peak in $\mathrm{Im}(\chi)$ at frequency $\Delta = \kappa' + \gamma_{ab}\frac{\beta}{2} = \gamma_{ab}(\kappa + \frac{\beta}{2})$ (the κ's here representing a slight shift in frequency from resonance), one finds:

$$\chi_{ab} = \frac{i|\wp|^2}{2\epsilon_0\hbar\gamma_{ab}} \frac{1}{1 + i(\kappa + \frac{\beta}{2}) + \underbrace{\frac{\beta^2}{4\alpha + i(\kappa + \frac{\beta}{2})}}_{\approx i2\beta, \quad \beta \gg \kappa, \alpha}} \tag{67}$$

$$= \frac{i|\wp|^2}{2\epsilon_0\hbar\gamma_{ab}} \frac{1}{1 + i\kappa}, \quad (\kappa = \gamma_{ab}\kappa') \tag{68}$$

   One may observe from (68), that the response around the peak frequency does not depend on β and therefore neither does its steepness. Interestingly, (68) shows that the response shape around the resonance peak displays a Lorentzian behavior. This is verified in Fig. 28a where the EIT response is plotted for a large value of Ω_c, setting $\beta = 60$. Therefore, as β becomes large the EIT response becomes two separated Lorentzian functions whose widths are determined by γ_{ab}. The EIT system then acts as if it were two separate Lorentzian functions, and if γ_{ab} is small these will be narrow. One may thereby achieve a steep variation around the peaks in this configuration.

   But what if β is made small instead? One may imagine the effect of this as though moving the two Lorentzian peaks in Fig. 28a towards each other so that they start overlapping. However, at $\nu = 10$ ($\Delta = 0$ in (66)) absorption will nevertheless be canceled due to the interference effect of the levels, and so one ends up with a response such as Fig. 28b. One is left with one approximately "Lorentzian" response with a sharp drop occurring around $\nu = 10$. Hence this arrangement also leads to a steep variation. If one considers only that part of the response below $\nu = 10$, one may say that this achieves an *asymmetric drop*, which therefore bears resemblance with the much discussed system in previous chapters displayed in Fig. 12 in section 3.2.2.

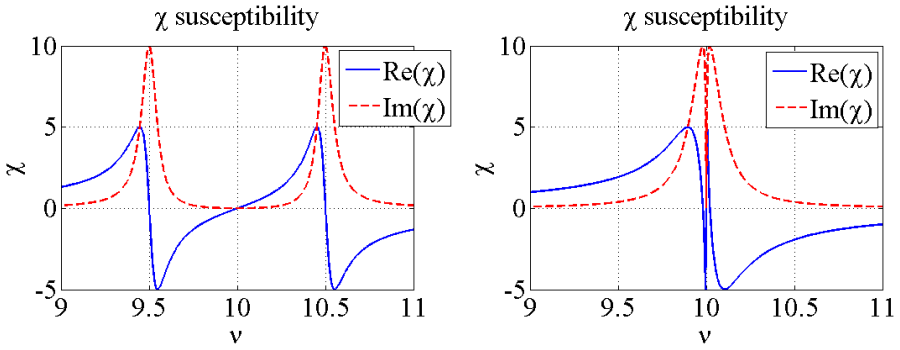

(a) Large Ω_c (b) Small Ω_c

Figure 28: Displaying the effect of changing the strength of the coupling field by varying the parameter Ω_c.

It has been shown that there exist several ways in which the EIT system may be used to cause *steep variations*. However, since one observes for example in Fig. 28a that the response shapes are Lorentzian, why not achieve the same steepness through normal Lorentzian responses instead? Why go through all the bother of setting up an EIT system? It is therefore clear that the steepness offered through an EIT system must be understood in the following way: The steep features in an EIT response are steep *in comparison* to those one could achieve by e.g. simply using Lorentzian responses. To understand this, consider Fig. 28a. It is clear that one should understand this response as a "hollowing-out" of a much wider Lorentz response due to the coherence effect. Stated otherwise: Without the coherence effect between the levels in an EIT system (i.e. if one had removed level $|c\rangle$ in Fig. 26), then instead of observing two separate Lorentzian functions in Fig. 28a, one would have one wide Lorentzian response. This means, that thanks to the EIT coherence effect, the obtainable Lorentzian responses in Fig. 28a are a lot narrower and sharper than that of a regular Lorentzian response realization.

5.3 EIT in the complex plane

Now that the EIT model has been presented and the methods of achieving steep variation in its response are known, one is ready to consider how the EIT system may be used towards achieving negative refraction. Based upon the insight offered in sections 3 and 4 with regard towards achieving negative refraction, it is useful to consider the EIT response in both the complex plane of ϵ_r and ν. This will therefore be done in this section, for which the aim is to discover possible routes through which negative refraction in the EIT response may be realized.

Fig. 29a displays the dielectric constant ϵ_r, Fig. 29c displays the refractive index n of an EIT system, and the complex plane of ϵ_r is displayed in Fig. 29b. By factoring the expression for $\epsilon_r = 1 + \chi$,

where χ is found from (64), the zeros and poles have been located and placed in the complex frequency plane, displayed in Fig. 29d. One observes in Fig. 29c that the EIT response is not able to achieve negative refraction, despite displaying steep variation. Why is this the case? Viewing the complex plane of ϵ_r in Fig. 29b it is clear that the polar path of ϵ_r never moves around the origin into the third quadrant. Comparing with Fig. 29a, this is consistent with there being *no gain* at any frequency. Considering that there is no inversion in the atomic levels of the model, displayed in Fig. 26, this is also to be expected. However, as discussed in section 3.1.1, one must require gain if one wishes to achieve negative refraction. Therefore, it is already clear that the conventional EIT response of (64) cannot permit negative refraction. Despite this, it is still worthwhile to analyze the conventional EIT system here, as the results of this will be useful when considering possible modifications to the EIT system in the next section.

Viewing the response of ϵ_r in Fig. 29a, one may analyze it in terms of the requirements discussed in section 3.2.3 stemming from the Kramers-Kronig relations. One then understands that the sharp drop in $\mathrm{Im}(\epsilon_r)$ immediately below $\nu = 10$ will contribute towards making $\mathrm{Re}(\epsilon_r) < 0$ in this region, which is indeed observed for $\nu < 10$. However, the steep rise in $\mathrm{Im}(\epsilon_r)$ immediately above $\nu = 10$ will contribute to make $\mathrm{Re}(\epsilon_r) > 0$, which indeed also is the case for $\nu > 10$. It therefore seems plausible to identify this second rise as the reason why the polar path of ϵ_r does not travel any closer towards the third quadrant in Fig. 29b than it does. This therefore suggests that the peak in $\mathrm{Im}(\epsilon_r)$ above $\nu = 10$ counteracts the achievement of negative refraction. A similar assessment can be performed upon the response of n in Fig. 29c: Here one can explain the fact that $\mathrm{Re}(n)$ does not become negative due to the steep rise in $\mathrm{Im}(n)$ immediately above $\nu = 10$. Two problems have therefore been identified: The fact that there is no gain, and that there is a sharp rise in $\mathrm{Im}(n)$ above $\nu = 10$, which is linked to the steep rise in $\mathrm{Im}(\epsilon_r)$ in the same region.

One may also analyze the situation in terms of the concepts outlined in section 4. Viewing the placement of zeros and poles in the complex frequency plane in Fig. 29d, one may ask why this arrangement does not allow for the polar path of ϵ_r to move around the origin in its complex plane, and into the third quadrant. Since $|\epsilon_r| > 0$ for all frequencies ν (both zeros lie below the real frequency axis), the answer must simply be that this arrangement does not allow for enough phase θ_ϵ. It therefore becomes interesting to ask: Is there any way in which the EIT system in the complex plane can achieve more phase at $\nu = 10$? Rather than start with a complicated process of varying the parameters of (64), one may first simply try moving the placement of zeros and poles in the complex plane a little, to observe what effect this gives. Doing this, however, means no longer treating the system as an EIT system, but rather as a general arrangement of zeros and poles. Anyhow, it is insightful to do this momentarily: Consider Fig. 30. Here it is observed that if one moves the uppermost zero in the plane a little towards the right, then the phase angle of this zero in-

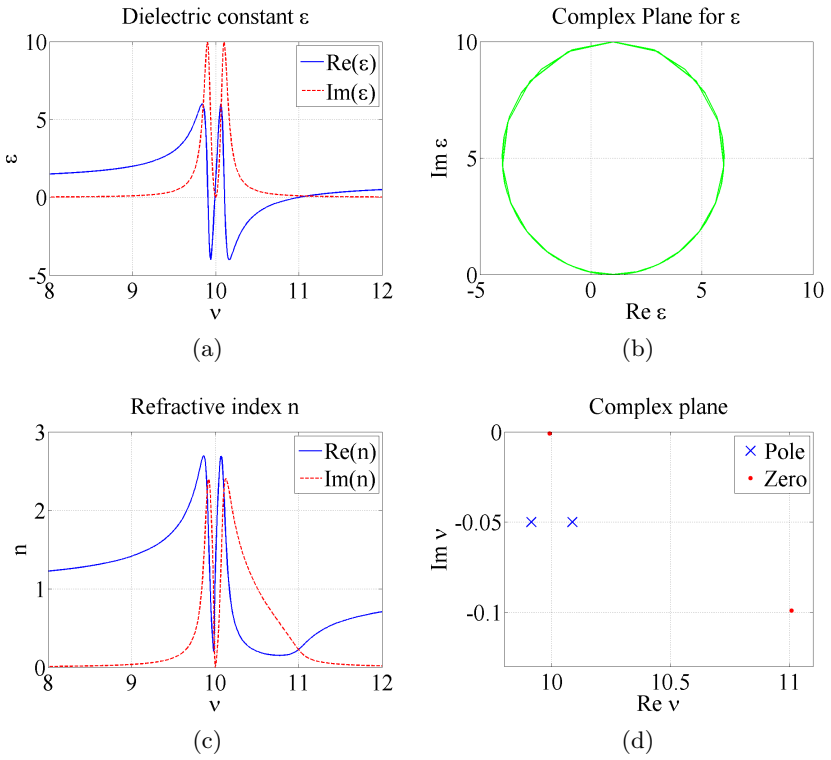

Figure 29: The conventional EIT system: Negative refraction does not occur due to $\mathrm{Im}(\epsilon_r) > 0$ for all frequencies in (a). One observes in (b) that the polar path of ϵ_r does not move around the origin. (d) Displays the arrangement of ZPPs: The symmetry of (a) can be attributed to the one zero being exactly in between two poles.

creases. Will this allow for negative refraction? Fig. 31 displays ϵ_r, n and the complex planes of ϵ_r and ν for this arrangement.

As is shown in Fig. 31c, negative refraction is now achieved. Looking at the dielectric function in Fig. 31a it becomes clear why: The amount of loss above $\nu = 10$ has been reduced, and gain occurs. Hence, the amount of rise in both ϵ_r and n above $\nu = 10$ has been reduced, thereby enabling the polar path of ϵ_r in its complex plane to move into the third quadrant. Hence it is clear that the complex plane of the EIT system does not need to be adjusted a lot in order for it to enable negative refraction. In a sense, one could call this configuration the *desired configuration* towards achieving negative refraction in this setting, and it is this configuration one should try to approach by using EIT. Note that this is due to the fact that the responses of ϵ_r and n in Fig. 31 are not symmetric about $\nu = 10$. However, can this arrangement actually be achieved as an EIT system? The answer is obviously no, as it has already been pointed out that the EIT response is fundamentally passive. However, what still remains interesting is: Can the symmetry

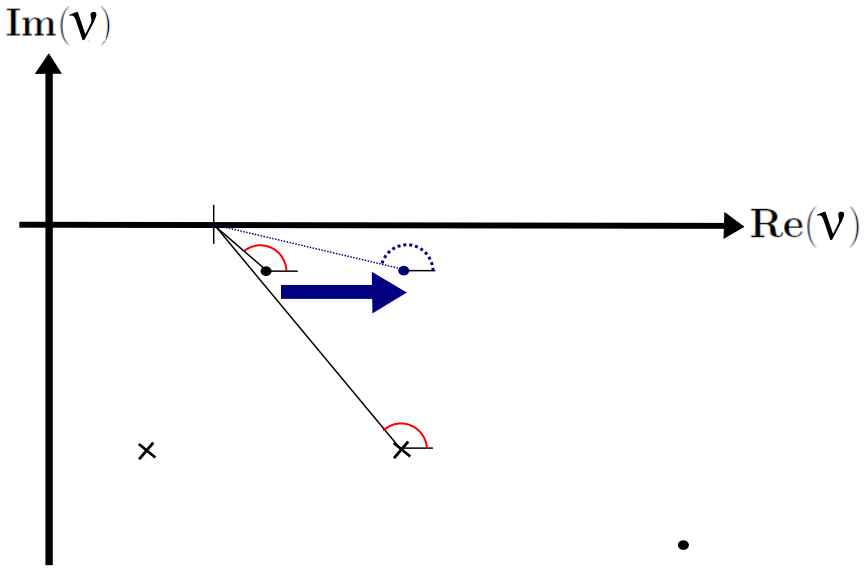

Figure 30: EIT in the complex plane: By moving the uppermost zero represented by a dot according to the blue arrow, one would achieve a larger phase.

in EIT be broken so as to make things easier with respect to achieve $\mathrm{Re}(n) \to 0$? Is there any way of choosing the parameters in (64) so that one ends up with a complex plane similar to that of Fig. 31d? Considering that the EIT response as given by (66) remains symmetric about $\nu = 10$ for all the changes in parameters evaluated in section 5.2, it is therefore not intuitive that one should be able to achieve anything near this *desired configuration*. One can in fact show that this symmetry cannot be broken: If one factorizes the numerator and denominator of χ from (64) under the EIT assumption that $\gamma_{cb} \ll \gamma_{ab}$ one finds a single zero at $\nu_0 = 0$ and two poles displaced at equal distances from it by $\nu_p = i\gamma_{ab} \pm \gamma_{ab}\sqrt{\frac{\Omega_\mu^2}{\gamma_{ab}} - 1}$. Hence the zero will always be between the two poles, no matter what parameters are chosen, meaning that the system remains symmetric under all parameter choices. Why are there two zeros in Fig. 29d and only one accounted for in (64)? This is because the complex plane in Fig. 29d represents ϵ_r and not of χ: The extra zero arrives from $\epsilon_r = 1 + \chi$. In the end, it is thereby clear that the zero cannot be moved in the way suggested in Fig. 30 in the EIT system.

To conclude this section, it is clear that the EIT system is fundamentally passive, and therefore cannot achieve negative refraction without modifying it somehow. What is more, it is also fundamentally symmetric, and this is also a significant obstacle towards using the EIT system to achieve negative refraction. Therefore how should one modify the EIT system to allow for negative refraction? This is the topic of the next section.

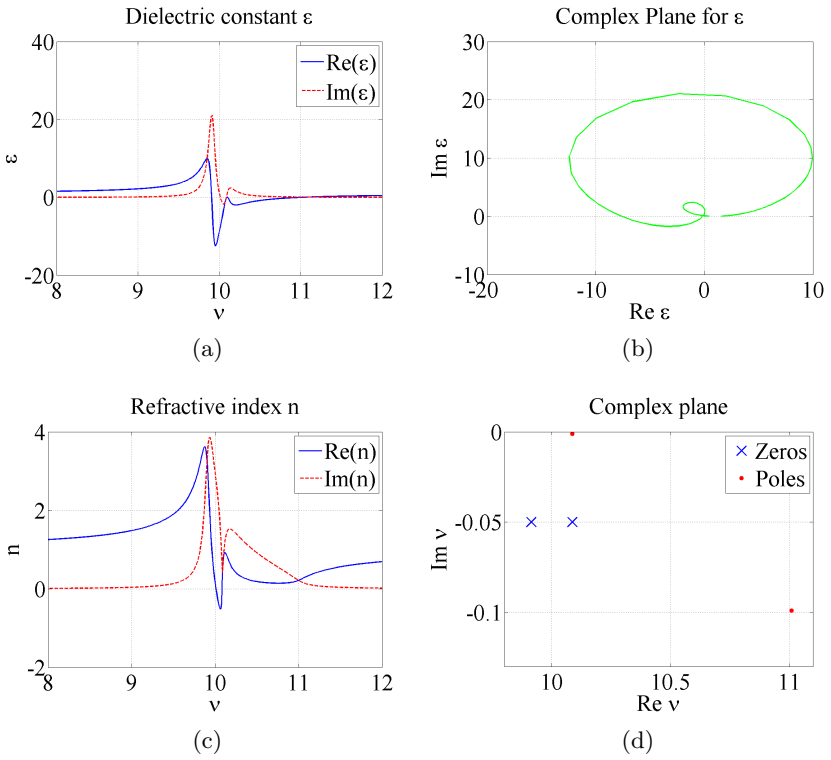

Figure 31: If one is able to alter the arrangement of ZPPs in EIT as suggested in Fig. 30, then this is the resulting system. On observes that negative refraction is achieved in (c), while symmetry is lost in (a). (b) Displays that gain is present.

5.4 Modified EIT systems: Five level symmetric system

Before dismissing the EIT system completely, it should be investigated whether the EIT system can be altered in some way to allow for negative refraction. After all, the system does provide sharp variations and therefore is interesting for the purposes of this report. In the previous section, the problem preventing negative refraction from occurring in the EIT system is the lack of gain, as well as the rise in $\mathrm{Im}(\epsilon_r)$ and $\mathrm{Im}(n)$ above resonance $\nu = 10$ in Fig. 29. What if one could counter this peak with an active component? What if one could for example design a *mirrored EIT system* that displays inversion in the atomic levels? This seems like a good approach, and will be evaluated in this section.

Before moving on to such considerations, however, one should first draw attention to one issue in particular: How does the superposition of other responses fit in with the atomic model presented in section 5.1? That is, if one for example superposes a mirrored EIT system

with the conventional EIT system, one will necessarily be dealing with more than three atomic levels and therefore more atomic transitions will be possible. Can one simply superpose responses without giving thought to the physical interpretation of the responses? This does not seem apparent. Therefore, in order to illuminate these questions, this section will first attempt to derive an atomic model for a superposition of a mirrored and conventional EIT system and investigate under what assumptions one is allowed to superpose responses. Such a system is described by a five-level atomic system, as displayed in Fig. 32.

The three bottom levels $|b\rangle, |d\rangle, |e\rangle$ in Fig. 32 constitute a mirrored system to that of Fig. 26 if the entire system population is place in state $|b\rangle$, as is the case in the figure. Upon calculation one may find that such a mirrored system, if independent of levels $|a\rangle$ and $|c\rangle$, would give a response $\chi_{\text{mirrored}} = -\chi$ where χ is given by the earlier found expression (64). Therefore it would give an identical response to that plotted in Fig. 27a with a sign change, being active all over. What happens then, if one includes levels $|a\rangle$ and $|c\rangle$ and derive the response for the entire five levels together?

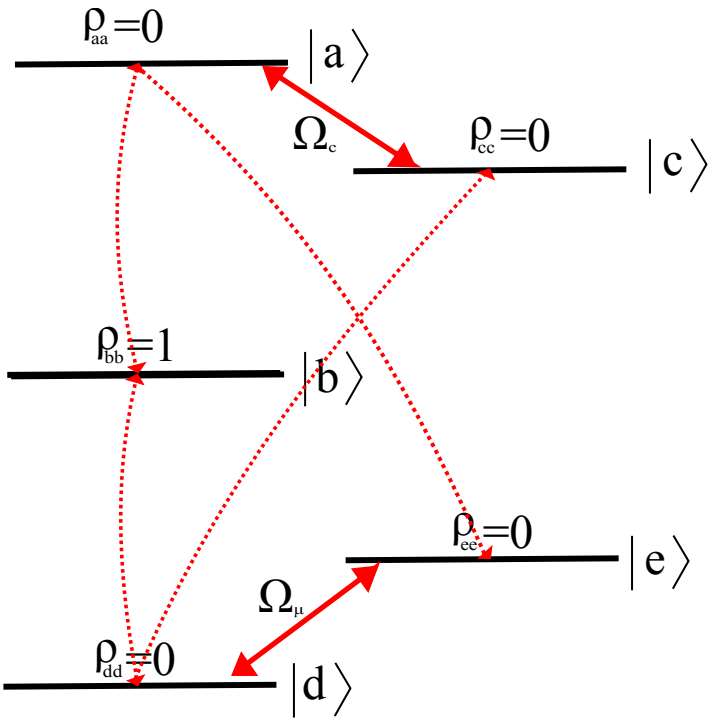

Figure 32: Five level symmetric system. Dipole allowed transitions are indicated in red, where the bold transitions represent transitions that are driven by strong coupling fields. Notice that transitions between $|a\rangle$ and $|e\rangle$, and between $|d\rangle$ and $|c\rangle$, emerge in the five level arrangement, and need to be considered.

One notices in Fig. 32 that some new transitions become possible:

$|d\rangle \leftrightarrow |c\rangle$ and $|e\rangle \leftrightarrow |a\rangle$. If one should assume that the response of this five level system is simply a superposition of χ and χ_{mirrored} then one would be neglecting these transitions. Under what circumstances may one do this? Following much the same procedure as in section 5.1 the response χ_{5level} will derived. From (56) it is clear that one must find the polarization:

$$P(t) = \wp_{ba}\rho_{ab} + \wp_{ca}\rho_{ac} + \wp_{ea}\rho_{ae} + \wp_{db}\rho_{bd} + \wp_{dc}\rho_{cd} + \wp_{ed}\rho_{de} + c.c. \quad (69)$$

Using the Von Neumann equation (58) one may express the density matrix elements for the five level system:

$$\begin{aligned}
\dot{\rho_{ab}} &= -(\gamma_{ab} + i\omega_{ab})\rho_{ab} - \frac{i\wp_{ab}E}{\hbar}(\rho_{bb} - \rho_{aa}) + \frac{i\wp_{ac}E}{\hbar}\rho_{cb} - \frac{i\wp_{db}E}{\hbar}\rho_{ad} + \frac{i\wp_{ae}E}{\hbar}\rho_{eb} \\
\dot{\rho_{cb}} &= -(\gamma_{cb} + i\omega_{cb})\rho_{cb} - \frac{i\wp_{ab}E}{\hbar}\rho_{ca} + \frac{i\wp_{ca}E}{\hbar}\rho_{ab} + \frac{i\wp_{cd}E}{\hbar}\rho_{db} - \frac{i\wp_{db}E}{\hbar}\rho_{cd} \\
\dot{\rho_{bd}} &= -(\gamma_{bd} + i\omega_{bd})\rho_{bd} + \frac{i\wp_{bd}E}{\hbar}(\rho_{dd} - \rho_{bb}) - \frac{i\wp_{ed}E}{\hbar}\rho_{be} + \frac{i\wp_{ba}E}{\hbar}\rho_{ad} - \frac{i\wp_{cd}E}{\hbar}\rho_{bc} \\
\dot{\rho_{be}} &= -(\gamma_{be} + i\omega_{be})\rho_{be} + \frac{i\wp_{bd}E}{\hbar}\rho_{de} - \frac{i\wp_{de}E}{\hbar}\rho_{bd} - \frac{i\wp_{ae}E}{\hbar}\rho_{ba} + \frac{i\wp_{ba}E}{\hbar}\rho_{ae}
\end{aligned} \quad (70)$$

Notice that these four differential equations are linked to each other. With the initial populations as in Fig. 32 one has $\rho_{bb}^{(0)} = 1$ and $\rho_{aa}^{(0)} = \rho_{cc}^{(0)} = \rho_{dd}^{(0)} = \rho_{ee}^{(0)} = 0$. If one assumes that the probe field is very weak, so that the populations do not change considerably, one is justified in assuming $\rho_{ae} = \rho_{ad} = \rho_{ca} = \rho_{cd} = \rho_{cb} = \rho_{de} = \rho_{eb} = 0$, hence (70) becomes:

$$\begin{aligned}
\dot{\rho_{ab}} &= -(\gamma_{ab} + i\omega_{ab})\rho_{ab} - \frac{i\wp_{ab}E}{\hbar}(\rho_{bb} - \rho_{aa}) + \frac{i\wp_{ac}E}{\hbar}\rho_{cb} + \frac{i\wp_{ae}E}{\hbar}\rho_{eb} \\
\dot{\rho_{cb}} &= -(\gamma_{cb} + i\omega_{cb})\rho_{cb} + \frac{i\wp_{ca}E}{\hbar}\rho_{ab} + \frac{i\wp_{cd}E}{\hbar}\rho_{db} \\
\dot{\rho_{bd}} &= -(\gamma_{bd} + i\omega_{bd})\rho_{bd} + \frac{i\wp_{bd}E}{\hbar}(\rho_{dd} - \rho_{bb}) - \frac{i\wp_{ed}E}{\hbar}\rho_{be} - \frac{i\wp_{cd}E}{\hbar}\rho_{bc} \\
\dot{\rho_{be}} &= -(\gamma_{be} + i\omega_{be})\rho_{be} - \frac{i\wp_{de}E}{\hbar}\rho_{bd} - \frac{i\wp_{ae}E}{\hbar}\rho_{ba}
\end{aligned} \quad (71)$$

Comparing the expressions for $\dot{\rho_{ab}}$ and $\dot{\rho_{cb}}$ with (59) and (60) it is clear that the last terms in both equations arise due to the possibility of having transitions between $|d\rangle \leftrightarrow |c\rangle$ and $|e\rangle \leftrightarrow |a\rangle$. What is more, it is due to these transitions that the four equations still remain linked.

One may insert the expression for the field E (61) used earlier (thereby assuming that $\Omega_\mu = \Omega_c$ in Fig. 32), and use the *rotating wave approximation (RWA)* in order to solve them. This means assuming

that the coupling frequency contributes only on the transitions $|a\rangle \leftrightarrow |c\rangle$ and $|d\rangle \leftrightarrow |e\rangle$, that the probe frequency contributes only to the $|a\rangle \leftrightarrow |b\rangle$ and $|b\rangle \leftrightarrow |d\rangle$ transitions, and that neither modes of the fields contribute to the $|d\rangle \leftrightarrow |c\rangle$ or $|a\rangle \leftrightarrow |e\rangle$ transitions. This therefore means that $\dot{\rho_{ab}}$ and $\dot{\rho_{cb}}$ are only coupled to each other, and likewise $\dot{\rho_{bd}}$ and $\dot{\rho_{be}}$ are only coupled with each other. The solution becomes:

$$\begin{aligned}\chi_{\text{5level}} &= \frac{\wp_{ba}\rho_{ab}}{\epsilon_0\mathcal{E}\mathrm{e}^{-i\nu t}} + \frac{\wp_{db}\rho_{bd}}{\epsilon_0\mathcal{E}\mathrm{e}^{-i\nu t}} \\ &= \frac{i|\wp|^2}{2\epsilon_0\hbar}\left[\frac{[\gamma_{cb}+i(\omega_{ab}-\nu)]}{[\gamma_{ab}+i(\omega_{ab}-\nu)][\gamma_{cb}+i(\omega_{ab}-\nu)]+\frac{\Omega_c^2}{4}}\right. \\ &\qquad \left. -\frac{[\gamma_{be}+i(\omega_{bd}-\nu)]}{[\gamma_{bd}+i(\omega_{bd}-\nu)][\gamma_{be}+i(\omega_{bd}-\nu)]+\frac{\Omega_\mu^2}{4}}\right]\end{aligned} \tag{72}$$

As it is through the RWA that one neglects the transitions $|d\rangle \leftrightarrow |c\rangle$ and $|e\rangle \leftrightarrow |a\rangle$, it is clear that it is under the RWA that one can justify superposing responses in the atomic level system dealt with here. So when is one justified in assuming this? Considering Fig. 32, it is clear that a RWA is only valid if the resonance between $|d\rangle \leftrightarrow |c\rangle$ and $|e\rangle \leftrightarrow |a\rangle$ do not overlap with the resonance between $|a\rangle \leftrightarrow |b\rangle$ and $|b\rangle \leftrightarrow |d\rangle$. This is ensured if:

$$(\omega_{ab} - \omega_{cd}) \gg (\gamma_{ab} + \gamma_{cd}) \tag{73}$$

In stating this condition it has been assumed that $\omega_{bd} = \omega_{ab}$, $\omega_{ae} = \omega_{cd}$, $\gamma_{bd} = \gamma_{ab}$ and $\gamma_{ae} = \gamma_{cd}$.

In (72) one can identify the expression χ from (64) in the second line, and hence χ_{mirrored} in the third line. This is hence a general result: If one would like to superpose the EIT sytem with a Lorentz response one can safely do this under the RWA, as long as an RWA is valid. Now that this has been understood, this section will move on to consider two modifications of the EIT system: One through the additions of an active EIT, and another through the addition of Lorentz responses.

5.4.1 Configuration 1: Active and passive EIT

It will now be attempted to achieve a response similar to that of Fig. 31a by use of a mirrored EIT response to diminish the rise of $\mathrm{Im}(\epsilon_r)$ above $\nu = 10$. Such a system is therefore described by (72) and Fig. 33 displays the responses to be considered. Here the resonance of the conventional EIT response is placed at $\nu = 5.5$ while the resonance of the mirrored EIT is placed at $\nu = 7.8$, as displayed in Fig. 33b. Superposing these two responses according to (72), gives Fig. 33a. This to some extent resembles the desired response, and at first glance Fig. 33c does indeed seem to lead to negative refraction. However, it turns out that there are two zeros in the upper complex plane which therefore makes the medium electromagnetically unstable. This has been verified by use of the *argument principle* described in [11, 14].

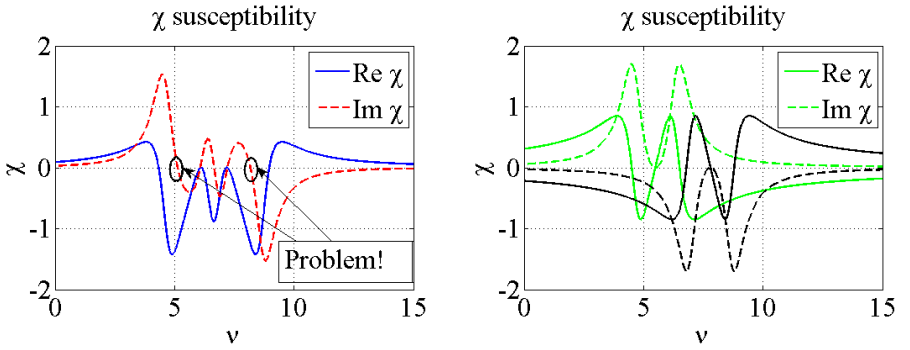

(a) Superposed response (b) Displaying the individual EIT responses

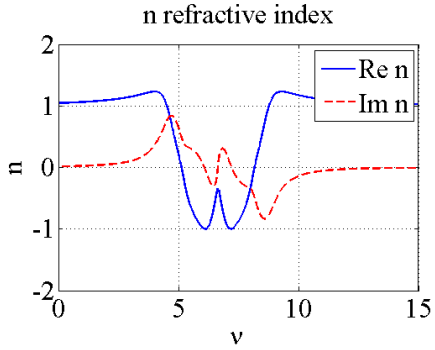

(c)

Figure 33: A system made out of a superposition of a passive and active EIT response

Many different combinations of the mirrored EIT and conventional EIT system have been attempted, however all systems that have lead to similar *apparent* negative refraction have proven to also be electromagnetically unstable. Why is this the case? The problem has been identified in Fig. 33a by two ellipses and arrows. At these frequencies, $\mathrm{Im}(\chi) \approx 0$ and $\mathrm{Re}(\chi) < -1$. It turns out that if one evaluates $\chi_{5\mathrm{level}}$ for frequencies in the upper complex plane, the tops and bottoms of the function peaks are washed out the higher up in the plane $\chi_{5\mathrm{level}}$ is evaluated. This fact can be made rigorous by considering the Poisson integral formula [14]. Somewhere in the upper complex plane the following criterion will therefore be met:

$$\begin{aligned} \mathrm{Re}(\chi) &= -1 \\ \mathrm{Im}(\chi) &= 0 \end{aligned} \tag{74}$$

When this occurs, one has $\epsilon_r = 1 + \chi = 0$, and hence this represents a zero. Therefore, all the EIT realizations in which the $\mathrm{Im}(\chi) < 0$ and $\mathrm{Re}(\chi) < -1$ for the same frequency stand in danger of having a zero

point somewhere in the upper complex plane. This has been the case in every attempted realization by the route proposed in this section.

5.4.2 Configuration 2: Addition of Lorentz functions

It will now be attempted to add a Lorentz function to the EIT system. Two combinations will be considered: A conventional EIT with an active Lorentzian response, and a mirrored EIT with a passive Lorentzian response.

Consider Fig. 34a. Here the passive EIT system χ by (64) is superposed with a weak active Lorentz response at $\nu = 10$ thereby leading to a slight gain at the resonance of the EIT response. This is done because it is known from section 3.1.1 that gain is necessary for negative refraction. It is also known from section 3.2 that gain above a given frequency can contribute to make $\mathrm{Re}(n)$ negative. Fig. 34b displays negative refraction, however the discontinuous behavior around $\nu = 10$ reveals that this medium is unstable: There is at least one zero in the upper complex plane. This for the same reasons as given for Fig. 33 of the previous section: $\mathrm{Im}(\chi) < 0$ where $\mathrm{Re}(\chi) < -1$.

Similarly, Fig. 34c presents a mirrored EIT system described by $\chi_{\mathrm{mirrored}} = -\chi$ with a weak passive Lorentz added at $\nu = 10$. As is viewed in Fig. 34d the same problems arise due to instability. Why is the EIT system so prone to lead to instability when superposed with other responses? When considering the arrangement of zeros and poles for the EIT system in Fig. 29d, this can be understood by the fact that there exists a zero placed very near the real frequency axis. It seems that it this zero is easily moved up into the upper complex plane upon the superposition of other responses with the EIT system.

After all the discussions presented, it is now clear that the EIT system cannot give negative refraction in itself and attempts at modifying the EIT system towards this end have been unsuccessful. The former because of the lack of gain and due to the symmetry of EIT the system, and the latter as a result of the problems with stability. Achieving negative refraction by an EIT system therefore does not seem very promising, and no further attempts will therefore be made here.

6 A strategy towards realization of an arbitrary dielectric response

In section 4.5 a sum of Lorentz functions is used to construct the sharp response displayed in the NIES system shown in Fig. 12b. The Lorentzian response arises out of the simple classical oscillator, however, it nonetheless successfully approximates a number of natural phenomena such as material absorption due to inter-band transitions [15]. What is more, it is quite straightforward to realize oscillatory responses. In *photonic crystals* one can for instance make optical band-gap materials by use periodically varying dielectric constants.

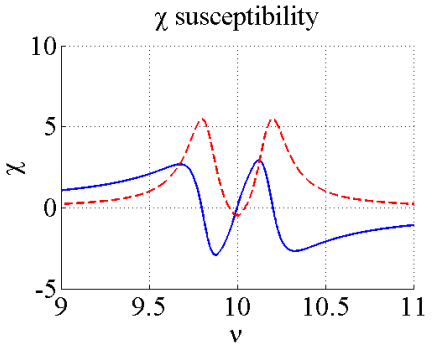

(a) Passive χ superposed with active Lorentzian

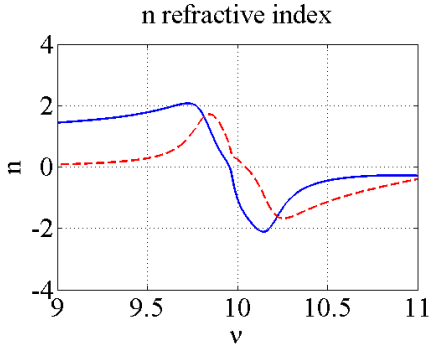

(b) Refractive index n corresponding to (a)

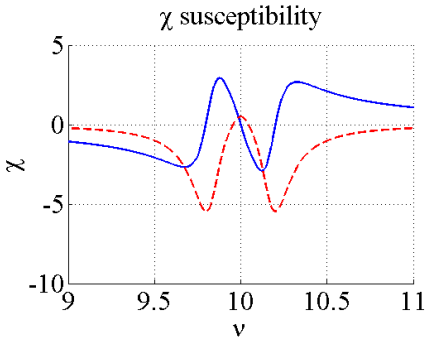

(c) Active χ_{mirrored} superposed with passive Lorentzian

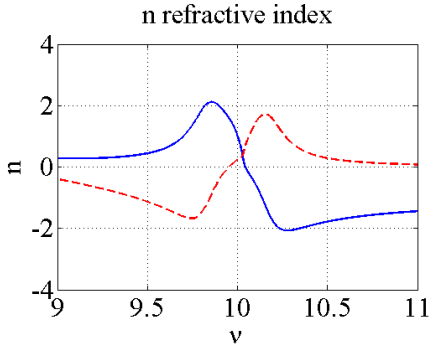

(d) Refractive index n corresponding to (c)

Figure 34: Superpositioning of Lorentz resonances with EIT resonances.

Similarly, it should be straightforward to make resonance structures in metamaterials. This suggests that if an arbitrary dielectric response can be approximated by Lorentzian functions, it should in principle be relatively straightforward to realize it. This section will offer some initial considerations on this possibility.

6.1 Approximation by a sum of Lorentz functions

Imagine that one desires to realize a particular chosen dielectric response $\epsilon_r(\nu)$. It could be for example a particular $\epsilon_r(\nu)$ that would produce negative refraction (as there have been several cases of in this report), or perhaps yield a desired optical filter. Can one always approximate such a response by a sum of Lorentz functions? Under what conditions can one do this? Consider the Lorentz-Cauchy function:

$$F_\lambda(\nu) = \frac{1}{\pi}\frac{\lambda}{\nu^2+\lambda^2} \quad \text{where} \quad \int_{-\infty}^{\infty} F_\lambda(\nu)\mathrm{d}\nu = 1 \tag{75}$$

The Lorentz-Cauchy function has the property that it tends towards a delta function as $\lambda \to 0$:

$$\lim_{\lambda \to 0} F_\lambda(\nu) = \delta(\nu) \tag{76}$$

Any function can be expressed as an integral of delta functions. This integral may again therefore be approximated by a sum of Lorentz-Cauchy functions with a finite width. Consider this for the imaginary part of a desired ϵ_r as expressed below:

$$\begin{aligned} \text{Im } \epsilon_r(\nu) &= \int_{-\infty}^{\infty} \text{Im } \epsilon_r(\omega_0)\delta(\nu - \omega_0)\mathrm{d}\omega_0 \\ &\approx \sum_{m=-\infty}^{\infty} \text{Im } \epsilon(m\Delta\omega_0)F_\lambda(\nu - m\Delta\omega_0) \end{aligned} \tag{77}$$

Here $\Delta\omega_0$ represent the step size between Lorentzian resonances. One must of course assume λ to be sufficiently small and that enough terms are added in the sum for the approximation to be valid. This nevertheless shows that Im $\epsilon_r(\nu)$ can be expressed as a sum of Lorentz-Cauchy functions.

Consider the imaginary part of the Lorentz function, now to be called $L(\nu)$, used in the sum (55) in section 4.5:

$$\text{Im } L(\nu) = \frac{\omega_0^2 \nu \Gamma}{(\omega_0^2 - \nu^2)^2 + (\nu\Gamma)^2} \tag{78}$$

It turns out that one can arrive at a similar expression by summing two Lorentz-Cauchy functions (75) in the following manner:

$$F_\lambda(\nu - \omega_0) - F_\lambda(\nu + \omega_0) = \frac{1}{\pi}\left[\frac{4\lambda\omega_0\nu}{(\omega_0^2 - \nu^2)^2 + 2\lambda^2(\nu^2 + \omega_0^2) + \lambda^4}\right] \tag{79}$$

If one considers this expression near resonance so that $\nu \approx \omega_0$ and assume that λ is small enough that $\lambda^4 \approx 0$, then (79) may be written as:

$$F_\lambda(\nu - \omega_0) - F_\lambda(\nu + \omega_0) = \frac{2}{\pi}\left[\frac{\omega_0\nu[2\lambda]}{(\omega_0^2 - \nu^2)^2 + ([2\lambda]\omega_0)^2}\right] \tag{80}$$

One may set $\Gamma = 2\lambda$, and it is clear from comparing (78) and (80) that both share the same functional form. One may perhaps ask why the particular sum $F_\lambda(\nu - \omega_0) - F_\lambda(\nu + \omega_0)$ in (79) is taken: As has been shown in section 2 and 4.1, the Kramers-Kronig relations demand that any function f must obey $f(-\nu) = f^*(\nu^*)$, therefore meaning that the imaginary part obey:

$$\text{Im}\{f(-\nu)\} = -\text{Im}\{f^*(\nu^*)\} \tag{81}$$

Im $L(\nu)$ expressed by (78) obeys this requirement since the Lorentzian response is causal, however F_λ expressed by (75) does not. The sum in (79) is therefore chosen in order to make the resulting sum obey (81).

Having shown that (78) displays the same functional form as (80), it follows that one may approximate the imaginary parts of causal functions by Im $L(\nu)$ in a similar manner by which Lorentz-Cauchy functions approximate general functions in (77). That is, one can write:

$$\begin{aligned} \text{Im } \epsilon_r(\nu) &= \int_0^\infty \text{Im } \epsilon_r(\omega_0) \Big[\lim_{\Gamma \to 0} \text{ Im } L(\nu - \omega_0) \Big] \mathrm{d}\omega_0 \\ &\approx \sum_{m=0}^{\infty} \text{Im } \epsilon(m\Delta\omega_0) \Big[\text{Im } L(\nu - m\Delta\omega_0) \Big] \end{aligned} \tag{82}$$

Notice here that the integral and sum only range over positive frequencies, in contrast to the case in (77). This follows from the fact that both Im $\epsilon_r(\nu)$ and Im $L(\nu)$ obey (81): Therefore by approximating Im $\epsilon_r(\nu)$ for positive frequencies, Im $L(\nu)$ has automatically approximated Im $\epsilon_r(\nu)$ for negative frequencies as well.

If one wishes to approximate a dielectric function $\epsilon_r(\nu)$, and not just the imaginary part Im $\epsilon_r(\nu)$, one is actually required to approximate two separate functions: Re $\epsilon_r(\nu)$ and Im $\epsilon_r(\nu)$. These must again be related to one another by the Kramers-Kronig relations (because $\epsilon_r(\nu)$ is causal). As it turns out, this is also taken care of through causality by summing Lorentzian functions in the following way:

$$\epsilon_r(\nu) \approx 1 + \sum_{\omega_0} \text{Im } \epsilon_r(\omega_0) \frac{\omega_0^2}{\omega_0^2 - \nu^2 - i\nu\Gamma} \tag{83}$$

From (82) one understands that Im $\epsilon_r(\nu)$ should be successfully approximated through this expression as long as Γ is sufficiently small, but what about Re $\epsilon_r(\nu)$? It is known that $\epsilon_r - 1$ obeys the Kramers-Kronig relations due to causality (section 2):

$$\begin{aligned} \text{Re}(\epsilon_r) - 1 &= -\mathscr{H}\text{Im}(\epsilon_r) \\ \text{Im}(\epsilon_r) &= \mathscr{H}\Big[\text{Re}(\epsilon_r) - 1\Big] \end{aligned} \tag{84}$$

Hence $\text{Re}(\epsilon_r)$ is uniquely defined by $\text{Im}(\epsilon_r)$ and vice versa. The Lorentzian functions in (83) are also causal and hence obey the same relations, and since the Hilbert transform $\mathscr{H}$ is linear so does their sum in (83). This has the following consequence: If (83) successfully approximates Im $\epsilon_r(\nu)$, then it has automatically also successfully approximated Re $\epsilon_r(\nu)$. The value 1 is added to the sum of Lorentzians in (83) in order that $\epsilon_r \to 1$ as $\nu \to \pm\infty$ (this must be done since Im $\epsilon(\nu) \to 0$ as $\nu \to \pm\infty$).

Therefore, it has been argued that it is possible to approximate any dielectric function $\epsilon_r(\nu)$ as a sum of Lorentz functions by (83). Needless to say this is only possible under certain conditions: Sufficiently small Γ and sufficiently many Lorentzian functions in the sum.

6.2 Causal extrapolation of a limited bandwidth dielectric response

In designing a particular dielectric response $\epsilon_r(\nu)$ one would like to be able to choose both Re $\epsilon_r(\nu)$ and Im $\epsilon_r(\nu)$ freely of each other. Consider for example Fig. 35a: Imagine that one would like to construct a dielectric function where Re $\epsilon_r(\nu) = -1$ along a bandwidth where there is no loss or gain, i.e. Im $\epsilon_r(\nu) = 0$, as depicted. However, if one assumes that Re $\epsilon_r(\nu) =$ Im $\epsilon_r(\nu) = 0$ for all ν outside the depicted bandwidth in Fig. 35a, then it is clear that this ϵ_r does not represent a causal response: If one takes the Hilbert transform of Re $\epsilon(\nu)$ according to (84), one is given a varying Im $\epsilon_r(\nu)$ as depicted in Fig. 35b. Hence, it is clear that the desired response of Fig. 35a is not *causality-friendly* within the bandwidth, and therefore not realizable left as it is.

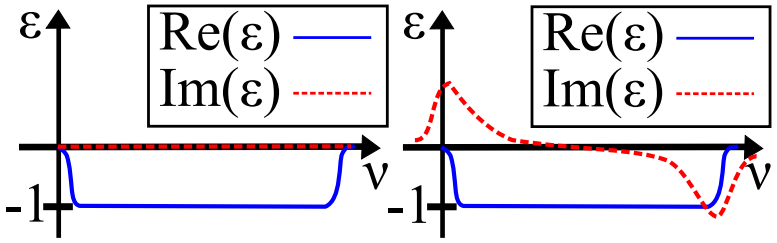

(a) Desired response $F(\nu)$ (b) Causal response

Figure 35: Defining desired response behavior (goal functions) within a bandwidth.

Does this mean that the ability to tailor a dielectric response is severly limited from the start? No, on the contrary, it turns out that one can have a causality-unfriendly response ϵ_r *within a bandwidth* by causally extrapolating it outside this bandwidth. Consider Fig. 36: Through the help of a certain extrapolation outside the band we are interested in, one can ensure that $\epsilon_r(\nu)$ remains causal for all frequencies (note that the figure does not give the valid extrapolation, but only serves to illustrate the concept), including within the band. In other words, the desired response displayed in Fig. 35a ceases to be problematic due to how $\epsilon_r(\nu)$ behaves outside this frequency bandwidth. As is explained in [16] there exists a unique extrapolation for this bandwidth and the question therefore becomes how one may find it. In this section this will be achieved by use of a numerical algorithm based upon the Krein and Nudel'man approximation of arbitrary functions by minimum-energy transfer functions as presented in [16].

One may call the ϵ_r in Fig. 35a within the displayed frequency bandwidth the *goal function* $F(\nu)$. One desires therefore to find the causally extrapolated function, which one may call $f(\nu)$, corresponding to the response shown in Fig. 36. That is, given the goal function $F(\nu)$ for a bandwidth $\Omega = (\omega_1, \omega_2)$ where $0 \leq \omega_1 < \omega_2 < \infty$, one needs to find the extrapolation $f(\nu)$ for $-\infty < \nu < \infty$. Krein and Nudel'man

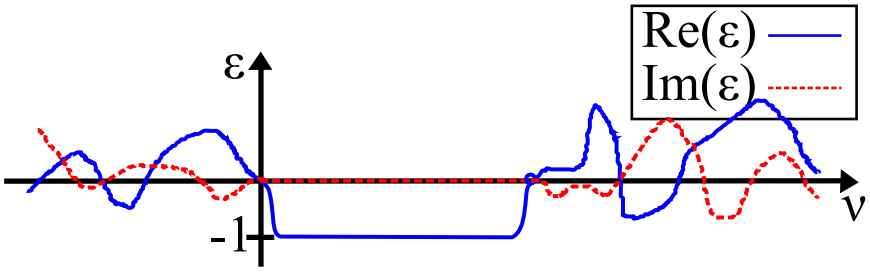

Figure 36: Extrapolated response $f(\nu)$ by Krein and Nudel'man.

formulate the problem as follows: Given a precision number δ such that $0 < \delta < \|F(\nu)\|_\Omega$, find an $f(\nu) \in H^2$ so that:

$$\begin{aligned} \|f - F\|_\Omega^2 &< \delta, \quad \text{where } \Omega = (\omega_1, \omega_2) \\ \|f\|_{\bar{\Omega}}^2 &\quad \text{minimum}, \ \bar{\Omega} = \mathbb{R} \backslash \Omega \end{aligned} \tag{85}$$

The requirement that $f(\nu) \in H^2$ means that $f(\nu)$ belongs to the Hardy space: This is an equivalent way of stating that $f(\nu)$ is causal, having its real and imaginary parts connected by the Hilbert transforms in (84). The $\|\cdot\|$ represents the norm:

$$\begin{aligned} \|f - F\|_\Omega^2 &= \int_\Omega |f(\nu) - F(\nu)|^2 \mathrm{d}\nu \\ \|f\|_{\bar{\Omega}}^2 &= \int_{\bar{\Omega}} |f(\nu)|^2 \mathrm{d}\nu = \left(\int_{-\infty}^{\omega_1} + \int_{\omega_2}^{\infty} \right) |f(\nu)|^2 \mathrm{d}\nu \end{aligned} \tag{86}$$

Demanding the minimum of $\|f\|_{\bar{\Omega}}^2$ ensures the uniqueness of the solution: The solution given is the one that minimizes the energy outside Ω. Having now defined the problem, the solution $f(\nu)$ is given by [16]:

$$f(\nu) = \frac{1}{2} f_e(\nu) - \frac{1}{2\pi i} \int_{\hat{\Omega}} \frac{f_e(\omega)\ \mathrm{d}\omega}{\omega - \nu} \tag{87}$$

The interval of integration is defined as $\hat{\Omega} = (-\omega_2, -\omega_1) \cup (\omega_1, \omega_2)$, and the function $f_e(\nu)$ is found from solving the equation:

$$\left(\eta + \frac{1}{2} \right) f_e(\nu) - \frac{1}{2\pi i} \int_{\hat{\Omega}} \frac{f_e(\omega)\ \mathrm{d}\omega}{\omega - \nu} = F(\nu), \quad \nu \in \Omega \tag{88}$$

The $\eta = \eta(\delta)$ is here a positive function of δ which decreases monotonically to zero as $\delta \to 0^+$. It determines the precision of the imitation of the goal function $F(\nu)$ within Ω, where the smaller η is chosen, the greater the precision. Choosing η, and hence δ, smaller will make $f(\nu)$ more similar to $F(\nu)$ within Ω, however it will also generally require a higher energy outside Ω in (86). It is not necessary to know the function $\eta(\delta)$ explicitly; it suffices therefore to use η as a parameter directly.

In order to solve for $f(\nu)$ numerically one must discretize and invert (88) to solve for $f_e(\nu)$. Since the integrals in both (87) and (88) represent Hilbert transforms which are linear operations, the whole process can be performed by matrix calculations. This process is straightforward and presented clearly in [16], to which interested readers are referred. In the proceeding it will be taken for granted that $f(\nu)$ can be found by implementing straightforward numerical calculations.

Since Krein-Nudel'man gives $f(\nu) \in H^2$, it is clear that the extrapolated function is causal. However, there remains a slight problem: Though a medium is causal, there may in fact still exist odd order zeros in the upper complex plane of $\epsilon(\nu)$. These are zeros that do not make $n(\nu)$ discontinuous, however, upon a slight perturbation of the medium may lead to this result nonetheless. For this reason, no zeros at all are desired in the upper complex plane for stability reasons. Unfortunately, though, the Krein and Nudel'man approach presented so far does not prevent such zeros from being present. As is suggested in [6], one may therefore avoid the problem by defining a new goal function $G(\nu)$:

$$G(\nu) = \ln(F(\nu)) \tag{89}$$

Here $F(\nu)$ is defined as earlier. One may then use (87) and (88) by the Krein-Nudel'man procedure to find the extrapolated $g(\nu)$. By exponentiating both sides of (89), one has $F(\nu) = \exp(G(\nu))$. Therefore, if $g(\nu)$ successfully extrapolates $G(\nu)$, one may also exponentiate $g(\nu)$ and find:

$$f(\nu) = \exp(g(\nu)) \tag{90}$$

Since an exponential function never equals zero, this method therefore achieves to find an extrapolation $f(\nu)$ which is zero free in the upper complex plane, and may therefore be used to extrapolate causal dielectric functions for electromagnetically stable media.

In summary, a method has now been devised in which a desired $\epsilon_\Omega(\nu)$ can be freely determined within a bandwidth, and then extrapolated in order to ensure causality and electromagnetic stability, giving $\epsilon_r(\nu)$. In section 6.1 it was demonstrated that any causal response can be approximated by a sum of Lorentz functions. In the introduction to this part of the report it was argued that photonic crystals and metamaterials can provide feasible means towards realizing Lorentzian responses. Hence the outline of a route towards realizing arbitrary dielectric responses has been presented. In the next section, an example will be presented.

6.3 Demonstration

Having outlined the procedure it becomes interesting to apply it on a particular example. The procedure to be performed consists of the following steps:

1. Define a function $F(\nu)$ of a desired response $\epsilon(\nu)$ within a band $\Omega \in (\omega_1, \omega_2)$ where $0 < \omega_1 < \omega_2 < \infty$.
2. Define the goal function of extrapolation as the logarithm of $F(\nu)$: $G(\nu) = \ln(F(\nu))$.
3. Extrapolate $G(\nu)$ by Krein and Nudel'man numerically to find $g(\nu)$ for a desired frequency interval.
4. Exponentiate the solution in order to find $f(\nu)$: $f(\nu) = \exp(g(\nu))$, thereby recovering the desired response within Ω described by $F(\nu)$.
5. Having found $f(\nu)$ approximate it by a sum of Lorentzian functions.

As a first attempt, the response displayed in Fig. 35a will once again be considered. The result from performing steps 1 to 5 is displayed in Fig. 37.

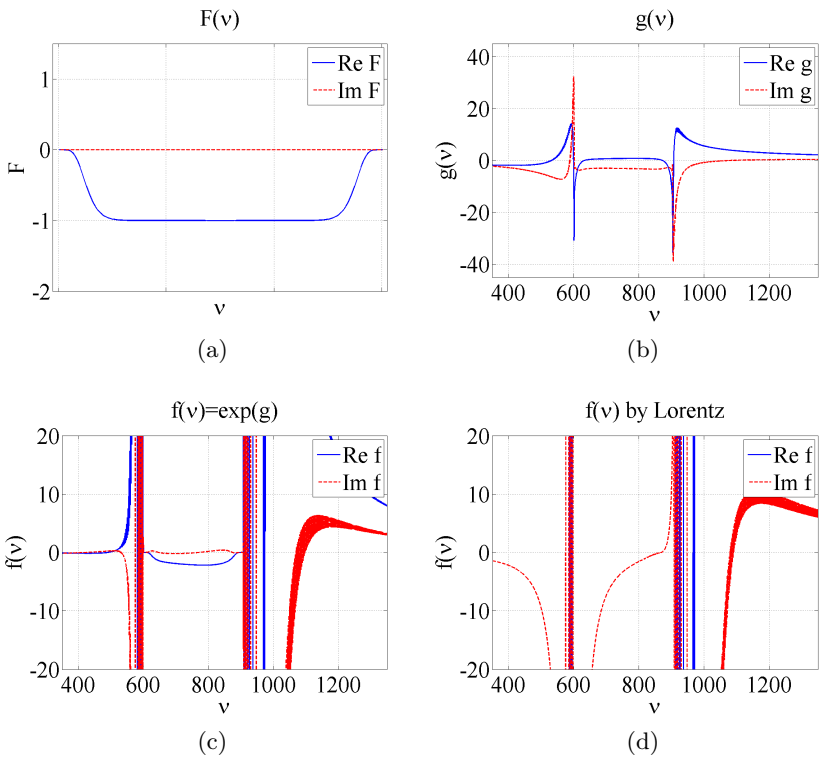

Figure 37: A demonstration of the procedure outlined in steps 1-5. Due to the desired response in (a) being *causality-unfriendly* dramatic responses result in the extrapolation, as displayed in (c).

Fig. 37a shows the desired response $F(\nu)$ within the bandwidth Ω. It may be described as follows:

$$\begin{aligned} \text{Re } F(\nu) &= -\exp\left(-\frac{(\nu-\nu_0)^2}{2\sigma^2}\right)^n \\ \text{Im } F(\nu) &= 0 \end{aligned} \tag{91}$$

In Fig. 37a the parameters have been chosen as $n = 8$ and $\sigma = 0.3$. Furthermore the regulation parameter has been chosen to be $\eta = 10^{-3}$. The result after step 3 above leads to Fig. 37b yielding $g(\nu)$. Performing step 4 gives $f(\nu)$ in Fig. 37c. It is clear that although the desired response $F(\nu)$ is more or less recreated, the extrapolation outside this bandwidth leads to a severely drastic response. The amplitude of the sharp peaks ouside the bandwidth are as large as on the order of 10^6. One also observes considerable oscillation along the curves leading to the "thick" curves displayed. Attempting to approximate this behavior by Lorentz functions in step 5 does not recreate the desired response, as displayed in Fig. 37d. This is because the step-size between Lorentzians in the sum (83) is too large to account for the sharp variation that is present.

By making η larger it is possible to make this behavior less drastic. If rather $\eta = 10^{-1}$ one achieves a less drastic behavior outside the bandwidth, as may be viewed in Fig. 38. Now, however, the desired response $F(\nu)$ from Fig. 37a not accurately recreated in the extrapolation shown in Fig. 38a. It is apparent that there is a trade-off between accuracy within the bandwidth Ω and having a manageable response outside Ω. With a more manageable response outside Ω, it is clear from Fig. 38b that one achieves greater success in approximating $f(\nu)$ by a sum of Lorentzian functions.

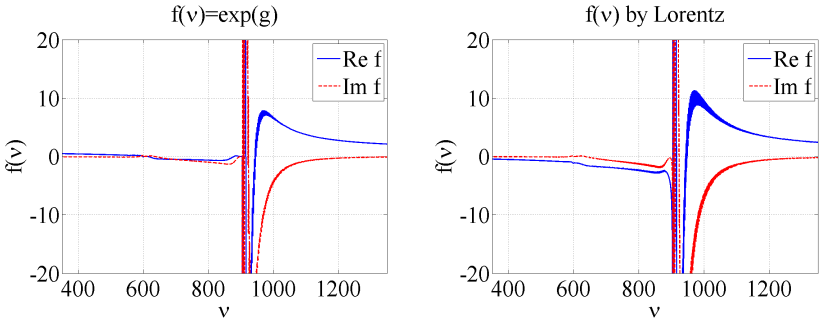

(a) (b)

Figure 38: By increasing the precision parameter from $\eta = 10^{-3}$ to $\eta = 10^{-1}$, the extrapolated response becomes less dramatic. However, this at the cost of precision: The goal function is not approximated well. Now the sum of Lorentzians from (83) succeed in approximating the response.

It was noted in section 6.2 that the desired response $F(\nu)$ in Fig. 35a, which is here described by (91) and shown in Fig. 37a, is not

causality-friendly. The rather dramatic functional response outside Ω in Fig. 37 and Fig. 38 may therefore be understood as a consequence of this: This rather peculiar behavior becomes necessary in order to make the desired response causal. One cannot expect to "bend" the rules of causality for *free*. What if one instead chooses to start with a $F(\nu)$ which is more causality-friendly? One would then expect a less dramatic response outside Ω. This is indeed the case, as is shown in Fig. 39.

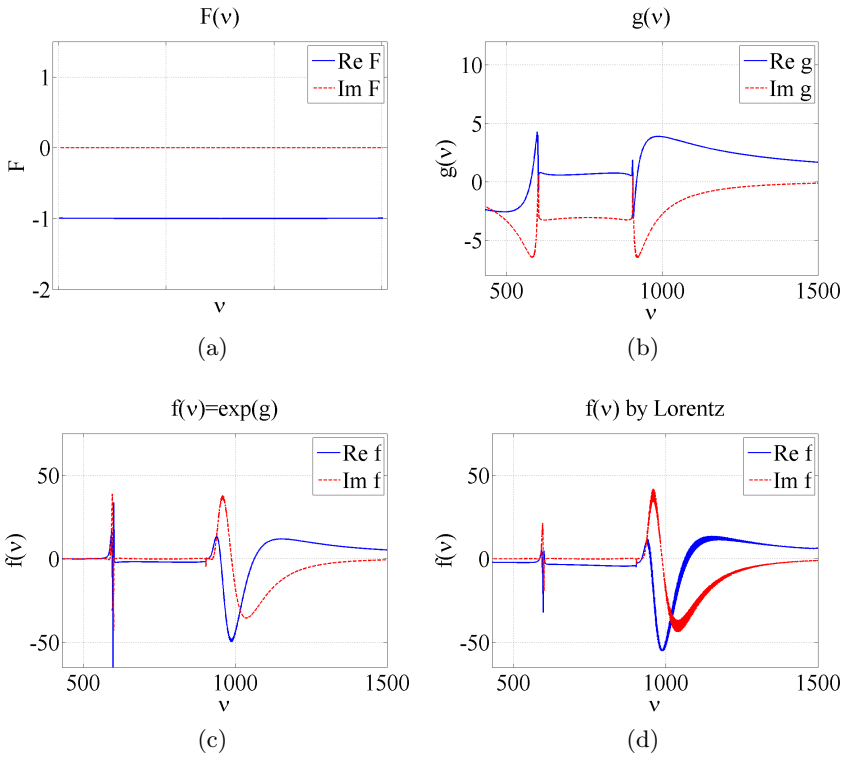

Figure 39: Performing steps 1-5 once again: This time with a *causality-friendly* goal function: The extrapolated response is not severe and can be approximated by a sum of Lorentzians according to (83).

The desired response $F(\nu)$ is here presented in Fig. 39a, and is causality-friendly: That is, if you assume that $\mathrm{Re}(\epsilon_r) \to 1$ slowly as $\nu \to \pm\infty$ and take the the Hilbert transform of the real part by (84) one will end up with the imaginary part displayed. Performing steps 2 and 3 upon $F(\nu)$ one therefore ends up with an extrapolation without the severe rapid behavior earlier observed (Fig. 39c). Here $\eta = 10^{-3}$. Since the behavior is a lot less rapid than in the previous examples, it is accurately approximated by a sum of Lorentz functions as displayed in Fig. 39d. If the spacing between each Lorentz function in the sum had been made slightly smaller, one would avoid the "thick" section of the curves, and can readily be done.

Fig. 39d comes about from the sum of more than 1000 Lorentz functions with equal widths, but differing amplitudes and resonance frequencies. Should one wish to realize this medium, therefore, one would have to tailor a considerable number of resonances. Is it possible to approximate this response with fewer Lorentzian resonances? Considering Fig. 39c it is clear that the distinctive features of this response all seem Lorentzian in nature. That is, it seems intuitively possible to recreate the general features of this response by a small number of Lorentzians with differing widths, resonances and amplitudes. This has been attempted and the result is displayed in Fig. 40. Here Fig. 40a is the superposition of four separate Lorentz responses, which are distinguished from one another in Fig. 40b.

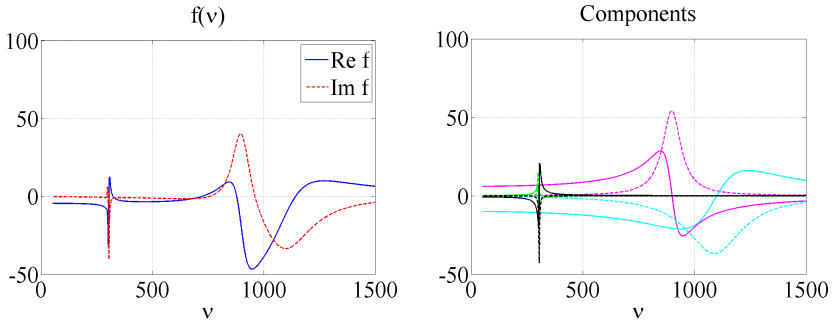

Figure 40: Attempting to approximate the $F(\nu)$ in Fig. 39c with only four Lorentzian functions. (a) The main features are recreated. (b) The individual Lorentzian responses that are superposed in order to get (a).

Comparing Fig. 39c with Fig. 40a, one observes a high degree of similarity. The desired response $F(\nu)$ is not recreated exactly, but its important characteristics are present: Re $f(\nu)$ is negative and relatively constant for an extended bandwidth, while Im $f(\nu)$ is relatively constant and close to zero within this bandwidth. Since this is achieved by only four Lorentz functions, this response should be considerably easier to realize than the previous one.

6.4 Evaluation of method

This section has succeeded in starting from a desired response within a bandwidth, and ended with an extended, causal response that might be feasible to realize. While the last step of approximation displayed in Fig. 40 does not follow the sum equation (83) derived in section 6.1, it follows the same principle: By considering the imaginary part of the extrapolated response $f(\nu)$ in Fig. 39c one sums Lorentz functions to attempt to approximate this.

However, there are some apparent short-comings with the proposed procedure. First and foremost is the fact that the Krein and Nudel'man

extrapolation does not distinguish between gain and loss in the minimization outside Ω. Krein and Nudel'man simply minimizes the energy, and therefore targets gain and loss equally. Ideally, one would rather minimize gain at the cost of higher loss, since gain is a problem for realization whereas loss is not. A second problem is the drastic responses that occur outside Ω if one wishes to design a response that is causality-unfriendly: Obviously one would not be able to realize a response such as the one displayed in Fig. 37c. Though it has been shown that any freely designed response within the bandwidth Ω can be causally extrapolated, this in turn does not imply that any causal response can be realized. Therefore, the procedure seems limited to causality-friendly responses.

Nonetheless, the aim of this section was merely to present some first considerations on the possibility of realizing an arbitrary dielectric response. It is therefore a result that the procedure in fact has succeeded.

7 Concluding remarks

7.1 General summary

After outlining the relevant concepts to metamaterials and negative refraction in section 1, and to the refractive index in active media in section 2, this report has addressed the issue of achieving negative refractive index through a given dielectric function ϵ_r. Section 3 outlines general criteria towards this end in terms of the *complex plane* of ϵ_r and in terms of requirements stemming from *causality*. The former identifies that a *polar path of ϵ_r moving around the origin* is a sufficient condition for achieving negative refraction, and represents a new perspective not found in literature. Ideally, one would have the polar path enclose an ellipse moving through all four quadrants in the complex plane: Constructing such a response becomes the goal of much of the rest of the report. In the latter considerations upon the causal Kramers-Kronig relations, there are identified two paths by which $\mathrm{Re}(n)$ becomes negative: (i) Large positive $\mathrm{Im}(n)$ below, or large negative $\mathrm{Im}(n)$ above, the negative index frequency, (ii) A steep drop in $\mathrm{Im}(n)$ immediately below the negative index frequency.

Despite the insights of section 3, it leaves the exact requirements upon ϵ_r remaining somewhat ambiguous. The driving question for the section 4 becomes: *How must ϵ_r be in order to achieve negative refraction at low gain?* In particular, now in the direction of *can this be achieved at arbitrarily low gain without the need for steep variation?* As a result of these questions, rational functions are chosen in order to understand the requirements of section 3 in terms of concrete examples. The rational functions serve to give both the polar path of ϵ_r and the Kramers-Kronig requirements a mathematical reality that is not found in literature: The requirements may now be understood in terms of zero-pole placements. That is, the polar path of ϵ_r arises out of the phase θ_ϵ and the magnitude $|\epsilon_r|$, accounted for by the position-

ing of zeros and poles in the complex plane, and the Kramers-Kronig requirements are built into the rational equations by demanding that (i) there be equally many zeros and poles present, (ii) one includes the corresponding negative frequency zeros and poles, (iii) there be no zeros or poles in the upper complex plane. One is thereby able to unify all the requirements in section 3, to *one set of tasks* regarding θ_ϵ and $|\epsilon_r|$: The goal becomes to achieve $\pi < \theta_\epsilon < 3\pi$ with an $|\epsilon_r|$ that ensures the polar path of ϵ_r to move around the origin in the complex plane, for a system containing equally many poles as zeros in the lower complex plane. As one generally has $|\epsilon_r| > 0$ (as long as zeros are not placed on the real frequency axis), the primary issue of achieving negative refraction becomes therefore to achieve *enough phase*.

From the investigation on rational functions, one observes that the causal requirements are rediscovered: Section 4 argues that (i) there is a trade-off between achieving enough phase θ_ϵ for negative refraction and having low gain/loss, and likewise (ii) there is a trade-off between achieving enough phase θ_ϵ and having little steepness. Hence, one may achieve enough phase and thereby negative refraction through either significant gain/loss, steep variation, or both, which is essentially restating the Kramers-Kronig requirements. The occurrence of (i) and (ii) arise from the two ways in which one may achieve a large phase θ_ϵ in the complex plane of ν by the movement of zeros and poles: In the first case by increasing the distance between the zeros and poles in each zero-pole pair (ZPP), and in the latter case by moving the ZPPs closer to the real frequency axis. The main constraint towards achieving negative refraction at low gain is identified to be the necessity of having equally many poles as zeros in the complex plane of ϵ_r. If one for example, has less poles than zeros, the task of achieving enough phase and have $|\epsilon_r|$ small in the active regions of ϵ_r would be straightforward.

Three systems from literature have been considered with regards toward achieving negative refraction: The *Two-Component* system from [5] is discussed in sections 3.2.1 and 4.6, the *Negative Index by Exponential Steepness (NIES)* system presented in [6] is discussed in sections 3.2.2 and 4.5, and the *Electromagnetically Induced Transparency (EIT)* system from [13, 12] is discussed in section 5. In the first case, the Two-Component system demonstrates much of what is possible to achieve in non-magnetic media without steep variation: Negative refraction occurs at a frequency for which considerable $\mathrm{Im}(n)$ is present, which thereby means that there will be considerable attenuation here. The amount of $\mathrm{Im}(n)$ can be lowered by increasing the amount of gain in the medium. In either case, this system therefore does badly on the figure of merits defined in section 4.3. It is also argued that the amount of gain must *at least* be on the order of $|\max\{-\mathrm{Im}(\epsilon_r)\}| \approx 1$ for the onset of negative refraction to occur. Since the Two-Component system therefore depends on achieving considerable gain and nevertheless has a lot of attenuation present, this system is not considered promising.

The NIES system demonstrates that it is possible to achieve negative refraction at arbitrarily small gain and without having any atten-

uation at the negative index frequency. It therefore does very well on the figure of merits defined in section 4.3. However, when comparing the NIES system with a single steep Lorentzian response one realizes that the key feature of the NIES system is not simply a steep drop in $\mathrm{Im}(n)$, but an *asymmetric drop* in $\mathrm{Im}(n)$. It is therefore argued that the NIES system achieves its desirable characteristics due to two properties: (i) Due to making the drop in $\mathrm{Im}(n)$ steep, and (ii) due to the area enclosed by the $\mathrm{Im}(n)$ curve below the drop remaining unchanged during this process. One observes in the NIES system therefore that *shape*, as well as steepness, is important. The asymmetric drop in this system is given a complementary explanation in terms of the zeros and poles in its complex frequency plane of n: Here it is observed that the asymmetry is explained by a horizontal *band of zeros and poles* that serve to *smear out* the presence of the pole in the ZPP that leads to negative refraction. That is, the band makes the presence of this pole *less present*. One must have enough ZPPs in the band to ensure that this smearing takes place, which corresponds with having enough ZPPs to make the $\mathrm{Im}(n)$ curve smooth. The question arises as to whether one can use this band-smearing effect towards achieving negative refraction at arbitrarily low gain without the use of a steep drop, however it is argued that this is not possible: The smearing-effect does not depend to the number of ZPPs in the band indefinitely, but reaches a maximum when the $\mathrm{Im}(n)$ curve is smooth.

Finally, the EIT system is considered as a possible system for which negative refraction through steep variation may be physically realizable. The conventional model of EIT is first derived from an atomic three level system by semi-classical theory, and its capacity of achieving steep variation is then evaluated. The concepts of negative refraction presented in sections 2, 3 and 4 are introduced to the EIT model, and the possibility of obtaining negative refraction in it is evaluated. Apart from the fact that conventional EIT lacks gain, it is argued that negative refraction is opposed due to symmetry: There is a steep rise as well as a steep drop in vicinity of the response resonance, where one would hope to achieve negative refraction. As this symmetry cannot be broken within the conventional EIT model, it is considered whether this can be done by modifying the system through superposing other responses to it. The criteria under which such superposition is consonant with the atomic model is developed before considering two cases: (i) Adding a *Mirrored EIT system*, or (ii) Lorentzian functions, to the EIT system. Neither of them lead to *valid* negative refraction, as the EIT system proves to be dispositioned towards electromagnetic instability upon such additions. For the above reasons, therefore, it is therefore suggested that the EIT system is not a likely route towards realizing negative refraction through steep variations.

Section 6 proposes an initial attempt at a procedure towards tailoring and realizing desired material responses in ϵ_r. It is shown that any causal response ϵ_r can be approximated by a sum of Lorentz-functions, and it is argued that the resulting a sum can in principle be realized in terms of photonic crystals or metamaterials. This bears resemblance

to how the response of the NIES system was constructed in sections 3.2.2 and 4.5. The section also demonstrates how one can choose a desired behavior of $\mathrm{Re}(\epsilon_r)$ and $\mathrm{Im}(\epsilon_r)$ independent of each other *within a bandwidth*, and then causally extrapolate the response for all frequencies. Here, the Krein and Nudel'man approximation is used to do this. The expanded response is calculated numerically, and a specific procedure is outlined to avoid having any zeros present in its upper complex plane. The method is demonstrated in terms of a couple of examples. The greatest drawback of this method is that it does not differentiate between gain and loss in its causal extrapolation, thereby there is no possibility of demanding that there be little gain present in the causally expanded response. This being said, the method does however demonstrate that one in fact can extrapolate functions in this manner. It is observed, that the more *causality friendly* $\mathrm{Re}(\epsilon_r)$ and $\mathrm{Im}(\epsilon_r)$ are chosen within the desired bandwidth, the smoother the extrapolation outside this bandwidth becomes.

7.2 Outlook and last discussions

On the basis of this thesis it does not seem probable that one should be able to achieve negative refraction for a non-magnetic medium requiring little gain. It seems that achieving low gain and non-steep responses are competing goals, and it has therefore been argued that the best-case realization without a steep response will resemble the Two-Component medium. Such media acquire negative refraction through having significant loss in ϵ_r below the frequency at which $\mathrm{Re}(n) < 0$, and will require gain on the order of $|\epsilon_r| \approx 1$.

This thesis report has developed the conceptual framework needed to understand how a given ϵ_r may lead to negative refraction by identifying the main parameters and constraints involved in the process. Within this framework, the Two-component system, the NIES system and the EIT system have all been successfully analyzed, as well as a number of attempts at achieving negative refraction through the positioning of ZPPs. This amounts to a significant result. Though some previous literature does present certain of the concepts that have been presented in this report (e.g. [6, 5]) these have been less extensive and have not set out to find conditions upon ϵ_r in general. On the contrary, this thesis gives clear and concrete instructions on how ϵ_r must be chosen in non-magnetic media towards achieving negative refraction. For instance, rather than qualitatively understand the success of the Two-Component and NIES systems of achieving negative refraction through ambiguous terms like *high loss* and *steep drop* respectively, one can on the basis of this thesis quantitatively and clearly understand both systems in terms of *phase* θ_ϵ and *magnitude* $|\epsilon_r|$ in the complex frequency plane. Therefore, one stands much better equipped for determining whether a given material response ϵ_r has the potential of leading to negative refraction or not. The results of this thesis are therefore relevant to a number of possible directions for further inquiry.

For example, for further inquiry into the possibility of achieving

negative refraction, the concepts presented here may be of good use and apply equally well to media that include magnetic responses, as well as non-magnetic, media. Considering the challenges this thesis has discovered in achieving negative refraction in non-magnetic systems, perhaps further inquiry should once again examine magnetic media, though this time empowered with the concepts developed here. On the basis of this report, one knows more on how one must demand ϵ_r and μ_r to be. An interesting idea could be to have an active ϵ_r and a passive μ_r response. This could compensate for the high losses often found in magnetic responses for optical frequencies. One could perhaps use the Two-Component medium displayed here for ϵ_r along with a passive magnetic response μ_r: The magnetic response could contribute by adding to the amount of phase achieved by the Two-Component system alone.

On the other hand, one may of course choose to continue examining non-magnetic media, for which the concepts of this thesis remain equally important. With the possible exception of the NIES system, the placements of ZPPs considered so far have been relatively simple: Perhaps there exist complex arrangements of zeros and poles that could lead to desirable results in ϵ_r and n? It could be interesting to see if there exist other systems than the NIES-system that do well on the figure of merits. A possible way of evaluating this may be to first define a desired refractive index response n_Ω which displays negative refraction with low $\mathrm{Im}(n)$ and without steep variation within a bandwidth Ω and then use the causal extrapolation method of section 6 to find n for all frequencies. One can then find the functional form of ϵ_r corresponding with this. Following such a procedure, where a number of possible refractive indexes $n_{\Omega 1}, n_{\Omega 2}, n_{\Omega 3}, ...$ are designed, a number of different dielectric responses $\epsilon_{r1}, \epsilon_{r2}, \epsilon_{r3}, ...$ can be found. Evaluating these in the complex plane may lead to interesting placements of ZPPs. However, such an approach is not likely to lead towards realizable ϵ_r if the desired n_Ω is not *causality friendly*: That is, since it does not seem possible to achieve negative refraction with low gain and low steepness on the basis of causality, any n_Ω with these properties is likely to lead to a very dramatic response within the extrapolated frequencies. Further investigation within non-magnetic media is therefore more likely to reduce into a task of optimizing the possibilities already suggested in this report, as there do not seem to be any other available. This could for example consist in optimizing a variation of the Two-Component System or the NIES system.

A possibly more promising direction of further inquiry in non-magnetic media could be to investigate to a greater extent what polar paths of ϵ_r are possible in its complex plane on the basis of causality. Considering that a polar path of ϵ_r around the origin in the complex plane would be a sufficient condition towards achieving negative refraction, such considerations could bring valuable results. This report has argued that e.g. an elliptic path such as that of Fig. 9d in section 3.1 is not possible without steep variation due to causality, because it would then achieve negative refraction without any of the require-

ments derived from the Kramers-Kronig relations: Loss, gain or steep variation. Therefore, this thesis has indirectly argued for what is not possible in the complex plane of ϵ_r, however an interesting question remains: What polar paths in fact are possible?

Despite the failure of the EIT system to provide a route towards realizing negative refraction by steep variation, further investigation could involve searching for other systems that display steep variations in $\mathrm{Im}(\epsilon_r)$ and $\mathrm{Im}(n)$. Perhaps it would also be reasonable to continue evaluating atomic coherence systems. After all, this thesis has shown that the EIT system could have produced negative refraction if its symmetry had been broken. Perhaps given a different atomic level arrangement, it is possible to derive a model that allows for an asymmetric response? Since atomic coherence systems have the desirable characteristics of steep variations, it could be worth a try. Hence, a future route of inquiry could be to employ the semi-classical formalism presented in this thesis to evaluate other atomic systems.

Further inquiry could also be related to the design and realization of desired responses through metamaterials. This would be a continuation of the proposed outline presented in section 6, and is therefore not primarily preoccupied with achieving negative refraction. The concepts from this thesis will then be helpful when designing desired responses. A significant question remains how one may causally extrapolate the goal functions while minimizing the amount of gain that is present. One should evaluate other possible extrapolation methods, and perhaps investigate the derivation leading to the Krein and Nudel'man approximation in order to see if there are any ways in which it can be modified. Another interesting question is if it is possible to find a method that allows for the approximation of the resulting function by as few Lorentzians as possible.

A Positioning of poles in the complex plane

Here the various possibilities of placing the zero-pole-pairs displayed in Fig. 18b are considered. The aim is to quantitatively show what was qualitatively argued for in section 4.4: That no matter which of the pole position possibilities suggested in Fig. 18b one uses, one faces problems with considerable gain. This is demonstrated in Fig. 41, Fig. 42, Fig. 44 and Fig. 45. Each system is analyzed in the caption belonging to every figure. Fig. 43 serves to demonstrate the fact that by adding more zero-pole pairs one is able to get a larger phase θ_ϵ.

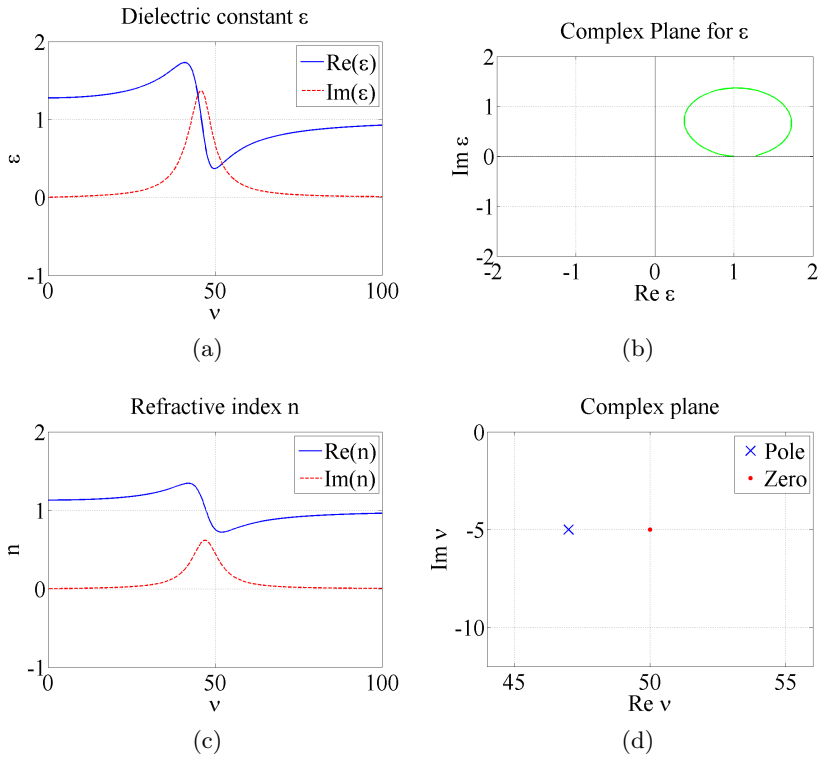

Figure 41: Two zero-pole-pairs. Both zeros are placed at $\nu_0 = 50 - 5i$ and both poles are placed at $\nu_p = 47 - 5i$, as displayed in (d). One observes in (b) that the phase θ_ϵ never becomes larger than 80^o and so $\mathrm{Re}(\epsilon_r) < 0$ in (a), or $\mathrm{Re}(n) < 0$ in (c) for all frequencies. That is, as discussed, one must require that the path passes around the origin in order to achieve negative refraction.

Upon moving along the real frequency axis in (d) from ∞ to a ν_{obs} placed to the right of the zero-pole-pair region, one may note that the phase given by (54) will yield $\theta_\epsilon = 2\theta_0 - 2\theta_p > 0$ because θ_p is small compared to that of θ_0. This is what is observed in the polar plot of (b): As one moves down in frequency from infinity one begins traversing the circle in the anticlockwise direction. As one continues moving ν_{obs} leftwards towards the origin, the phase θ_p begins increasing, thereby eventually causing θ_ϵ to decrease as is shown in (b) by the path turning back towards the start. Finally one will arrive at the point where $\theta_p = \theta_0$ and the path in (d) encloses a circle.

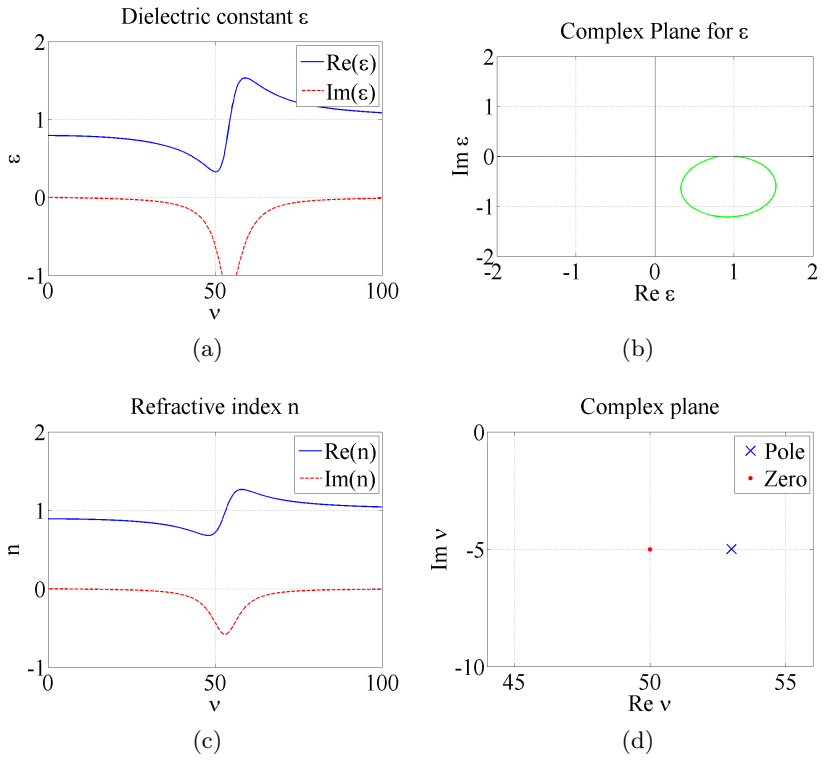

Figure 42: Two zero-pole-pairs, here placed in opposite order to those of Fig. 41. One therefore observes a mirrored image of (b) as compared to Fig. 41b. Both zeros are placed at $\nu_0 = 50 - 5i$ and both poles are placed at $\nu_p = 53 - 5i$, as displayed in (d). One observes in (b) that the path is located entirely in the fourth quadrant $-\pi/2 < \theta_\epsilon < 0$, and that the phase never becomes more negative than -80^o. This path therefore does not acquire enough phase to achieve negative refraction. Re(ϵ_r)> 0 in (a), and Re(n)> 0 in (c) for all frequencies, despite there being gain. If one whishes negative refraction, the path in (b) must pass *around* the origin.
One may understand the path taken in (b) by the same analysis as given in the caption of Fig. 41. As one moves along the real frequency axis in (d) from $\nu_{\text{obs}} = \infty \to 0$, θ_p in the beginning increases more rapidly than does θ_0 from which one gets the first half of the circle in the clockwise direction in (b). After this θ_0 catches up, giving the second half of the circle. As one achieves $\theta_0 = \theta_p$ the circle is completed.

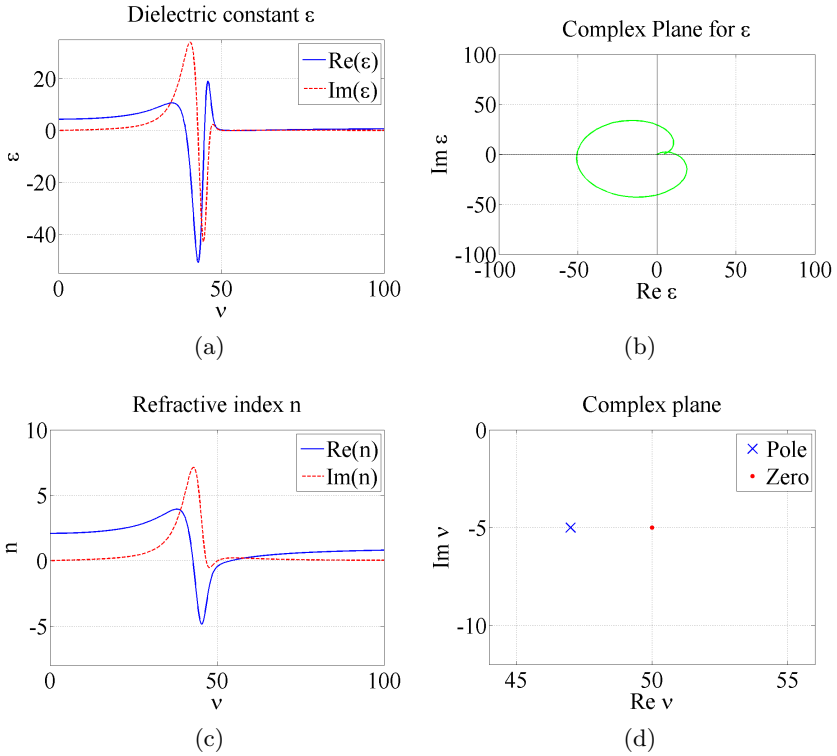

Figure 43: Twelve zero-pole-pairs placed in the same manner as in Fig. 41. All twelve zeros are placed at $\nu_0 = 50 - 5i$ and all twelve poles are placed at $\nu_p = 53 - 5i$, as displayed in (d).
The zero-pole-placements of Fig. 41 and Fig. 42 have not succeeded in leading to negative refraction due to the phase θ_ϵ not being large enough. As discussed, the amount of phase angle can be increased by increasing the number of zero-pole-pairs according to (53). This has been done here: Comparing with Fig. 41, one observes here that the path in (b) successfully passes around the origin, leading to both $\mathrm{Re}(\epsilon_r) < 0$ in (a), or $\mathrm{Re}(n) < 0$ in (c). However, one observes that there is significant gain involved, which is therefore not desirable. Notice the considerable magnitude of the *heart shape* in (b) and the response amplitude in (a) and (c).

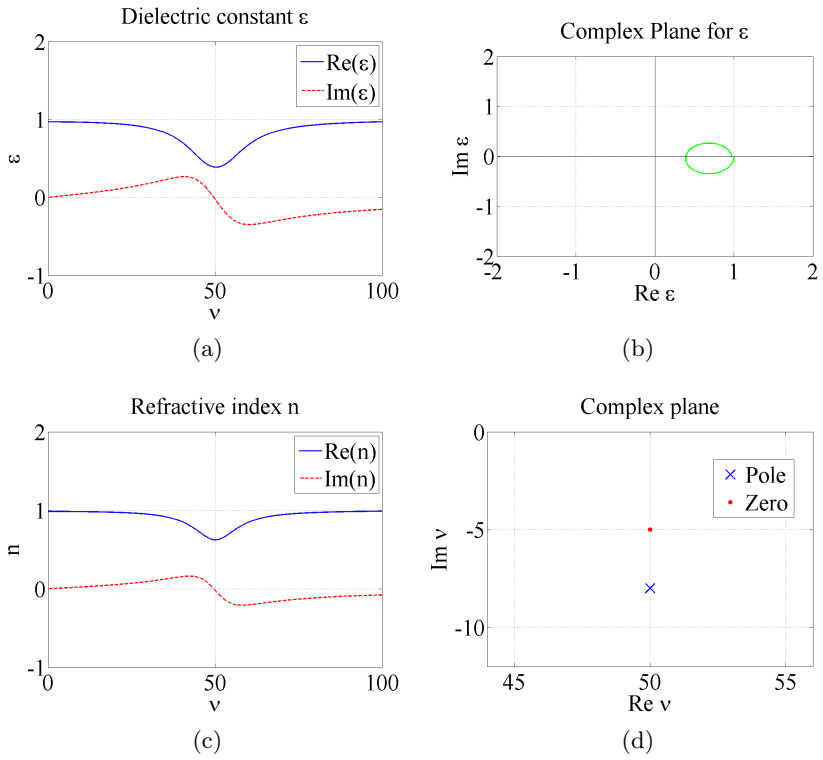

Figure 44: Two zero-pole-pairs. Both zeros are placed at $\nu_0 = 50 - 5i$ and both poles are placed at $\nu_p = 50 - 8i$, directly underneath the zeros in the complex plane as displayed in (d). One may analyze the path in (b) by noting that for frequencies along the real frequency axis to the right of the zero-pole pair $\theta_p > \theta_0$, therefore making $\theta_\epsilon < 0$ which leads to the lower part of the ellipse in (b), and hence gain. For frequencies to the left of the zero-pole pair the opposite is the case, having $\theta_p < \theta_0$ leading to the upper part of the ellipse in (b) and hence the passive part.
There are not enough zero-pole pairs present to give large enough phase to achieve negative refraction, however as was demonstrated in Fig. 43 this would be possible if enough zero-pole pairs are used. The goal of this figure, however, is to demonstrate that the zero-pole placement leads to gain which would nevertheless be the case for a larger amount of zero-pole pairs as well.

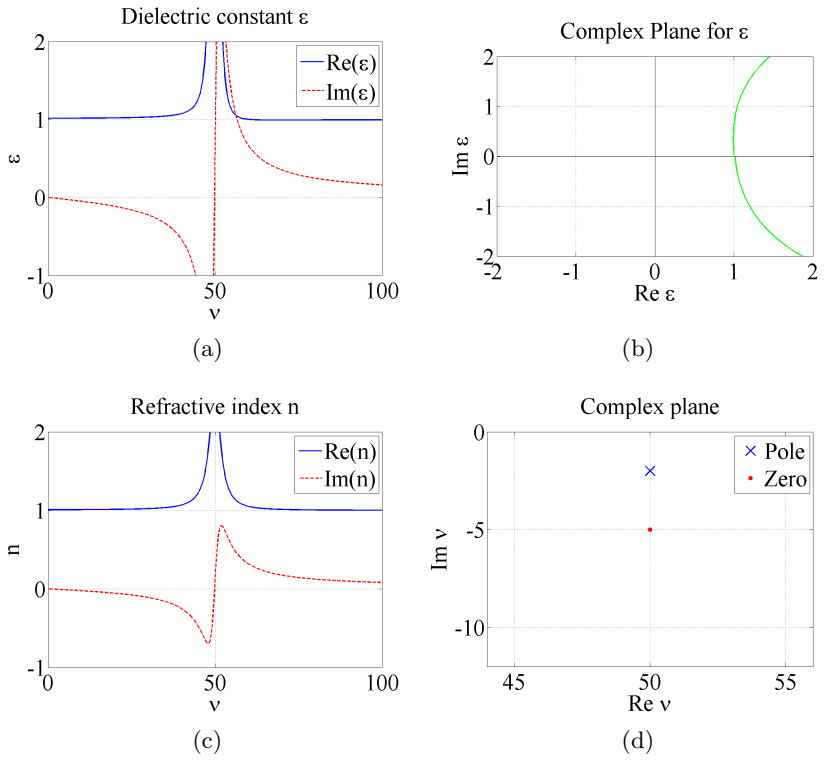

Figure 45: Two zero-pole-pairs, here placed in opposite order to those of Fig. 44: The poles above the zeros. Both zeros are placed at $\nu_0 = 50 - 5i$ and both poles are placed at $\nu_p = 50 - 2i$, directly above the zeros in the complex plane as displayed in (d). The behavior in (b) may be analyzed in the same way as was done in the caption to Fig. 44 except swapping the regions at which $\theta_p > \theta_0$ and $\theta_p < \theta_0$. However, the size of the ellipse in the polar plane of (b) is significantly greater due to the poles being so close to the real axis. There is a lot of gain present.

References

[1] J. B. Pendry, D. Schurig, and D. R. Smith. Controlling electromagnetic fields. *Science*, 312(5781):1780–1782, 2006.

[2] D. Schurig, J. J. Mock, B. J. Justice, S. A. Cummer, J. B. Pendry, A. F. Starr, and D. R. Smith. Metamaterial electromagnetic cloak at microwave frequencies. *Science*, 314(5801):977–980, 2006.

[3] J. B. Pendry. Negative refraction makes a perfect lens. *Phys. Rev. Lett.*, 85:3966–3969, Oct 2000.

[4] Liu Zhaowei Zhang, Xiang. Superlenses to overcome the diffraction limit. *Nat Mater*, (7):435 – 441, 2008.

[5] Yi-Fan Chen, Peer Fischer, and Frank W. Wise. Negative refraction at optical frequencies in nonmagnetic two-component molecular media. *Phys. Rev. Lett.*, 95:067402, Aug 2005.

[6] Bertil Nistad and Johannes Skaar. Causality and electromagnetic properties of active media. *Phys. Rev. E*, 78:036603, Sep 2008.

[7] D. R. Smith, Willie J. Padilla, D. C. Vier, S. C. Nemat-Nasser, and S. Schultz. Composite medium with simultaneously negative permeability and permittivity. *Phys. Rev. Lett.*, 84:4184–4187, May 2000.

[8] Johannes Skaar. Negative refraction: A tutorial.

[9] Viktor G Veselago. The electrodynamics of substances with simultaneously negative values of ϵ and μ. *Soviet Physics Uspekhi*, 10(4):509, 1968.

[10] Johannes Skaar. Fresnel equations and the refractive index of active media. *Phys. Rev. E*, 73:026605, Feb 2006.

[11] Christopher Dirdal. Metamaterials and coherent control. Dec 2011.

[12] Michael Fleischhauer, Atac Imamoglu, and Jonathan P. Marangos. Electromagnetically induced transparency: Optics in coherent media. *Rev. Mod. Phys.*, 77:633–673, Jul 2005.

[13] M.O. Scully and M.S. Zubairy. *Quantum optics*. Cambridge University Press, 1997.

[14] L.V. Ahlfors. *Complex analysis: an introduction to the theory of analytic functions of one complex variable*. International series in pure and applied mathematics. McGraw-Hill, 1979.

[15] B.E.A. Saleh and M.C. Teich. *Fundamentals of photonics*. Wiley series in pure and applied optics. Wiley-Interscience, 2007.

[16] Johannes Skaar. A numerical algorithm for extrapolation of transfer functions. *Signal Processing*, 83(6):1213 – 1221, 2003.